A STUDY OF SOLUTE: SOLVENT INTERACTIONS IN SOME ASSOCIATED LIQUIDS

Nicholas Martinus

A Thesis Submitted for the Degree of PhD
at the
University of St Andrews

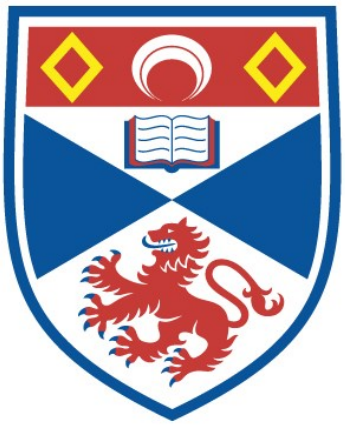

1977

A STUDY OF SOLUTE - SOLVENT INTERACTIONS IN SOME ASSOCIATED LIQUIDS

A Thesis

presented for the degree of

DOCTOR OF PHILOSOPHY

in the Faculty of Science of the

University of St. Andrews

by

Nicholas Martinus

ProQuest LLC.
789 East Eisenhower Parkway
P.O. Box 1346
Ann Arbor, MI 48106 – 1346

A STUDY OF SOLUTE-SOLVENT INTERACTIONS IN SOME ASSOCIATED LIQUIDS

A thesis presented for the degree of Ph.D. in the Faculty of Science of the University of St. Andrews by Nicholas Martinus.

ABSTRACT

The variation of the viscosity of aqueous and non-aqueous electrolyte solutions with salt concentration has been studied and the results interpreted in terms of a number of mathematical models. The effects of ion-association on the viscosity of electrolyte solutions has been investigated by measuring the viscosity of aqueous solutions of some thallous salts.

The viscosities of alkali halide salts in formamide have been determined over a range of temperatures and new methods for the division of viscosity B- coefficients into ionic contributions have been proposed. The results of these studies have been interpreted in terms of the ion-solvent interactions.

The intermolecular interactions present in binary liquid mixtures of formamide with methanol, ethanol propan-1-ol and butan-1-ol have been studied by viscosity measurements over the complete concentration range. Finally the usefulness of time domain dielectric spectroscopy in solute-solvent interaction studies has been briefly investigated.

DECLARATION

I declare that this thesis is my own composition, that the work of which it is a record has been carried out by me, and that it has not been submitted in any previous application for a Higher Degree.

This thesis describes results of research carried out at the Department of Chemistry, United College of St. Salvator and St. Leonard, University of St. Andrews, under the supervision of Dr. C.A. Vincent since 1st October, 1973.

Nicholas Martinus

CERTIFICATE

I hereby certify that Nicholas Martinus has spent twelve terms of research work under my supervision, has fulfilled the conditions of ordinance no. (St. Andrews), and is qualified to submit the accompanying thesis in application for the degree of Doctor of Philosophy.

C.A. Vincent
Director of Research

ACKNOWLEDGEMENTS

First and foremost I would like to thank Dr.C.A. Vincent for his continuous help and encouragement throughout the work.

My thanks go to Professor J.M. Tedder and Professor P.A.H. Wyatt for providing the research facilities and also for the award of a research grant from the Purdie fund.

I would also like to express my gratitude to Mr. C.D. Sinclair of the Department of Statistics for help with the statistical analysis in Chapter 3, and to Dr. M. Kent of the Department of Fisheries Aberdeen for help with the time domain spectroscopy work.

My thank are also due to Mr. J. Rennie and Mr. J.G. Ward for electronic and technical assistance, and to Mr. J.B. Martinus for his help with the diagrams in the thesis.

Finally I thank my wife Liz for skilfully typing this thesis and for all the help and encouragement she has given me.

SUMMARY

The variation of the viscosity of aqueous and non-aqueous electrolyte solutions with salt concentration has been studied and the results interpreted in terms of a number of mathematical models. The effects of ion-association on the viscosity of electrolyte-solutions has been investigated by measuring the viscosity of aqueous solutions of some thallous salts.

The viscosities of alkali halide salts in formamide have been determined over a range of temperatures and new methods for the division of viscosity B- coefficients into ionic contributions have been proposed. The results of these studies have been interpreted in terms of the ion-solvent interactions.

The intermolecular interactions present in binary liquid mixtures of formamide with methanol, ethanol propan-1-ol and butan-1-ol have been studied by viscosity measurements over the complete concentration range. Finally the usefulness of time domain dielectric spectroscopy in solute-solvent interaction studies has been briefly investigated.

TABLE OF CONTENTS

CHAPTER ONE

1.1 INTRODUCTION

The study of solution interactions has attracted attention for more than a century. Such studies fall naturally into two categories, i.e. the investigation of electrolytic and non-electrolytic solutions.. The major drawback to the development of a completely satisfactory theory to explain solution interactions is our lack of understanding of the liquid state itself, as was pointed out as early as 1889 [1]. Today it is accepted that any theory of liquid solutions must be considered in relation to the structure of the solvent concerned.

Current theories of liquid structure can be divided into two main categories, lattice theories and distribution function theories. The lattice theories assume a structure similar to a certain extent to the regular structure of a crystal e.g. Eyring [2], Podolsky [3] etc. Although lattice theories are not particularly successful as predictive models on an ab initio basis they can provide good agreement with experiment when certain constants have been determined.

Distribution function theories on the other hand investigate the forces arising from interactions between molecules and the manner in which these forces influence structure. Since liquids display only short-range order, as suggested by Samoilov [4], then the only quantitative way to describe liquid structure is by the construction of a radial distribution curve. This maybe achieved through X-ray and neutron diffraction studies. On the basis of these experiments, the radial distribution function of molecules is obtained from the first intensity maximum

of the radiation scattering. This function gives the probability of finding one molecule as a function of the distance from another. A knowledge of the distribution function is the minimum information required to develop a picture of the structure of liquids. This knowledge enables the calculation of the average distance of the adjacent molecules and the number of nearest neighbours. However, information is required not only on the relative positions of the molecules, but also on the forces of interaction between them. Although a general theory of intermolecular forces has not been successfully developed, various properties of these forces are known. The primary forces which keep the molecules of a liquid together are van der Waals type forces which include dispersion forces, dipole-dipole interactions, dipole-induced dipole and hydrogen bonding. The repulsive forces between the molecules arise from the overlapping of the electron shells of the neighbouring molecules and the mutual repulsion of the atomic nuclei. A liquid may be considered to fluctuate between a large number of equally likely structures.

Research into electrolyte solutions is currently centred on two broad areas: ion-ion interactions and ion-solvent interactions. The study of ion-ion interactions investigates the balance of electrostatic and thermal forces and the development of models for a time-averaged distribution of ions in solution. Since the successful interionic attraction theory of Debye and Hückel [5] a great deal of research has been concentrated in this area and refinements of their treatment of both equilibrium and transport properties have been made by numerous workers[6,7,8]. In

comparison, the study of ion-solvent interactions is much less advanced and has not received the same attention.

A large volume of work has also been carried out on the interactions of non-electrolyte mixtures. From the initial attempt by Arrhenius [9] to predict the viscosity of binary mixtures, work has progressed to statistical thermodynamic models and the study of thermodynamic excess functions and partial molal quantities.

1.2 METHODS OF STUDYING SOLUTION INTERACTIONS

There are perhaps three main groups of methods for studying solution interactions: thermodynamic measurements, spectroscopic investigations and studies of transport processes.

(1) THERMODYNAMIC MEASUREMENTS

Thermodynamic properties of solutions are not only useful for estimating the feasibility of reactions in solutions, but they also offer one of the better methods of investigating the theoretical aspects of solution structure. This is particularly true for the standard partial molal entropy, enthalpy and the partial molal volumes of the solutes, values of which are sensitive to the arrangement of solvent molecules around a solute molecule. Enthalpies and free energies of solvation and transfer between solvents have also been valuable in testing theoretical relationships such as the Born equation [10]. The main sources of experimental data for these functions have been equilibrium studies, direct calorimetric measurements, density determinations and electrochemical measurements. In considering the thermodynamics of ion

solvation, two equilibria of fundamental importance are:

$$MX_{(s)} = M^{+}_{(soln)} + X^{-}_{(soln)} \qquad (1.1)$$

$$M^{+}_{(g)} + X^{-}_{(g)} = M^{+}_{(solv)} + X^{-}_{(solv)} \qquad (1.2)$$

These two processes are related to one another through a Born-Haber type cycle such as

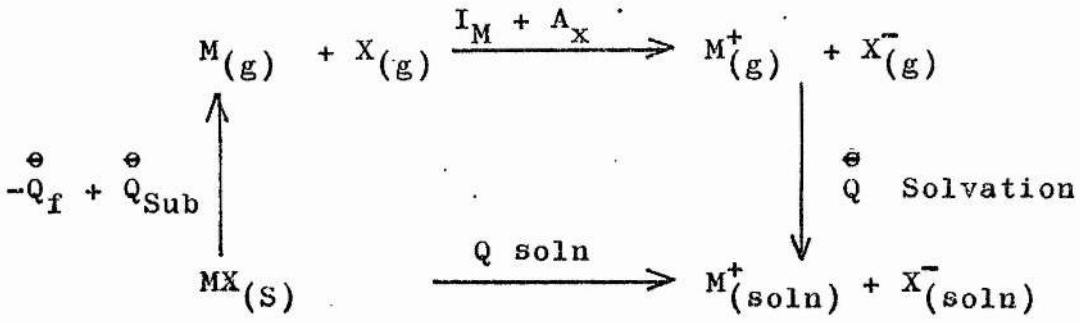

In this cycle I and A are the ionisation potential of the metal atom M and the electron affinity of the non-metal entity X respectively. $Q^{\ominus}$ is the energy or enthalpy of the process indicated e.g. $\Delta H^{\ominus}_{f}$ is an enthalpy of formation and $\Delta H^{\ominus}_{soln}$ and $\Delta H^{\ominus}_{solv}$ correspond to processes (1) and (2) respectively. The thermodynamic quantities for reaction (1) are directly measurable and those of reaction (2) must be calculated from

$$\Delta G^{\ominus}_{solv} = \Delta G^{\ominus}_{soln} + \Delta G^{\ominus}_{lattice} \qquad (1.3)$$

$$\Delta H^{\ominus}_{solv} = \Delta H^{\ominus}_{soln} + \Delta H^{\ominus}_{lattice} \qquad (1.4)$$

It is often preferable to work with $\Delta G^{\ominus}_{solv}$ and $\Delta H^{\ominus}_{solv}$ terms since they can be divided, using certain non-thermodynamic methods, into ionic contributions. However $\Delta G^{\ominus}_{soln}$ and $\Delta H^{\ominus}_{soln}$ are directly measurable quantities and are therefore much more accurate than the corresponding energies and

enthalpies of solvation. The entropies of solvation can then be calculated from

$$\Delta S^{\ominus}_{solv} = \frac{\Delta H^{\ominus}_{solv} - \Delta G^{\ominus}_{solv}}{T} \qquad (1.5)$$

The standard entropy of solvation is given by

$$\Delta S^{\ominus}_{solv} = \bar{S}^{\ominus}_{n} - S^{\ominus}_{g} \qquad (1.6)$$

where $\bar{S}^{\ominus}_{n}$ is the standard partial molal entropy of the electrolyte and $S^{\ominus}_{g}$ is the standard molal entropy of the electrolyte in the gas phase calculated from the Sackur-Tetrode equation [11]. A good example of the use of thermodynamic measurements in the study of ion-solvent interactions is the work of Parker et al,[12] on the solvation of ions. In this work use was made of transference cells to determine the thermodynamics of transfer between various solvents.

(11) SPECTROSCOPIC INVESTIGATION

Spectroscopic techniques are widely used to investigate solution interactions. Much work has been done on the selective solvation of ions by nuclear magnetic resonance spectroscopy. Infrared and Raman spectroscopy have proved invaluable in the study of hydrogen bonding and in elucidating the mechanisms of solvation. The use of dielectric spectroscopy techniques is a relatively new tool in solvation studies. Time domain spectroscopy enables the permittivity and loss factor of a solvent to be determined over a range of frequency. The relaxation time of molecules can also be measured by this technique. In this work some associated liquids have been analysed by time domain spectroscopy to assess its usefulness in solvation studies.

(111) TRANSPORT PROCESSES

This covers a range of experimental techniques including viscosity, diffusion and electrolytic conduction studies. Information from all three sources is usefull in solution interaction studies. The measurement of the viscosity of electrolyte solutions and binary liquid mixtures was the main source of experimental results in this project.

The theory of liquid viscosity was developed from the concepts of hydrodynamics, the study of fluids in motion. The early development of this subject took place in the eighteenth century and workers of this period were mainly concerned with so called "perfect fluids", which were characterised by the fact that they had no tangential component of stress. Earlier, in the seventeenth century Newton [13] showed that the force F required to maintain a constant difference between two laminae with an area of contact A was

$$F = \eta A \frac{dv}{ds} \qquad (1.7)$$

where η is called the coefficient of viscosity and is a characteristic constant for each liquid. The main development of the theory of viscous fluids was due to Navier and Stokes [14,15] and is given in standard texts[16].

Classical theories of solution were built upon the analogy between the behaviour of solute particles and that of molecules of an imperfect gas. The solvent was considered to be a mere provider of the atmosphere within which the solute particles moved. Modern theories of solution however stress the importance of considering not

only the effects of the ions on the structure of the particular solvent but also the specific ion-solvent interactions involved. A solvated ion is no longer thought of as an ion that moves through the solution with a certain number of solvent molecules bound to it. A dynamic situation is now envisaged whereby solvent molecules spend an average period of time as nearest neighbours to solute particles.

The viscosity of a liquid can be considered to be due to the interactions of the various solution species. In 1929 Jones and Dole [17] deduced an empirical relationship between the concentration of solute and the viscosity of electrolyte solution. i.e.

$$\eta / \eta_o = 1 + Ac^{\frac{1}{2}} + Bc \qquad (1.8)$$

where η is the viscosity of the solution, η_o that of the solvent, c the concentration of solute and A and B constants characteristic of a solute in a given solvent. Falkenhagen and Dole [18] then showed that the $Ac^{\frac{1}{2}}$ term in equation (1.8) corresponded to the ion-ion interactions within the solution. The B factor was shown to be a measure of the ion-solvent interactions.

The viscosities of aqueous solutions of thallous salts and alkali halide solutions in formamide have been determined and the results considered in terms of time-averaged physical models such as those of Frank and Wen [19] and Samoilov [4].

In general, the viscosity isotherms for non-electrolyte binary mixtures are not linear and theoretical predictions can be made only in non-associating mixtures

of components with similar molar volumes [20]. Viscosity studies therefore are unlikely to yield a clear moleculaf interaction mechanism for such binary liquids although it is possible to interpret the results in terms of specific interaction and complex formation.

CHAPTER TWO

EXPERIMENTAL TECHNIQUES

2.1 INTRODUCTION

Of the numerous methods of measuring viscosity, considerations of accuracy, simplicity and susceptibility to rigorous mathematical treatment have led to the continued use and refinement of only a few.

The measurement of resistances to flow through a tube is probably still the most accurate and widely used method at the present time. Capillary viscometers are comparatively simple and inexpensive, they require only a small quantity of test liquid, temperature control is easy and a full mathematical treatement is possible. In general, the liquid is made to flow through a capillary tube under a known pressure difference and the rate of flow is measured, usually by noting the time taken for a given volume of liquid to pass a graduation mark. In certain types of instruments, the liquid is forced through the capillary at a pre-determined rate and the pressure drop produced across the capillary is measured. Capillary viscometers were used throughout this project and the equations for laminar flow of a liquid through a cylindrical tube are derived in the subsequent sections. A full account of other methods of viscosity measurement has been given by Dinsdale and Moore and by Swindells and coworkers [20,21].

2.2 POISEUILLE'S LAW

Until 1842, there was little knowledge of fluid flow through capillaries. Previous experimental investigations concerning flow through tubes had been carried out by Hagen[22] who used wide brass tubes in his work. Poiseuille[23]

however, in an attempt to understand the flow of blood through the human body, undertook an exhaustive series of experiments to investigate the flow of liquid through capillaries. He proved that the conditions of flow through capillary tubes were much simpler than those in the wide tubes studied previously, and showed that

$$Q = K \frac{Pr^4}{l} \qquad (2.1)$$

where Q is the flux, P the applied pressure, r the radius of the capillary, l the length of the capillary and K a constant.

2.3 THEORETICAL DERIVATION OF POISEUILLE'S LAW

Consider a section of capillary tube of length l, and let a liquid flow from A to B. fig (2.1)
It is assumed:

(1) that the flow is everywhere parallel to the axis (i.e. streamline);

(2) that there is no acceleration of the liquid at any point (i.e. steady flow)

(3) that there is no slip at the walls of the capillary;

(4) that the fluid is incompressible;

(5) that the fluid will flow when subjected to the smallest shearing force, the viscous resistance being proportional to the velocity gradient.

Let the velocity of the liquid at a distance r from the axis of the capillary be v then the velocity gradient

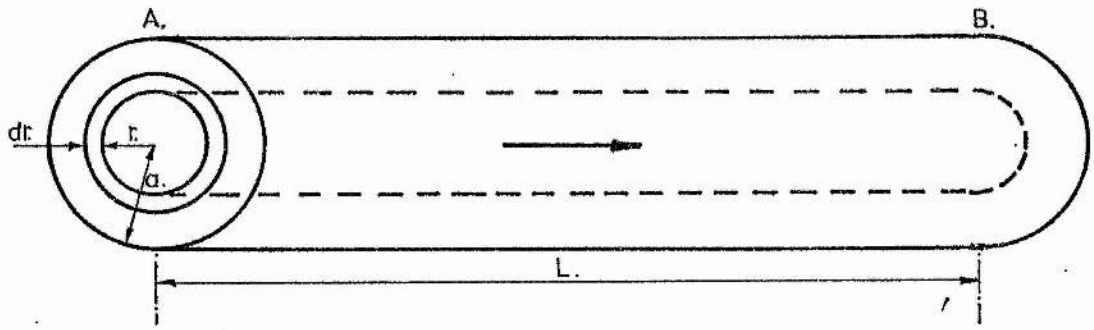

FIG. 2·1

$$D = \frac{dv}{dr} \qquad (2.2)$$

The fluid flows through the tube in the direction of the arrow by a pressure differential ΔP between A and B. The force exerted by the pressure P on a cylinder of radius r is

$$F_1 = \pi r^2 P \qquad (2.3)$$

acting in the direction of motion. The force due to the viscous resistance of the surrounding liquid on the surface of the cylinder is given by

$$F_2 = 2\pi rl\eta \frac{dv}{dr} \qquad (2.4)$$

Since there is no acceleration of the liquid, these forces must be equal and opposite. i.e.

$$Pr = -21\eta \frac{dv}{dr} \qquad (2.5)$$

then $$\frac{dv}{dr} = \frac{-Pr}{21\eta} \qquad (2.6)$$

$$\therefore \quad v = \frac{-P}{21\eta} \int_o^r r dr \qquad (2.7)$$

Thus $$v = \frac{-Pr^2}{41\eta} + C \qquad (2.8)$$

From condition (3) r = a when v = 0

$$\therefore \qquad C = \frac{Pa^2}{4l\eta} \qquad (2.9)$$

and the velocity of the fluid is given by

$$v = \frac{P}{4l\eta}\left(a^2 - r^2\right) \qquad (2.10)$$

The velocity distribution across the capillary is therefore parabolic. Since v is the distance travelled in unit time, the particles of liquid which were on the plane A at zero time will be on the surface of the parabola after unit time, in other words the volume of this paraboloid is the volume of liquid V which passes in unit time. The volume of this solid of revolution is given by

$$Q = 2\pi \int_0^a vrdr \qquad (2.11)$$

substituting for v

$$Q = \frac{\pi P}{2l\eta} \int_0^a (a^2 - r^2)\, r\, dt \qquad (2.12)$$

$$\therefore \qquad Q = \frac{\pi P a^4}{8l\eta} \qquad (2.13)$$

This formula corresponds to the empirical Poiseuille equation [23]. If Q_t is the total volume of efflux in time t, the formula becomes

$$Q_t = \frac{\pi P a^4 t}{8l\eta} \qquad (2.14)$$

2.4 CORRECTION FACTORS

STREAMLINE AND TURBULENT FLOW

In the theoretical derivation of Poiseuille's law it was assumed that the flow in the capillary was everywhere parallel to the axis. It has been found experimentally that deviations from this assumption occur at high rates of flow, and this was shown by Reynolds [24]

to be due to a change from streamline to turbulent flow. The type of flow can be characterised by a dimensionless quantity known as Reynolds Number R_n defined by

$$R_n = \frac{vd\rho}{\eta} \qquad (2.15)$$

where v, ρ and η are the mean velocity, the density and the viscosity of the liquid respectively, and d is the diameter of the tube. Turbulent flow normally occurs when the Reynolds number reaches a certain value, which experiment has shown to be about 1400 to 2000 for most capillary tubes. Flow behaviour will be the same in different tubes with different liquids where the Reynolds Numbers are the same.

THE KINETIC ENERGY CORRECTION

Viscometers for which condition (2) page (10) is fulfilled are characterised by very long efflux times and usually inconveniently small capillary bores. Long efflux times (in some of Poiseuille's work one run lasted several hours) are tedious and small bores inevitably result in difficulties due to dust particles lodging in the capillary and altering the characteristics of the viscometer. With most capillary viscometers, therefore, account must be taken of the work done in accelerating the liquid from rest, i.e. imparting kinetic energy. Hagenbach[25] (1860) was the first worker to attempt to make this correction. By 1891, Hagenbach[25], Wilberforce[26] Couette[27], and Finkener[28], had determined a theoretical calculation for the kinetic energy correction.

With reference to fig. (2.1) the volume of liquid passing through the thin cylinder dr in one second is given by:

$$V = 2\pi r\, dr\, v \qquad (2.16)$$

and it has been shown that this, integrated over the whole section of the capillary is the volume entering or leaving the tube in one second. The kinetic energy of this volume of liquid is:

$$U = \tfrac{1}{2}\rho\,(2\pi\, rv\, dr)\, v^2 \qquad (2.17)$$

or $$U = \pi\rho\, v^3 r\ \ dr \qquad (2.18)$$

where ρ is the density of the liquid.

From equation (2.10)

$$v = \frac{P}{4l\eta}\ \ (a^2 - r^2) \qquad (2.19)$$

substituting for v in (2.18), the kinetic energy given to the liquid in time t is,

$$U = \left(\frac{P}{4l\eta}\right)^3 \pi\rho t\ (a^6 r - 3a^4 r^3 + 3a^2 r^5 - r^7)dr \qquad (2.20)$$

Integrating between limits r = 0 to r = a gives

$$U = \left(\frac{P}{4l\eta}\right)^3 \pi\rho\, \frac{a^8}{8}\ \ t \qquad (2.21)$$

Now from Poiseuille's equation (2.13) the total efflux volume in t seconds is given by

$$Q = \frac{\pi P a^4\ t}{8l\eta} \qquad (2.22)$$

Or

$$V = \frac{\pi P a^4 t}{8l\eta} \qquad (2.23)$$

$\therefore$

$$\frac{P}{4l\eta} = \frac{2V}{\pi a^4 t} \qquad (2.24)$$

and

$$\left(\frac{P}{4l\eta}\right)^3 = \frac{8V^3}{\pi^3 a^{12}\ t^3} \qquad (2.25)$$

Therefore the energy dissipated is given by equating (2.21) and (2.25).

$\therefore$

$$U = \frac{\rho\, V^3}{\pi^2 a^4 t^2} \qquad (2.26)$$

The pressure differential ΔP between the A and B planes fig. (2.1) is used up doing various forms of work. If P is the pressure required to overcome the forces due to the viscosity then $(\Delta P - P)$ is the pressure dissipated in imparting kinetic energy to the fluid. The work done in imparting kinetic energy is then $(\Delta P - P)V$ and as shown above

$$(\Delta P - P)V = \frac{\rho V^3}{\pi^2 a^4 t^2} \qquad (2.27)$$

$$\therefore \quad (\Delta P - P) = \frac{\rho V^2}{\pi^2 a^4 t^2} \qquad (2.28)$$

This is a small correction which has to be deducted from the observed pressure difference in order to yield the pressure used in overcoming the viscosity forces.i.e. pressure used to overcome viscous resistance

$$Pv = P - \frac{\rho V^2}{\pi^2 a^4 t^2} \qquad (2.29)$$

Substitution in (2.23) gives

$$\eta = \frac{\pi a^4 t}{8lV}\left[P - \frac{\rho V^2}{\pi^2 a^4 t^2}\right] \qquad (2.30)$$

$$\therefore \quad \eta = \frac{\pi P a^4 t}{8lV} - \frac{\rho V}{8l\pi t} \qquad (2.31)$$

However the actual kinetic energy correction found experimentally was

$$U = \frac{m \rho V^3}{\pi^2 a^4 t^2} \qquad (2.32)$$

$$\therefore \quad \eta = \frac{\pi P a^4 t}{8lV} - \frac{m \rho V}{8l\pi t} \qquad (2.33)$$

where m is a constant, called the Hagenbach coefficient, which depends on the viscometer characteristics. Various values of m have been deduced theoretically ranging from 0.5 (Reynolds)[24] to 1.12 (Boussinesq)[29]. Experimental

values of m determined, range from 0 to 1.55 with values around 1.12 the most prevalent.

COUETTE CORRECTION

In addition to the work done in overcoming the viscous resistance in the capillary itself, a small amount of energy is expended in overcoming the viscous forces between the converging and diverging streamlines at the entrance and exit of the capillary respectively. The correction for this effect takes the form of a hypothetical increase λ to the length of the capillary; equation (2.33) then becomes

$$\eta = \frac{\pi P a^4 t}{8(1+\lambda)V} - \frac{m\rho V}{8(1+\lambda)\pi t} \qquad (2.34)$$

The value of λ cannot be deduced theoretically but must be found by experiment and is usually of the order of a few diameters.

For viscosity measurements in kinematic instruments the pressure term P is replaced by the hydrostatic pressure head $hg\rho$ to give

$$\eta = \frac{\pi a^4 hg\rho t}{8(1+\lambda)V} - \frac{m\rho V}{8(1+\lambda)\pi t} \qquad (2.35)$$

where h is the mean height of the liquid column and g is the acceleration due to gravity.

2.5 VISCOMETER DESIGN

For many of the original kinematic viscometers, which were basically glass U-tubes, difficulties arose in the determination of the exact mean hydrostatic pressure head ($h_m g \rho$). As flow progresses, the pressure changes continuously due to the drop in the height in the other

column. The Ostwald viscometer, used for the determination of relative viscosity, simplifies matters by using a fixed volume of liquid (delivered by means of a pipette) so that the mean height of the liquid column, h_m, is constant for each determination and can therefore be incorporated in a general viscometer constant.

Surface tension effects, arising from the adhesion of liquid to the walls of the bulbs immediately above the capillary and in the exit reservoir, can also alter the hydrostatic pressure head and give rise to uncertainties in measurements, particularly when the surface tensions of the calibration liquid and the liquid under investigation are very different.

The Ubbelohde suspended level viscometer[30] as used in this investigation, is considered to minimise these effects by the provision of the suspended level at the exit of the capillary. fig. (2.2). This 'suspended level' which is simply a bulb maintained at the same external pressure as that exerted on the liquid and of similar shape to the liquid reservoir, ensures that changes of the mean hydrostatic pressure head for the different solutions are determined only by the density of the solution, since the pressure is maintained constant. The total volume of liquid introduced into the viscometer does not need to be known accurately, since that which falls to or remains in, the lower reservoir does not contribute to the mean hydrostatic pressure head. This is of particular advantage when measurements at more than one temperature are required, since the actual volume under investigation is fixed by the marks on the upper reservoir, and expansion of the liquid in the

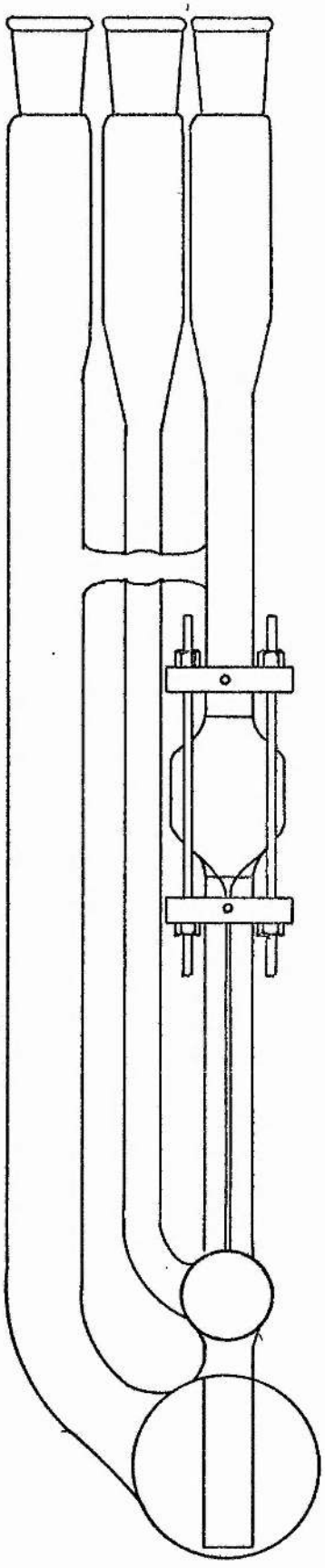

FIG. 2.2

viscometer need not be taken into account. Surface tension effects are also minimised by use of the Ubbelohde suspended level viscometers. At the curved surface of the bulb, at the exit of the capillary, a certain traction is developed which acts in the opposite direction to the surface tension of the liquid in the upper bulb of the viscometer.

It is essential that the viscometer be mounted firmly in a level position to maintain a constant hydrostatic pressure head. For a change of angle A to $A+\delta A$ in the vertical alignment of the capillary axis, the change in the liquid head is given by

$$\frac{1 - \cos (A - \delta A)}{\cos A}$$

A deviation of 0.0436 radians will therefore produce an inaccuracy of 0.1% in the measured viscosity. Jones and Dole[17] noted that, despite their efforts to maintain a rigid reproduceable mounting for their viscometer, the efflux time changed by approximately 0.1% over a certain period of time. The cause of this was attributed to the fact that their laboratory building was jacked up at one end to allow repairs to be carried out on the foundations !

Accurate temperature control is necessary for viscosity measurements. This is especially true for associated solvents which often have large temperature coefficients of viscosity.

2.6 APPARATUS

The viscometers used in the project were Ubbelohde suspended level viscometers conforming to British Standard BS.IP. SL(S)71 fig. (2.2). The capillary

sections were approximately 80 mm long and 1.0 mm in diameter and the quantity of solution required for each determination was between 10 and 15 cm^3. The viscometers were equipped with ground glass sockets enabling them to be stoppered firmly to the air. Size 2 viscometers were used throughout. These had efflux times of about 250s for water at 25°C and 900s for formamide at the same temperature.

The efflux times were measured by means of photocell lamp assemblies coupled to a Hewlett Packard auto-viscometer 5901 B in conjunction with a Hewlett Packard 5903 A programmer.

2.7 THE AUTO-VISCOMETER

The Hewlett Packard auto-viscometer, model 5901 B, measured efflux times in glass capillary viscometers and provided automatic influxing in preparation for the efflux measurement. Very accurate timing was realised, because the efflux time was measured with an electronic counter using a quartz-crystal oscillator as a time base reference. A neon display provided a digital readout that could be held for observation until released by the operator. Automatic influxing and timing eliminated errors between operators due to differences in technique and human fatigue. The accuracy of the timer was $\pm$ 0.001s. The electronic counter, measured efflux times automatically, through the use of detectors mounted above and below the fiducial marks on the glass viscometer, which activated electronic circuits during the liquid efflux time. The time interval for the meniscus to travel between the two detectors was

displayed on the instrument register. The detectors also controlled the limits of liquid transport during influx and the release of the liquid for the efflux measurement. A constant pressure pneumatic pump provided the pressure required to force the liquid back into the upper bulb and was automatically shut off by a signal from the upper detector when the meniscus passed on the way up. When the meniscus again passed this detector on the way down, a signal was sent to start the timer which was only stopped when the liquid meniscus passed the lower detector. When incorporated with the programmer printer a permanent record of the efflux time was obtained. The auto-viscometer was equipped with four sets of detectors and could therefore accommodate four viscometers.

2.8 THE PROGRAMMER/PRINTER

The Hewlett Packard model 5903 A programmer/printer was an electro-mechanical apparatus which programmed the output of the 5901 B auto-viscometer and provided a printed record of the efflux time measurements. It could program the operation of the auto-viscometer such that the measurement at any channel was repeated between 0 and 10 times with 25 second intervals between measurements. This sequence could be repeated indefinitely. The printer recorded the efflux time for each run to 0.001 or 0.01 seconds as selected on the auto-viscometer along with a coded identification of the programmed channel and the run number.

2.9 DETECTORS

Two detector systems were used in this work. The

Hewlett Packard detection system consisted of minature tungsten lamp photocell assemblies which were contained in water-tight blocks and firmly attached to the viscometers above and below the efflux volume reservoirs. The viscometers were placed in the thermostatted bath completely immersing the detectors. With the passage of time, the detectors insulation failed causing lamp failure. This system has been criticised for causing heating effects[31] but this has not been observed here.

Various workers[32,33] have used detection systems in which the light source and detector were remote from the viscometer. In the second detector system, which has some similarities to that of Adolph and Siedel[33] pairs of 1 mm glass fibre light guides (Jena Glaswerk, Schott e Gen., Mainz, No. LKF1.40) were attached to the viscometers above and below the efflux reservoirs by nylon clamps. The light guides were led out of the thermostatted bath and into a nylon block containing pairs of infrared emitters and detectors (Texas Instruments Ltd., TIL31 and TIL78 respectively) The auto-viscometer described previously was modified to make it compatible with this detection system. The light guide system has proved very sensitive and can be used to detect the passage of a meniscus in a capillary tube of 0.5 mm diameter.

2.10 THERMOSTAT BATH

This was a water filled bath supplied by Townson and Mercer Ltd., (model E.270 series 33) of approximately 45 dm^3 capacity. The temperature was controlled by means of a thyristor and thermistor bridge arangement and was

considered to be accurate to at least $\pm$ 0.01°C throughout its temperature range of 10°C to 120°C. The water in the bath was circulated over a weir and around a serpentine cooling coil which was attached to a refrigeration unit. Coolant was pumped through the cooling coil from the refrigeration unit, by means of a totally immersed electric pump controlled by a variac. Provision was also made to pass cold water, from the domestic supply, through the cooling coil for high temperature work. The cold water flow rate was controlled by a flow meter (Rotameter 1100). Figure (2.3) shows the flow diagram for the two cooling systems used. Two mercury filled glass precision thermometers were used to measure the temperature. These were total immersion thermometers supplied by Zeal Ltd. One covered the range 0.0°C to 25°C and the other from 25°C to 50°C with graduations every 0.05°C. Both these thermometers were standardised at the ice point.

2.11 VISCOSITY MEASUREMENTS

For accurate measurements of viscosities in capillary viscometers there are three practical areas of importance:

(1) efflux time measurement;

(2) temperature control;

(3) efficient cleaning of the viscometer and protection against solid particles lodging in the capillary.

The human error in the measurement of efflux time with manually operated chronometers can now be eliminated by using electronic triggers. As early as 1933, Jones and Tally[34] used photo-electric cells to measure efflux times automatically. One of the problems discovered was the

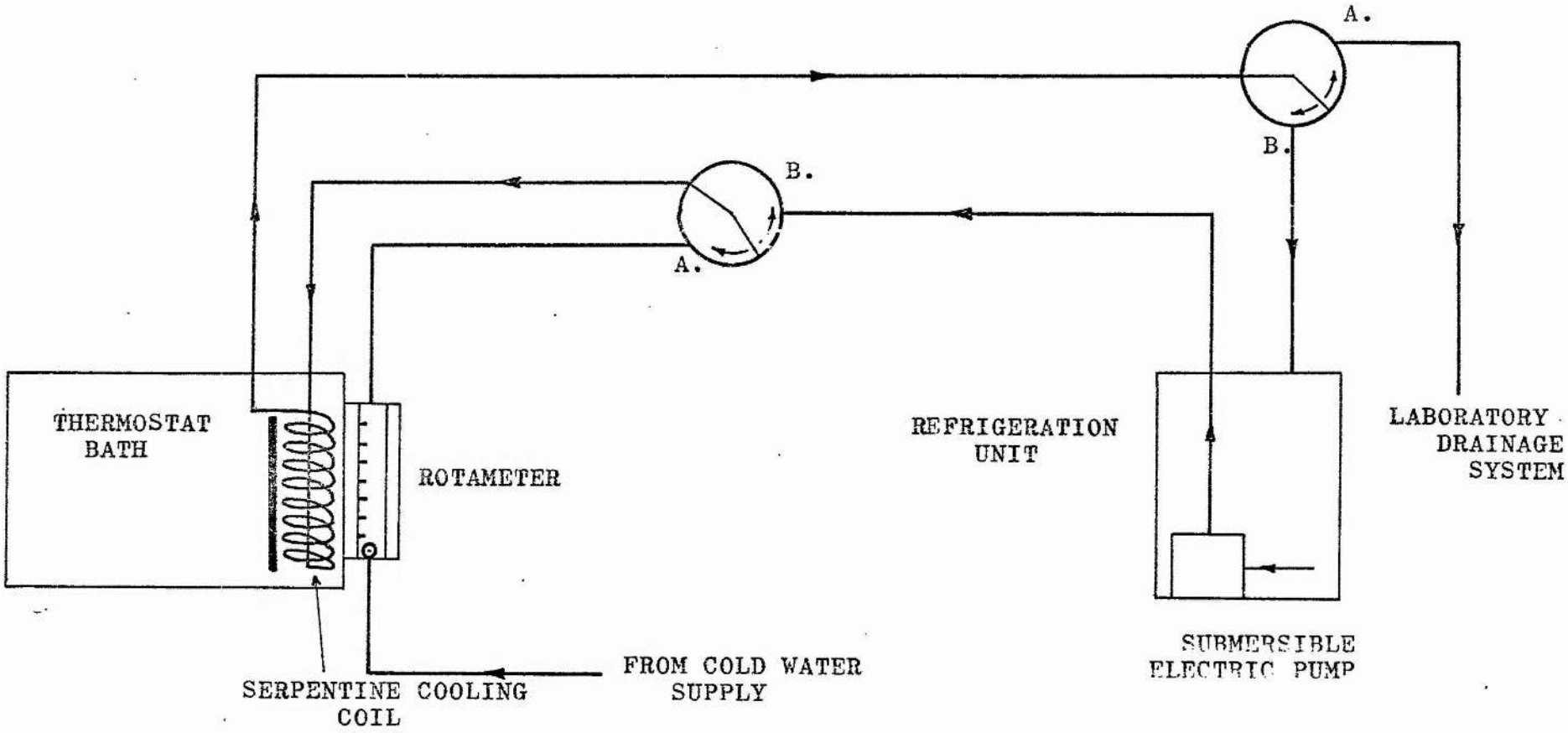

FIG. 2.3 FLOW DIAGRAM FOR THERMOSTATTED BATH

difficulty in cleaning the apparatus without altering the position of the recording apparatus and thus changing the viscometer characteristics. An important advantage of the detection system used in this project was that the detectors were firmly attached to the viscometer and were not moved during the cleaning operation. Spurious efflux times, caused by false triggering due to air bubbles were infrequent and the efflux times did not vary by more than 0.02%.

Bad triggering was usually associated with faulty mounting of the detector unit. The units were mounted firmly by their securing screws, and in the case of the Hewlett Packard detectors, were sealed against interference from air bubbles in the water bath with a silicone sealant (Dow Corning no. 0470-0256). A further cause of bad triggering was due to insufficient filling of the viscometers. If the quantity of fluid was too small, air bubbles were forced into the top reservoir of the viscometer, and the timer was activated prematurely.

In practise, the minor fluctuations in efflux time for the same solution in the same viscometer were due to variations in the bath temperature. In general viscosities were measured at only one temperature each day. The thermostatted bath was set to the required temperature the previous evening and given at least 8 hours to equilibrate. However even with these precautions, it was often found necessary to maintain a steady temperature by careful manipulation of the coarse and fine adjusters on the thermostatted bath which was found to be sensitive to the room temperature, and opening and closing laboratory doors caused temperature fluctuations.

The thermometers were read with a telescope, care being taken to ensure that the operators' eye was in line with the actual reading to avoid parallax error.

The viscometers were cleaned by flushing three times with distilled water and then three times with analytical grade acetone and finally with a stream of dust free dry nitrogen, all of which were initially passed through a number 2 glass filter, to trap any solid particles. This procedure was followed before each viscometer was filled with a new solution. At intervals of about three months the viscometers were completely filled with concentrated nitric acid and left to soak for two days. They were then washed out and filled with distilled water and soaked for about a week to ensure that no traces of acid remained.

2.12 CALIBRATION OF VISCOMETERS

Capillary viscometers may be used for absolute or relative measurements. The absolute instruments are normally used only for the establishment of primary standards and require very accurate control of applied pressure and a precise knowledge of the capillary dimensions. Relative viscometers, as used in this project, require calibration with standard liquids.

The viscosity of freshly distilled water at $20^{o}C$ has been determined by an absolute method and found to be $1.0019 \times 10^{-3} \pm 3.0 \times 10^{-7}$ J $m^{-3}s$. The rounded off value of 1.002×10^{-3} J $m^{-3}s$ has been generally accepted[16] and is used as the primary calibration standard for relative viscometers.

This primary standard has been used to determine the viscosity of water at all temperatures between 0°C and 100°C and also the viscosity of aqueous sucrose solutions to be used as secondary standards[16] . The viscosity of water, between 0°C and 20°C has been shown to follow from the relationship [36]

$$\log \eta_T = \left[\frac{1301}{998.333+8.1855\ (T-20)+0.00585(T-20)^2}\right]-3.30233 \qquad (2.36)$$

and between 20°C and 100°C by[37]

$$\log \frac{\eta_T}{\eta_{20}} = \frac{1.3272\ (20-T)\ -0.001053\ (T-20)^2}{(T\ +\ 105)} \qquad (2.37)$$

The Übbelohde suspended level viscometers used in this work were calibrated with freshly distilled water over the temperature range 10°C - 50°C, by measuring the efflux times at the chosen temperatures. Assuming that the viscometer characteristics do not change significantly over this temperature range, equation (2.35) can be written as

$$\frac{\eta}{\rho t} = A - \frac{B}{t^2} \qquad (2.38)$$

The known viscosity and density and the measured efflux times were substituted into equation (2.38) and a plot of $1/t^2$ against $\eta/\rho t$ was constructed. fig. (2.4) From equation (2.38) the plot should be linear, with gradient -B and intercept A. Inspection of fig. (2.4) however indicates a slight curvature, which has also been demonstrated by McDowall[38] . The most accurate calibration is obtained when a calibration standard of similar viscosity to the test solution is employed. The solvent, formamide, used in this work had a viscosity 3.3×10^{-3} J m^{-3}s at 25°C; however the viscosity of distilled water does not extend into this region. To obtain calibration points in the

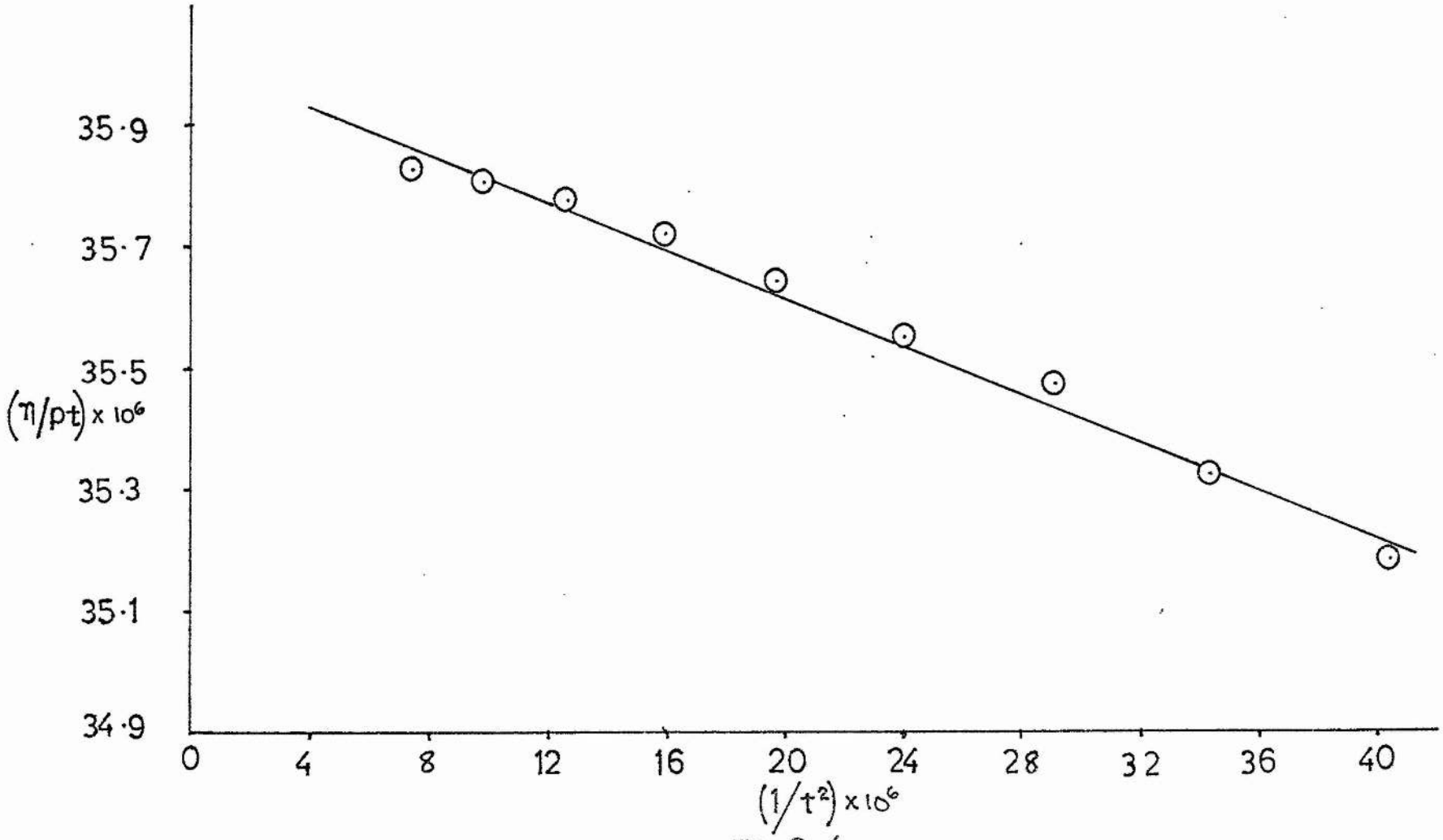
35·9
35·7
35·5
35·3
35·1
34·9
$(\eta/pt) \times 10^6$
0
4
8
12
16
20
24
28
32
36
40
$(1/t^2) \times 10^6$

FIG. 2·4

higher viscosity region, 20% and 30% aqueous sucrose solutions in the temperature region 15°C - 25°C were studied. When the efflux times for these solutions were determined and the plot of $1/t^2$ against $\eta/\rho t$ constructed, the points fell below the line indicated by the distilled water calibration fig (2.5). The efflux times for the sucrose solutions were completely repeatable and were the same for independent freshly prepared solutions. No reason could be found for the discrepancey of the two calibration liquids. The sucrose points were eliminated from the calculation and the distilled water calibration data was extrapolated to higher viscosity regions.

As the function

$$\eta / \rho t = A - B/t^2 \qquad (2.39)$$

was not linear, the mathematical function used to analyse the calibration data was a quadratic equation of the form

$$y = A + Bx + Cx^2 \qquad (2.40)$$

where $y = \eta/\rho t$ and $x = 1/t^2$.

The coefficients for equation (2.40) were determined by regression analysis and values for these coefficients are shown in table (2.1) for two typical viscometers.

TABLE 2.1

	VISCOMETER 1	VISCOMETER 2
A	3.59×10^{-5}	3.6138×10^{-5}
B	-8.64×10^{-3}	-1.236×10^{-2}
C	-2.35×10^{2}	-65.00

Table (2.2) gives the precision with which the efflux times used for the calibration were measured.

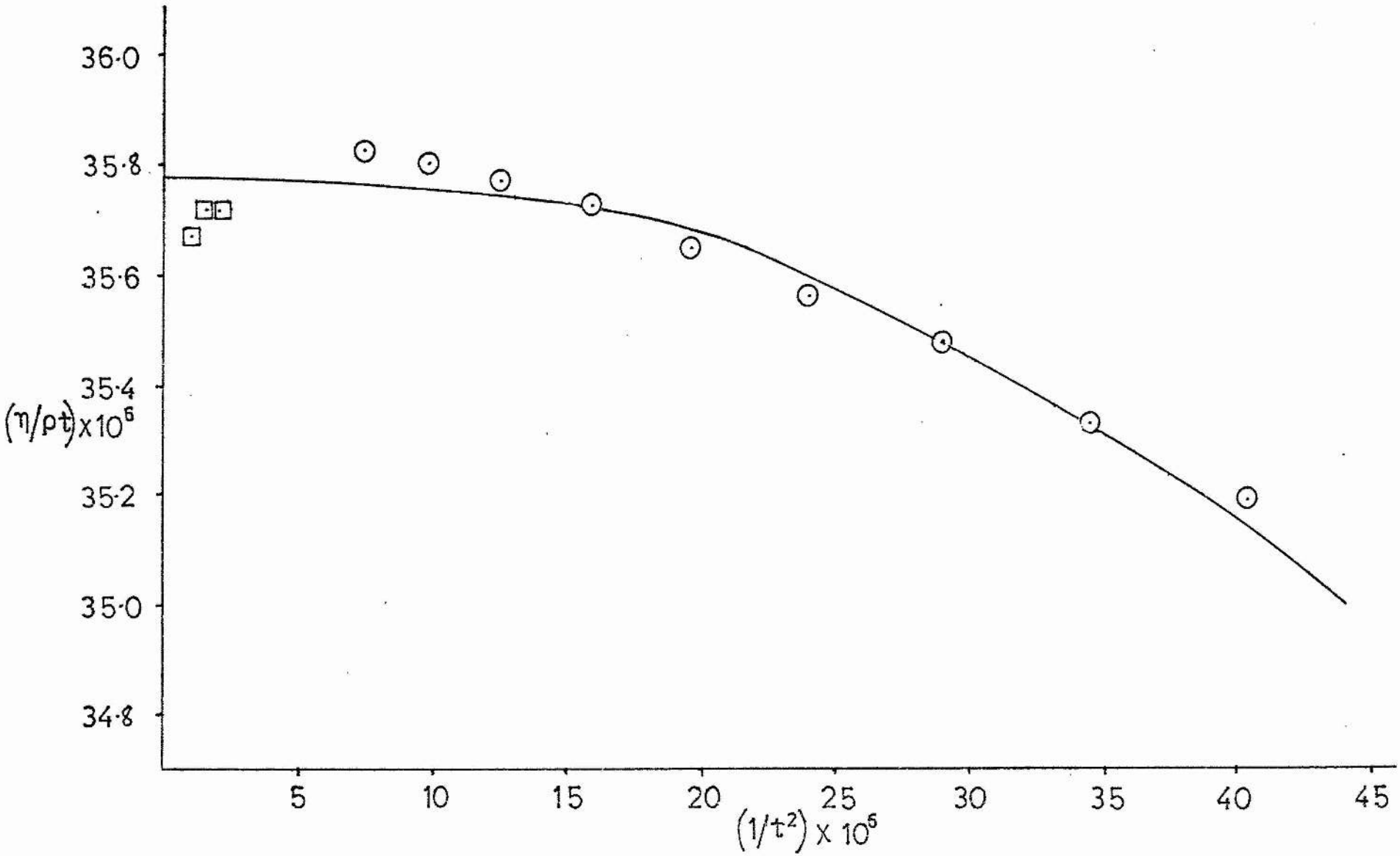
36·0
35·8
35·6
35·4
35·2
35·0
34·8
$(\eta/\rho t) \times 10^6$
5
10
15
20
25
30
35
40
45
$(1/t^2) \times 10^5$

FIG. 2.5

TABLE 2.2

STANDARD DEVIATION OF EFFLUX TIMES		
	$TIME_c$ (t)/s	$(t-\bar{t})^2$
	369.42	0.0016
	369.49	0.0009
	369.46	0.00
	369.48	0.0004
$\bar{t} = \sum t/n$	369.42	0.0016
$= 369.46s$	369.49	0.0009
	369.48	0.0004
	369.45	0.0001

where $\bar{t}$ is the mean efflux time for n measurements. Therefore $\sigma = (t-\bar{t})^2 / n-1 = 0.0008$ where σ is the standard deviation. The values for the density and viscosity of distilled water required in the calibration are given in appendix 1. Fig. (2.6) shows a typical calibration curve for an Ubbelohde Viscometer.

2.13 DENSITY MEASUREMENT

The density of the solutions was determined using Lipkin bicapillary pycnometers [39]. The pycnometers were constructed from 1 cm^3 pipettes (Pyrex 3240/20) with graduations every 0.01 cm^3 and had a capacity of approx. 30 cm^3 fig. (2.7). The pycnometers were calibrated with freshly distilled water at 2.5°C intervals from 15°C to 50°C by filling with a known weight of water and noting

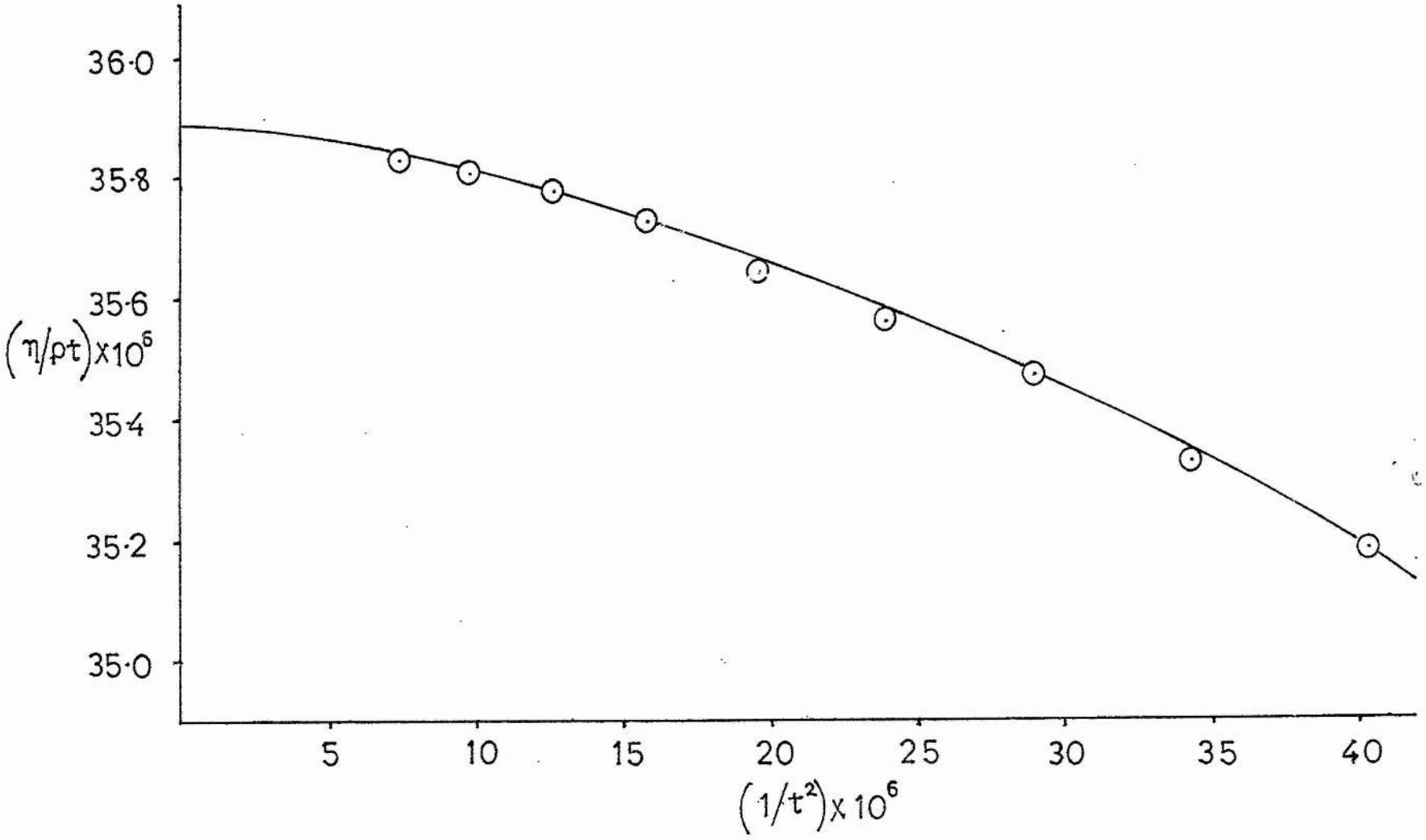
36·0
35·8
35·6
35·4
35·2
35·0
$(\eta/\rho t)\times10^6$
5
10
15
20
25
30
35
40
$(1/t^2)\times10^6$

FIG. 2·6

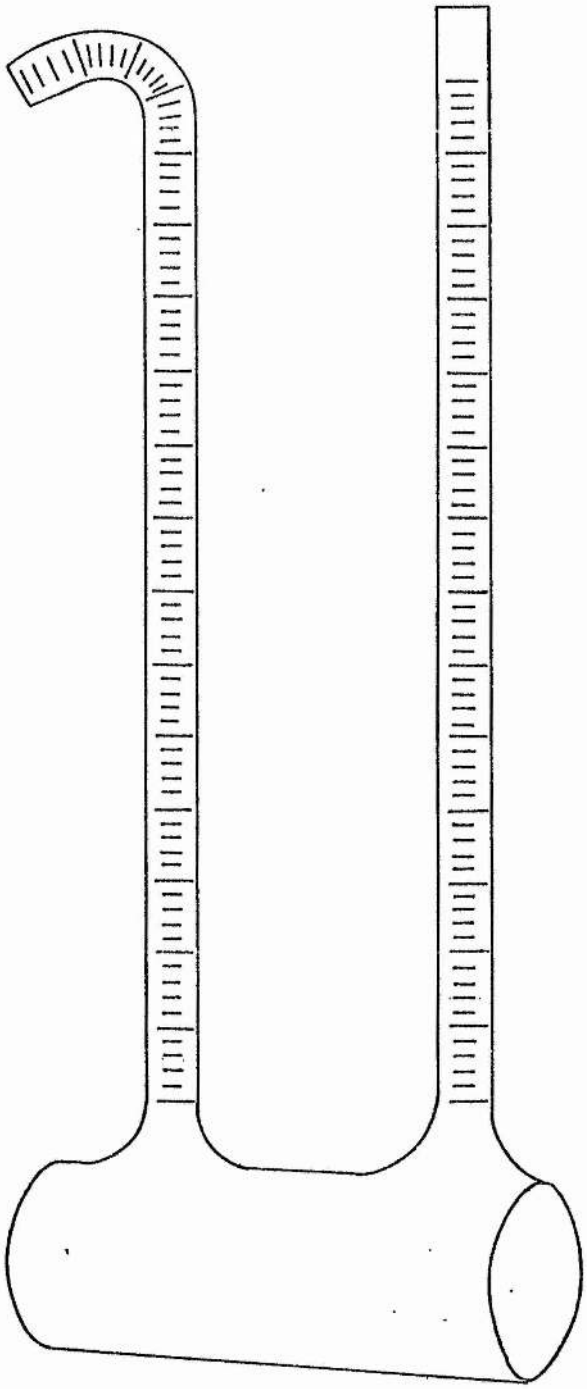

FIG. 2·7

the limb reading at those temperatures. From the known density of water at the chosen temperatures a calibration graph of volume against total limb readings was constructed. This relationship was linear for all pycnometers used. The data was then analysed by a least squares programme and the calibration constants for each pycnometer were computed. The left hand limb of each pycnometer was bent through an angle of approximately 140^{o} to allow self-filling by syphoning. The limb readings were observed using a cathetometer. One of the calibration points near the top of the limb was taken as the standard point and the difference between the height of the solution in the limb, and the standard point was taken as the limb reading. The cathetometer permitted a reading accuracy of $\pm$ 0.002 cm^3 in 30 cm^3 of solution. Since the weighing was more accurate than this, the accuracy of the density measurements was therefore considered to be 0.01%.

The procedure adopted for the density measurements, was to wash out the pycnometer three times with distilled water and then three times with Analar acetone. The pycnometer was then flushed with a stream of dust free dry nitrogen and weighed. Care was taken when weighing the pycnometers to avoid contact with the skin. The pycnometer was then filled with the test solution by capillary action and any liquid which lodged in the top of the left hand limb was removed and the pycnometer reweighed. It was then clamped firmly in position in the water with the limbs vertical so that the latter could be observed through the glass front of the bath. The cathetometer was then set up and correctly levelled. When determining the density at

different temperatures, in all cases, the level of the meniscus was found to be steady after five minutes equilibration.

2.14 PREPARATION OF SOLVENT

FORMAMIDE

Formamide is a particularly difficult solvent to work with. It is thermally unstable, photosensitive and hygroscopic.

The most common method used for the purification of formamide is fractional crystallisation [40]. This method however is very wasteful and inconvenient for the preparation of large quantities.

The major impurities in commercial formamide are water and dissolved ions. A purification method proposed by Notley and Spiro[41] involving the use of ion exchange resins and molecular sieves yields formamide with the lowest recorded specific conductance ($2 \times 10^{-7} S\ m^{-1}$). This method of purification proved impractical for viscosity studies since formamide prepared in this manner yielded spurious efflux times. These were considered to be due to dust particles, from the molecular sieves, lodging in the viscometer capillaries despite filtration of the solvent.

The method adopted for the purification of formamide was repeated fractional distillation of the solvent under reduced pressure. The still used, was equipped with ground glass joints throughout (it was necessary to lubricate these joints with formamide to ensure a good vacuum) and had a vertical fractionating column, 0.025 m broad and packed with glass helices (Fenske rings) to a height of 0.5 m. A pressure of

less than 100 N m^{-2} was obtained using a rotary oil pump and a liquid nitrogen trap. The solvent formamide (reagent grade Hopkin and Williams) was neutralised, if necessary, by the addition of dilute aqueous sodium hydroxide solution to a bromothymol blue end point. The neutral liquid was heated to 65°C - 75°C under reduced pressure, the ammonia and water pumped off, and the formamide again neutralised. This procedure was repeated until the liquid remained neutral when distillation began. The solvent was then distilled repeatedly at pressures of less than 100 N m^{-2}. Only the middle fraction of the solvent distilling between 65°C and 70°C was collected. This procedure yielded formamide with a water content 0.025% as determined by Karl Fischer[42] titration, and specific conductance 2.50 x 10^{-4}S m^{-1}.

Due to the difficulty of keeping formamide in a high state of purity, the material was used as soon as possible after purification. When formamide was not used within seven days of preparation, it was redistilled before use. Formamide and all formamide solutions were stored in a cold room in the dark in ground glass stoppered flasks and sealed to the atmosphere with a paraffin film.

2.15 METHANOL

Solvent grade methanol was dried by the method of Lund and Bjerrum using a Grignard type reaction[43]. 20 g of magnesium turnings 0.1 g iodine and 50 cm^3 methanol were allowed to react in a dry flask. When the reaction subsided, 1 dm^3 of methanol was added, and the solution refluxed for two hours. The anhydrous methanol was then

distilled at atmospheric pressure, using a similar still to that described above, into a dry flask protected from atmospheric moisture. Methanol prepared in this manner was found to have a water content of 0.02% as determined by Karl Fischer titration.

2.16 ETHANOL

Solvent grade ethanol was distilled with 5% benzene to remove water present [44]. The benzene-ethanol solution formed a ternary azeotrope of benzene-ethanol-water, which distilled over at 64.5°C. A fractionating column similar to that used for formamide was employed to redistill the dry ethanol. The middle fraction distilling at 78°C was collected. The sample prepared thus, had a water content of 0.015%.

2.17 PROPAN-1-OL AND BUTAN-1-OL

Reagent grade samples (Fisons Ltd.) were twice fractionally distilled through a 1 metre column packed with glass helices according to the method of Mathews and McKetta[45]. The distillations were carried out at reduced pressure and gave final products with a boiling range of less than 0.02°C.

All the alcohols were stored in ground glass stoppered flasks sealed with a paraffin film.

2.18 PREPARATION OF SALTS

LITHIUM BROMIDE

Due to the possibilities of forming some extremely stable hydrates (e.g. LiBr $2H_2O$) the reagent grade lithium

bromide was recrystallised three times from absolute alcohol. The white crystals were dried in a vacuum oven at 135°C and 100 N m^{-2} for seven days before use.

2.19 POTASSIUM CHLORIDE

Analar grade potassium chloride was used without further purification after drying at 120°C for three days.

2.20 RUBIDIUM IODIDE

Reagent grade rubidium iodide was dried at 120°C for twenty four hours and stored in vacuum over P_2O_5.

2.21 CAESIUM SALTS

Caesium chloride, caesium bromide and caesium iodide were each recrystallised twice from freshly distilled water. The salts were then dried at 140°C in a nitrogen atmosphere and stored in vacuum over P_2O_5.

2.22 THALLOUS SULPHATE

Reagent grade thallous sulphate was twice recrystallised from boiling freshly distilled water. The needle-like white crystals were then dried in vacuum over P_2O_5.

2.23 THALLOUS HYDROXIDE

Solutions of thallous hydroxide were prepared by precipitation of barium sulphate from solutions of thallous sulphate and carbonate free barium hydroxide at 100°C. Since aqueous solutions of thallous hydroxide were required, no attempt was made to isolate solid thallous

hydroxide or its hydrate. The concentration of the stock solutions (0.3 mol dm^{-3}) of thallous hydroxide prepared in this manner were accurately determined by potentiometric titration with standard acid. More concentrated solutions of thallous hydroxide were prepared, but these tended to produce yellow insoluble crystals of thallous hydroxide monohydrate TlOH. H_2O. Other concentrations of thallous hydroxide solutions were prepared by dilution of the stock solutions by weight.

2.24 THALLOUS NITRATE

Thallous nitrate was prepared by precipitation from thallous hydroxide solution with concentrated nitric acid. The white thallous nitrate crystals were washed with small volumes of ice-cold distilled water and dried in vacuum over P_2O_5.

2.25 TETRABUTYLAMMONIUM IODIDE & TETRAPENTYLAMMONIUM IODIDE

Both salts were used as received without further purification or drying. Attempts at drying in vacuum, or over dessicants produced a brown discolouration on the surface of the materials. The salts showed the same discolouration when they were dried at 120°C in an oven at atmospheric pressure. Test samples when left exposed to the laboratory atmosphere remained white for a much longer time than the treated samples. No reference could be found in the literature to explain these effects. A possible reason for the discolouration was considered to be some photochemical reaction on the surface of the salts, with this reaction inhibited by atmospheric moisture.

Microanalysis of the salts as received showed them to be extremely pure and dry. The salts were therefore used without further treatment.

CHAPTER THREE

VISCOSITY OF ELECTROLYTE SOLUTIONS

3.1 INTRODUCTION

In 1847, Poiseuille[46] showed that some salts increased the viscosity of water, whereas others decreased it. Arrhenius[47] made some viscosity measurements on solutions and found that the change in viscosity caused by addition of a salt was roughly proportional to the concentrations at low molarities, but increased more rapidly than the concentrations at moderate molarities. He proposed the relationship

$$\eta_R = A^c \qquad (3.1)$$

where η_R is the relative viscosity of the solution equal to the viscosity of the solution divided by the viscosity of the solvent, c is the concentration of the solution and A is a constant for any given salt and temperature.

At the beginning of this century, Grüneisen[48] measured the viscosities of electrolyte solutions down to a very low concentration and found that, in dilute solutions the viscosities were not linear with concentrations but showed a characteristic curvature. This curvature was always negative i.e. the viscosity increased irrespective of whether or not at higher concentrations, the salt increased or decreased the relative viscosities.

In 1906, Einstein[49] deduced theoretically that, if the solute could be regarded as being composed of spherical incompressible uncharged particles, which were large in comparison to the solvent molecules, the relative viscosity of the solution would be given by

$$\eta_R = 1 + 2.5\varphi \qquad (3.2)$$

where φ is the total volume of the solute particles per unit volume of the solution. This equation implied a linear relationship between viscosity and concentration.

3.2 JONES - DOLE EQUATION

In 1929, Jones and Dole[17] measured the viscosities of dilute barium chloride solutions with great precision. By plotting $\frac{\eta-1}{c}$ against c they showed that the Grüneisen effect was magnified at concentrations of 0.005 mol dm^{-3}. It was then evident that although the principle effect of dissolved salts on viscosity or fluidity was proportional to the concentration, there was some other effect which was of relatively greater importance in dilute solutions, which was responsible for the curvature found at lower concentrations. At about the same time, the interionic attraction theory of Debye and Hückel was a focus of theoretical interest.[5] This theory showed that the effect of the interionic forces in opposing the motion of ions in an electric field was proportional to the square root of the concentrations in very dilute solutions. Jones and Dole therefore, without attempting a rigorous justification postulated equation (3.3) to explain their results

$$\phi_R = 1 + Ac^{\frac{1}{2}} + Bc \qquad (3.3)$$

where ϕ_R is the relative fluidity equal to $1/\eta_R$, c is the molar concentration of the solution, A is a constant which is negative for all electrolytes but zero for non-electrolytes and B is a constant which could either be positive or negative depending on the salt used.

Jones and Tally[34] later pointed out that for salts that diminish the viscosity of water a more suitable equation was

$$\eta_R = 1 + Ac^{\frac{1}{2}} \pm Bc \qquad (3.4)$$

where η_R is the relative viscosity of the solution, A has the same meaning as in equation (3.3) with reversed sign and B is identical in value within experimental error to B in equation (3.3), but also with reversed sign. Equation (3.3) and (3.4) are substantially equivalent for dilute solutions. This can be seen by taking the reciprocal of both sides of equation (3.3) and considering the magnitude of the terms:

$$1/\phi_R = 1/(1 + A\ c^{1/2} + Bc) \qquad (3.5)$$

Also $$\eta_R = 1/\phi_R \qquad (3.6)$$

$$\therefore \quad \eta_R = \frac{1 - A\ c^{1/2} - Bc}{(1 + A\ c + Bc)(1 - A\ c - Bc)} \qquad (3.7)$$

$$= \frac{1 - A\ c^{1/2} - Bc}{1 - A^2c - 2ABc^{3/2} - B^2c^2} \qquad (3.8)$$

For LiBr in formamide at 25°C A = 0.0068 $dm^{3/2}\ mol^{-\frac{1}{2}}$ by calculation and B = 0.436 $dm^3\ mol^{-1}$ by experiment (see chapter IV). Calculation of the terms in equation (3.8) assuming a maximum concentration of 0.1 mol dm^{-3} gives

$$1 - A^2c - 2ABc^{3/2} - B^2c^2$$

$$= 1 - 4.6 \times 10^{-6} - 1.87 \times 10^{-4} - 1.9 \times 10^{-3}$$

$$= 0.9979$$

The denominator is 0.2% too small. However the B value is not generally measured to better than 1% therefore the equivalence of the parameters in (3.3) and (3.4) is within experimental error up to this concentration.

3.3 THE A PARAMETER IN THE JONES - DOLE EQUATION

The experimentally determined $Ac^{\frac{1}{2}}$ term in the Jones - Dole equation which becomes predominant at low concentrations is consistent with that calculated on the basis of the Debye - Hückel theory. On the basis of this theory, the simultaneous effects of the electrostatic attraction and repulsion and thermal motion is to surround each ion by an excess of ions of opposite charge. fig (3.1a)

The ionic atmosphere surrounding each ion and having an opposite charge from that under consideration, is on a statistical average spherically symmetrical. The resultant force acting on the ion in the middle of the ionic atmosphere is therefore zero. When a linear velocity gradient is imposed on such a solution, as in a capillary viscosity measurement, these ionic atmospheres will be distorted from their symmetrical distribution by the associated shearing forces. Interionic attraction and thermal movements will tend to restore the equilibrium distribution and since there is a finite time of relaxation for this process, an ellipsoidal distribution results and persists. fig. (3.1b)

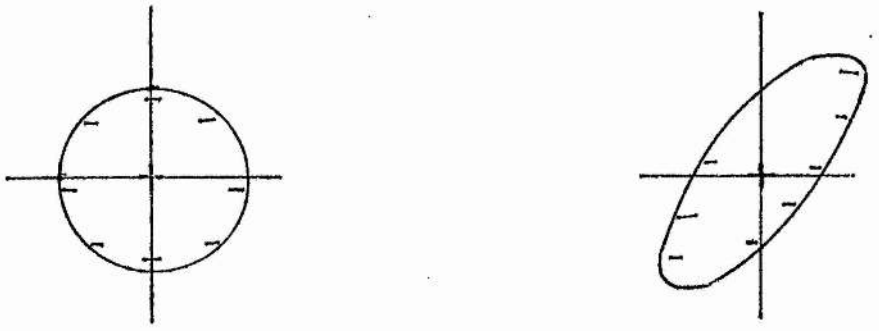

FIG. 3·1

This restoring force will act against the flow and therefore increase the viscosity. The A- coefficient is thus taken as a measure of the ion-ion interactions in solution. On the basis of the Debye - Hückel theory, Falkenhagen and Vernon[50] have shown that the A- coefficient can be calculated from the expression

$$A = \frac{1.461}{\eta_0 \varepsilon^{1/2} T^{1/2}} \frac{(\nu_1 z_1)^{1/2}}{(z_1 + z_2)^{1/2}} \left[\frac{1}{4} \frac{\lambda_1^\circ z_2^2 + \lambda_2^\circ z_1^2}{\lambda_1^\circ \lambda_2^\circ} - K \right] \times 10^{-5} \; dm^{3/2} \; mol^{-1/2} \qquad (3.9)$$

And

$$K = \frac{(\lambda_1^\circ z_2 - \lambda_2^\circ z_1)^2}{\lambda_1^\circ \lambda_2^\circ \left\{ (\lambda_1^\circ + \lambda_2^\circ)^{1/2} + (\lambda_1^\circ z_2 + \lambda_2^\circ z_1)^{1/2} \left[\frac{z_1 + z_2}{z_1 z_2} \right]^{1/2} \right\}^2}$$

where λ°_1 and λ°_2 are the limiting ionic equivalent conductances of the cation and anion respectively in S $m^2 mol^{-1}$, z_1 and z_2 are the valence of the ions, ν_1 is the number of types of ions formed from a molecule, η_0 is the viscosity of the solvent in J m^{-3} s, ε is the absolute permittivity of the solvent in F m^{-1} and T is the absolute temperature. For binary electrolytes equation (3.9) reduces to[51]

$$A = \frac{0.2583 (\lambda_1^\circ + \lambda_2^\circ)}{\eta_0 (\varepsilon T)^{1/2} \lambda_1^\circ \lambda_2^\circ} \left[1 - 0.6863 \left(\frac{\lambda_1^\circ - \lambda_2^\circ}{\lambda_1^\circ + \lambda_2^\circ} \right)^2 \right] \times 10^{-5} \; dm^{3/2} \; mol^{-1/2} \qquad (3.10)$$

A- coefficients calculated by these equations show excellent agreement with experimental values for both aqueous and non-aqueous solution. Theoretically only positive A values are meaningful. Kaminsky[52] has verified experimentally that the temperature coefficient of A, $\partial A / \partial T$, is positive and most A values determined experimentally are positive in agreement with theory. Attempts to extend the range of this derivation including ion size parameters e.g. Pitts[53] have not significantly improved agreement with experiment. Davies and Malpass[54] however, have argued that the limiting Falkenhagen-

- Vernon expression incorrectly describes the ion-ion interactions at higher concentrations and have empirically extended this equation. They have used

$$\left(\eta/\eta_0 - 1\right) - A^1 F(I) = Bc \qquad (3.11)$$

where F (I) is a function of the ionic strength taken as $I^{\frac{1}{2}} / (1 + I^{\frac{1}{2}}) - 0.2I$ and A^1 is the theoretically calculated value of the Falkenhagen coefficient restated in terms of ionic strength. The result of this modified Jones - Dole equation is to make B- coefficient values more positive although the effect is rather small for 1 : 1 electrolytes. In common with most other workers it was decided in this project, to retain the simple $Ac^{\frac{1}{2}}$ term and accept that the resulting B- coefficients contain a small contribution due to the ion-ion effects which are linear functions of concentration.

3.4 THE JONES - DOLE B- COEFFICIENT

Above a concentration of about 0.002 mol dm^{-3} the $Ac^{\frac{1}{2}}$ term is swamped by the concentration of the Bc term. The Jones - Dole B- coefficient may be either positive or negative. A positive B value indicates that the salt present in the solution increases the viscosity of the pure solvent, while a negative B value shows that the salt decreases the viscosity of the solvent. Negative B- coefficients are normally confined to highly associated solvents such as water and glycerol. The B- coefficient is therefore related to the structural disturbance of the solvent due to the presence of the ion. The generally accepted viewpoint is that the B- coefficient is a measure of the ion-solvent interactions. It is related to the size of the solvated

ion, the amount of long range orientation of solvent molecules caused by the electric field of the ion and the structural decomposition of the solvent arising from peculiar centrosymmetric solvent molecular orientations in the ionic co-spheres.

Gurney[55] used the term"ionic co-spheres" to refer to the region of solvent immediately surrounding the ion and somewhat modified by the presence of the ion. Each ion is encompassed in its own co-sphere and the remainder of the solvent between the ions is unaffected by the ions. He considered that the B- coefficients represent the contributions of the ionic co-spheres to the viscosity, and that in dilute solutions the contributions from the positive and negative ions would be independent and therefore additive. This was shown from the fact that the differences in B values of cations with a common anion, or anions with a common cation were constant. With suitable assumptions B ion values have been determined (Chapter IV) and most correlations with other solution properties are made in terms of ionic B- coefficients.

Kaminsky[52] has correlated the effect of ions on solvent structures with the temperature coefficent of B i.e. $\partial B/\partial T$. He has suggested that an ion with a negative $\partial B/\partial T$ is a structure maker, and an ion with a positive $\partial B/\partial T$ is a structure breaker. Structure-makers are viewed as ions which strengthen or enhance the structure of the solvent by their presence thus increasing the viscosity, while structure-breakers are viewed as ions which loosen the structure of their co-sphere and therefore lower the viscosity. A linear relationship between ionic B- coefficients

and the partial molar entropy of the ions has been demonstrated by Gurney. He also showed the striking resemblance between the temperature coefficient of mobility ($C_0^{18} = \frac{\eta^{18}\lambda^{18}}{\eta^{o}\lambda^{o}}$) against equivalent ionic conductances and C_0^{18} against ionic B- coefficients. Podolsky [3] using a lattice model, has shown that the B- coefficient of an ion is proportional to the perturbation of the activation energy accompanying transformation of a lattice particle from a solvent molecule to an ion. Further, differences in ionic mobility may be shown as exponential functions of this same perturbation i.e. the theory predicts that the logarithm of the ionic mobility will be a linear function of ionic B- coeffient.

As yet no general theory has been developed for the B- coeffficient but important qualitative explanations have been advanced in terms of ion-solvent interactions.

3.5 EXTENDED JONES - DOLE EQUATION

In 1933 it was reported [56] that for aqueous solutions of KBr and KCl having concentrations above 0.1 - 0.2 mol dm^{-3} experimental results indicated the need for the addition of a further term, proportional to the square of the concentration, to the Jones - Dole equation. On examining a number of salts in methanolic solution, Jones and Fornwalt [57] found that while equation (3.4) adequately described experimental data up to a concentration of 0.01 mol dm^{-3} , it failed badly above this value. They therefore used only the results below this concentration in the evaluation of the B- parameter. In 1957 Kaminsky [58] used an extended equation

$$\eta/\eta_o = 1 + A\ c^{1/2} + Bc + Dc^2 \qquad (3.12)$$

in order to fit the results of very precise measurements in aqueous systems at high concentrations. The fitted D- parameter was a small number compared with the corresponding value of B, and the latter was not greatly affected by the introduction of the extra term. However in a study of electrolyte solutions in N- methylformamide, Feakins and Lawrence[59] reported that the use of the extended equation (3.12) altered the derived B- values by some 0.015 or 3% from the values derived using equation (3.4). Up to 0.1 mol dm^{-3} the Dc^2 term contributed less than 3% to $(\eta/\eta_o - 1)$, but this increased to around 10% for a system studied with concentrations up to 0.4 mol dm^{-3}. Sodium iodide solutions in dimethyl sulphoxide have been studied by two groups of workers. Adolph and Siedel[33] using a maximum concentration of approximately 0.08 mol dm^{-3} fitted equation (3.12) to their data which at 25° C gave

$$(\eta/\eta_o - 1) = 0.0145c^{\frac{1}{2}} + 0.734c + 0.685c^2 \qquad (3.13)$$

for c = 0.1 mol dm^{-3}, the Dc^2 term contributed some 8% to $(\eta/\eta_o - 1)$. Recently Feakins et al.[60] have re-examined this system, and, finding no significant deviations from equation (3.4) over the range 0 - 0.08 mol dm^{-3}, evaluated their B- coefficients using the simpler equation over this restricted concentration range. They reported the viscosity concentration function at 25° C as

$$(\eta/\eta_o - 1) = 0.009c^{\frac{1}{2}} + 0.802\ c \qquad (3.14)$$

It is likely that B and D parameters will be highly interdependent and therefore that B- parameters determined

using equation (3.4) will not be directly comparable with those derived using equation (3.12). Further, the physical significance of the D- parameter is not obvious and the question arises as to its usefulness in the interpretation of solution properties. Desnoyers and Perron[61] suggested that it is a more complex parameter than the B- coefficient namely a function of the size of the ions, of structural solute-solute interactions and of higher terms of the long-range Debye -Hückel type of forces. They concluded that the D- parameter could not be used unambiguously to obtain information on ion-ion or ion-solvent interactions. A series of experimental measurements were therefore examined statistically for both aqueous and non-aqueous systems with a view to determining the best way of evaluating the B-parameter. In all cases a theoretically established value for the A- coefficient was used. This procedure has been shown to be the best method of fitting results to the Jones - Dole or extended Jones - Dole equations because of the rapid increase in experimental error on measuring relative viscosity at very low concentrations.[60]

3.6 METHOD 1

This method involved the fitting of equation (3.12) to the data in stages estimating the B and D coefficients by least squares, and then successively reducing the number of data points in the analysis by omitting the point which was currently at the highest concentration. The aim was to determine the stage at which equation (3.12) provided an adequate description of the data. For example, the results of applying this process to the data of Adolph and Siedel

for sodium iodide in dimethyl sulphoxide at 25°C are shown in table (3.1)

TABLE 3.1

N	ESTIMATE OF		ESTIMATED STANDARD ERROR OF		E_D/SE_D	R.S.S. x 10^7	
	B	D	B	D		Eq(3·12)	Eq(3.4)
7	0.754	0.550	0.0042	0.059	9.26	0.767	13.90
6	0.763	0.322	0.0048	0.104	3.10	0.314	1.069
5	0.775	-0.233	0.0090	0.379	-0.62	0.179	0.201

R.S.S. is the residual sum of squares , E_D is the estimate of D and SE_D is the estimated standard error of D.

Using as an indicator for stopping the data reduction, the criterion that the value of D was not significantly different from zero, involved comparing the ratio of the estimated value of D to its estimated standard error with the appropriate percentage point of the t- distribution. Using either the 10% or 5% point, the two highest concentrations were discarded in this case, giving a point estimate of B of 0.775 with an estimated standard error of 0.009. However the interval of $0.775 \pm (3.18 \times 0.009)$ or 0.746 - 0.803 did not necessarily provide a good 95% confidence level for B, as will be seen later. Using an alternative criterion of stopping-viz. when the reduction in the residual sum of squares obtained by adding the term in D was not significant - and applying the F-test, it was again decided to stop at the same stage of the data reduction.

Viscosity measurements on sodium sulphate at 15°C by Kaminsky[58] provided a set of extremely good data, which is analysed in table (3.2).

TABLE 3.2

N	E_B	E_D	SE_B	SE_D	E_D/SE_D	R.S.S. × 10^8	
						Eq.(3.12	Eq.(3.4
9	0.3609	0.0422	0.00033	0.0029	14.51	0.278	8.653
8	0.3604	0.0487	0.00052	0.0062	7.82	0.227	2.547
7	0.3613	0.0332	0.00055	0.0081	4.09	0.109	0.472
6	0.3605	0.0499	0.00079	0.0146	3.42	0.075	0.295
5	0.3607	0.0445	0.00103	0.0224	1.99	0.072	0.167
4	0.3573	0.2480	0.00160	0.0890	2.79	0.019	0.095

Both stopping criteria discussed above indicated a reduction to six points, which led to an estimated B- value of 0.3607 $\pm$ (2.78 x 0.00103) i.e. 0.357 - 0.364 for a 95% confidence level.

3.7 METHOD 2

This approach was a modification of Method 1 in which the coefficients B and D were highly correlated. The correlation in the three fits for the data of Adolph and Siedel[33] shown in table (3.1) were -0.959, -0.955 and -0.966, which reflected the similarity of the behaviour of c and c^2 over the range of concentration studied. It was therefore considered more informative to construct a two - dimensional confidence region for the B and D parameters jointly. Making the usual assumptions about the error term, a 95% confidence ellipse for the values of B and D is given by

$$\left\{ (B-\hat{B}) /SB\right\}^2 - 2R(B-\hat{B}) (D-\hat{D})/(SB.SD)+\left\{(D-\hat{D})/SD\right\}^2 \leqslant 2(1-R)^2_F \quad (3.15)$$

where $\hat{B}$ and $\hat{D}$ are the estimated values of B and D respectively SB and SD are their estimated standard errors, R is the coefficient of correlation between B and D, and F is the appropriate percentage point of the F distribution with 2 and $(\flat-2)$ degrees of freedom, where $\flat$ is the number of data points in the fit. For example, in the case quoted above at the five lowest concentration points, the 95% confidence is the interior of the ellipse

$$12373(B-\hat{B})^2 + 567\ (B-\hat{B})\ (D-\hat{D}) + 6.962\ (D-\hat{D})^2 = 1.277 \qquad (3.16)$$

The portion of the line D = 0 which lies inside this region is that between the roots of the quadratic equation in B :-

$$12373(B - 0.775)^2 + 132.1\ (B- 0.575) - 0.277 = 0 \qquad (3.17)$$

i.e.

$$B = 0.760 \text{ to } B = 0.780$$

Figure (3.2) shows the elliptical confidence regions obtained in this way based on 7, 6 and 5 data points. Note that when the parameters were estimated using all seven data points the ellipse did not intersect the B-axis, confirming that the term in D was required for a satisfactory fit of the data. As the number of points was reduced the ellipse became larger and its centre moved. In practise however the segment of the B- axis cut off by the ellipse was moderately stable while there was still a reasonable number of points in the fit. A practical lower limit for the number of observations is seven - five more than the number of parameters to be estimated. From figure (3.2) it is seen that the interval 0.760 to 0.780 is likely to contain the true value of B.

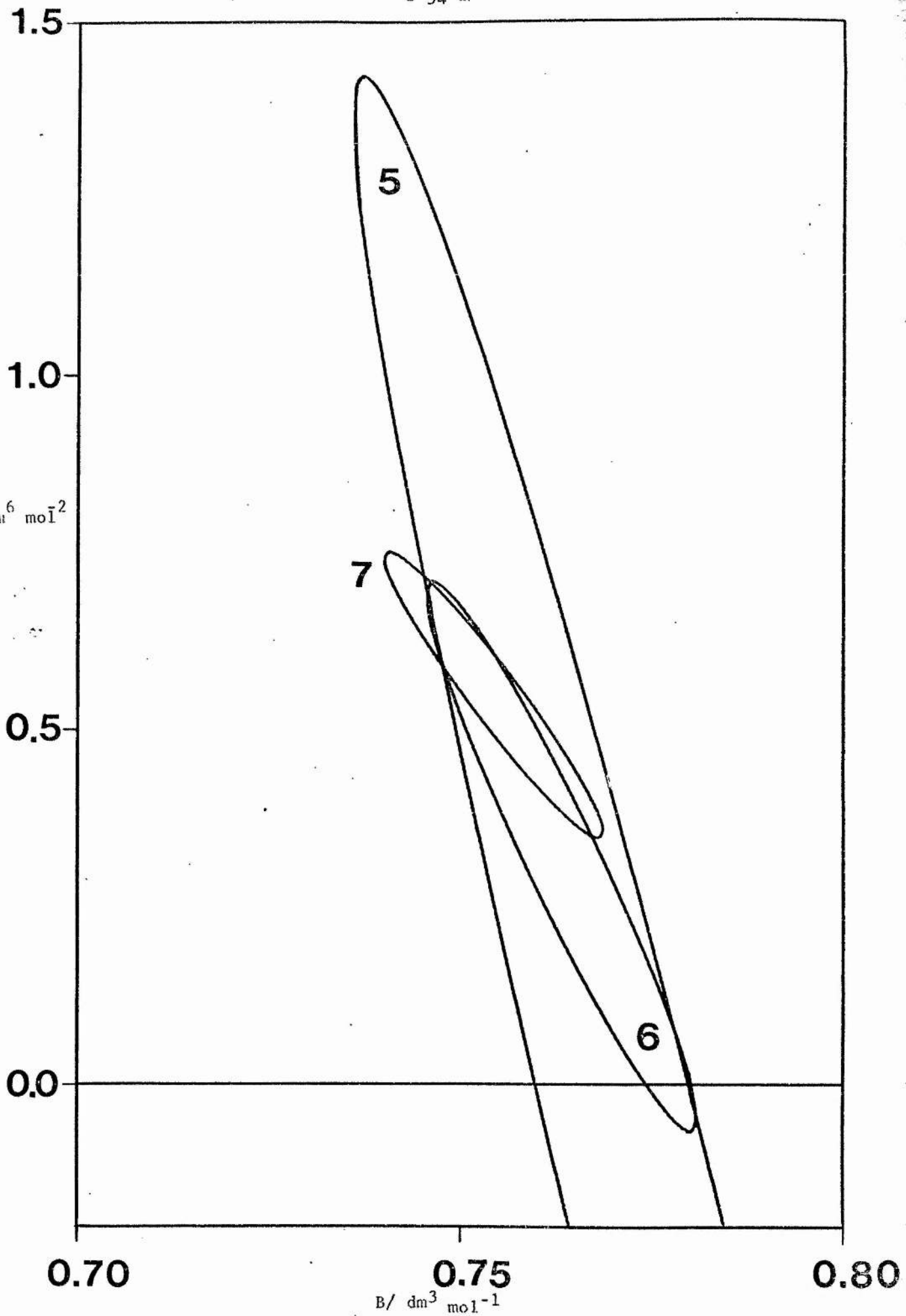

FIG. 3·2

Applying this method to the sodium sulphate data of Kaminsky led to the confidence regions shown in figure (3.3). The very large negative correlation coefficients (-0.956 - -0.977) produced long thin ellipses sloping from left to right. The portion of the B- axis cut off by the five observation ellipse was 0.3616 to 0.3638 providing a point estimate for B of 0.363. Application of method 2 to the results of measurements of sodium bromide in N-methylformamide[59] at 35°C is illustrated in figure (3.4)

3.8 METHOD 3

In this method a different approach was used. In order to avoid the problem of correlation between the estimates for B and D, equation (3.12) was reformulated as

$$(\eta/\eta_0 - 1) = Ac^{\frac{1}{2}} + Bc + PQ(c) \qquad (3.18)$$

where Q (c) was a second degree polynomial in $c^{\frac{1}{2}}$ and whose coefficients β and γ were chosen so as to make Q(c) orthogonal to $c^{\frac{1}{2}}$ and c over the range of concentration values, c_i, involved in the fit:-

$$Q(c) = \beta c^{\frac{1}{2}} + \gamma c + c^2 \qquad (3.19)$$

Now $$\sum_i c_i^{\frac{1}{2}} Q(c_i) = 0, \text{ and } \sum_i c_i Q(c_i) = 0 \qquad (3.20)$$

And Thus

$$\beta = \left(\sum_i c_i^{3/2} \sum_i c_i^3 - \sum_i c_i^2 \sum_i c_i^{5/2}\right) \Big/ \left\{\sum_i c_i \sum_i c_i^2 - \left(\sum_i c_i^{3/2}\right)^2\right\} \qquad (3.21)$$

And

$$\gamma = \left(\sum_i c_i^{3/2} \sum_i c_i^{5/2} - \sum_i c_i \sum_i c_i^3\right) \Big/ \left\{\sum_i c_i \sum_i c_i^2 - \left(\sum_i c_i^{3/2}\right)^2\right\} \qquad (3.22)$$

where the summation is over these values of i which correspond to the observations being used in the fit at any stage.

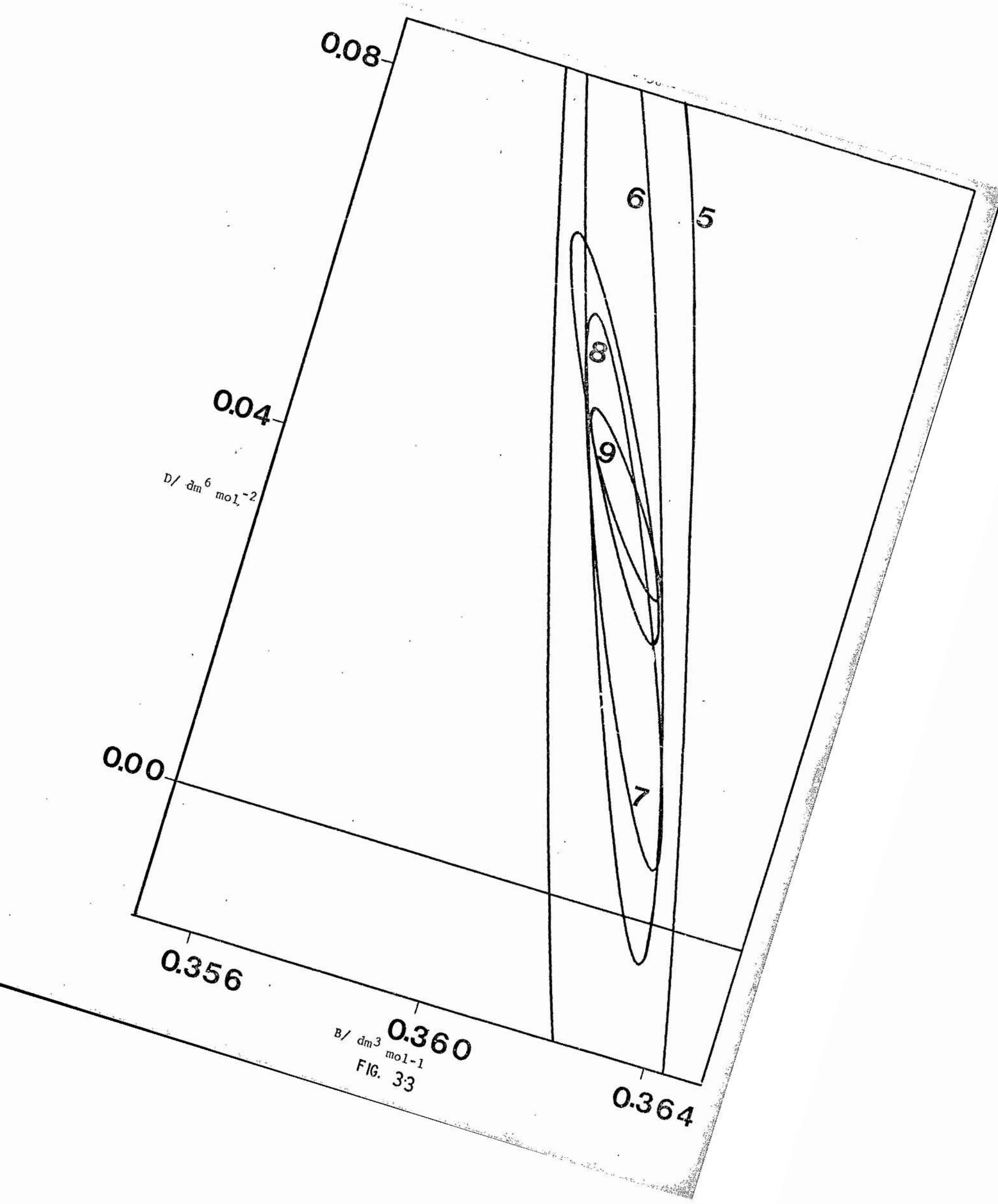

FIG. 33

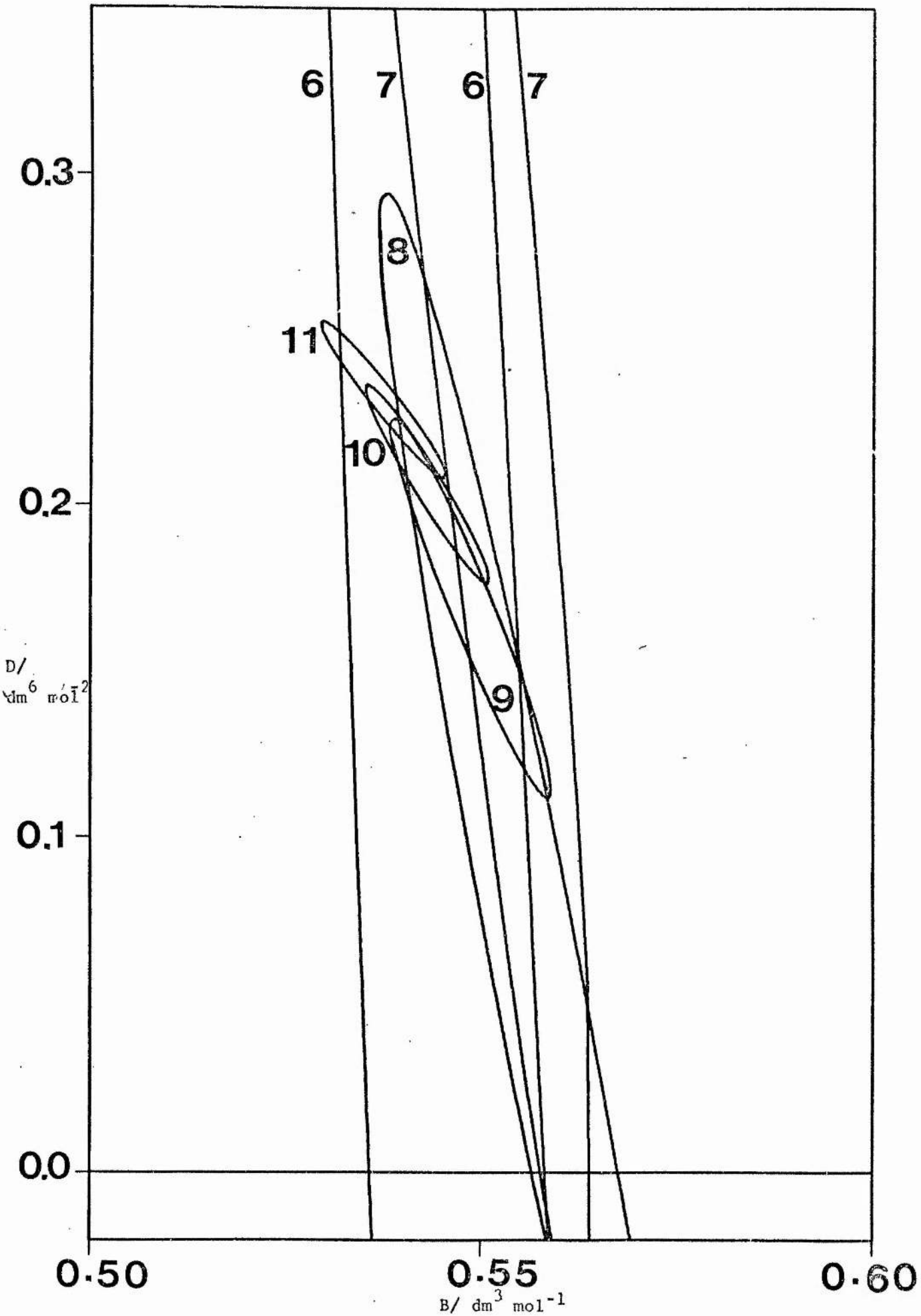

FIG. 3·4

For example, Table (3.3) shows the values of Q (c) for the data of Feakins and Lawrence[59] discussed above, first for all eleven observations and then for the data reduced by the highest and by the two highest concentrations. When the coefficients B and P were fitted their estimated values were uncorrelated because the variance matrix of the estimated values was $\sigma^2 (X^TX)^{-1}$ and it had been ensured that X^TX had zero entries at all points of the diagonal and consequently so did $(X^TX)^{-1}$

[X is the matrix $\begin{pmatrix} \sum_i c_i^2 & \sum_i c_i Q(c_i) \\ \sum_i c_i Q(c_i) & \sum_i Q(c_i)^2 \end{pmatrix}$]

Since the coefficients β and γ changed from stage to stage of the data reduction, the coefficient P was estimating a different quantity each time and was of little interest.

TABLE 3.3

i	c_i	$Q_{11}(c_i)$	$Q_{10}(c_i)$	$Q_9(c_i)$
1	0.000622	0.002916	0.001903	0.001015
2	0.002471	0.005116	0.003257	0.001662
3	0.004759	0.006358	0.003951	0.001925
4	0.008303	0.007289	0.004371	0.001983
5	0.01183	0.007667	0.004433	0.001855
6	0.02366	0.007262	0.003587	0.000927
7	0.05013	0.003344	0.000029	-0.001612
8	0.09652	-0.004868	-0.005973	-0.004414
9	0.2004	-0.015160	-0.008803	0.002159
10	0.3041	-0.008225	0.007028	-
11	0.3954	0.013840	-	-

Table (3.4) shows the estimates of B together with their standard errors and 95% confidence intervals. It is seen that the latter are ambiguous in their description of B since the fit was at first very poor but became reasonable when the number of observations was reduced to eight. Moreover the point estimate of B at first moved rapidly and systematically with the reduction in observations. The width of the confidence interval is a function both of the number of points and the standard error of the estimated values of B.

TABLE 3.4

No. of points	Estimate of B	Estimated standard error of B	95% confidence interval for B	R.S.S. $\times 10^6$ Eq.(3.18)
11	0.614	0.0051	0.602-0.625	69.92
10	0.596	0.0041	0.586-0.605	19.20
9	0.578	0.0029	0.562-0.593	3.051
8	0.562	0.0018	0.558-0.566	0.258
7	0.561	0.0034	0.552-0.570	0.192
6	0.547	0.0015	0.543-0.551	0.074
5	0.556	0.0054	0.539-0.573	0.021
4	0.552	0.0092	0.512-0.591	0.017

Figure 3.5 shows how it decreased as the point estimate settled down and then increased again. The interval corresponding to fitting the eight lowest concentrations is in the narrow range 0.558-0.566. However a more reliable interval contains these values which are common to the 6, 7 and 8 point intervals, viz. 0.543 - 0.570.

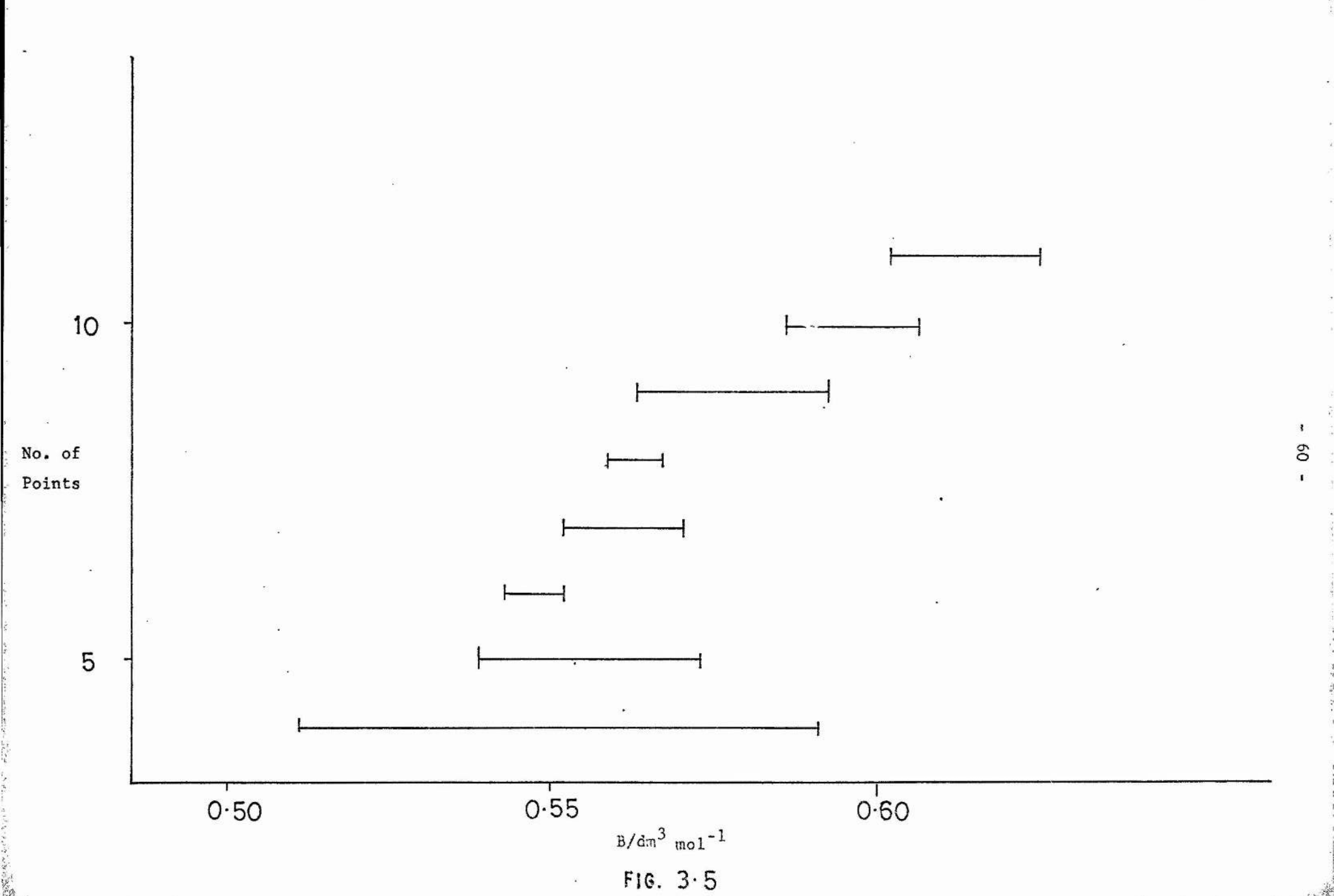

FIG. 3·5

3.9 COMPARISON OF METHODS 1,2 and 3

A comparison of the results obtained using Methods 1,2 and 3 of data analysis on the three sets of experimental observations above is given in Table (3.5).

TABLE 3.5

Data source	Method 1	
	Point	Interval
Adolph and Siedel (ref.33)	0.775	0.746 - 0.803
Kaminsky (ref.58)	0.361	0.357 - 0.364
Feakins and Lawrence (ref.59)	0.557	0.541 - 0.572

Data Source	Method 2	
	Point	Interval
Adolph and Siedel (ref. 33)	0.770	0.760 - 0.780
Kaminsky (ref. 58)	0.363	0.362 - 0.364
Feakins and Lawrence (ref.59)	0.563	0.558 - 0.568

Data Source	Method 3	
	Point	Interval
Adolph and Siedel (ref. 33)	0.770	0.765 - 0.775
Kaminsky (ref. 58)	0.363(5)	0.363 - 0.364
Feakins and Lawrence (ref. 59)	0.562	0.558 - 0.566

Method 1 while simplest both in concept and in calculation, is unlikely to provide good values for B since it does not allow for the correlation between estimated values of B and D. Method 2, takes account of this correlation and produces a narrower range of B values. While it is not necessary to draw the ellipses in order to find where they cut the B- axis, the confidence region diagram is useful for inspecting the consistency of the reduced sets of data in estimating B. Method 3, gives apparently more precise estimates at certain stages of data reduction, however a more conservative estimate is made by choosing values of B common to several confidence intervals. From table (3.5) it may be noted that the results obtained by methods 2 and 3 are comparable both for point and interval estimates whether the observations exhibit a greater degree of accuracy (as in the aqueous data studied) or a lesser degree (as in the non-aqueous systems).

3.10 INCOMPLETELY DISSOCIATED ELECTROLYTES

Davies and Malpass[54] have reported the effect of ion association on the viscosity of dilute electrolyte solutions. However, the salts studied had very low stability constants and it was therefore decided to investigate salts with a sufficient proportion of associated species to make possible the interpretation of viscosity changes due to their presence. As the thallous ion in aqueous solution is known to associate to a considerable extent with a number of anions in the concentration range suitable for viscosity studies, a number of thallous solutions were investigated.

3.11 EXPERIMENTAL RESULTS

Relative viscosities of thallous nitrate, sulphate and hydroxide solutions were determined at 25° C and are shown in table (3.6). The experimental data for these systems are compiled in Appendix II. The range of concentrations which could be studied was restricted by solubility limitations to approximately 0.1 mol dm^{-3} for the first two salts and 0.3 mol dm^{-3} for TlOH. A 0.5 mol dm^{-3} solution of this last compound was also studied by carrying out the measurements immediately after the solution had been prepared. The mean standard error of the relative viscosities was 3.0×10^{-4}.

TABLE 3.6

c/mol dm^{-3}	α	η/η_o	$(\eta/\eta_o)_{calc.}$
		THALLOUS NITRATE	
0.02011	0.9645	0.99945	0.99949
0.03381	0.9435	0.00880	0.99887
0.04037	0.9341	0.99866	0.99856
0.06364	0.9038	0.99721	0.99745
0.07895	0.8860	0.99705	0.99671
0.10121	0.8623	0.99550	0.99562
		THALLOUS SULPHATE	
0.02038	0.6116	1.00595	1.00566
0.02984	0.5377	1.00821	1.00775
0.04002	0.4807	1.00987	1.00992
0.04914	0.4415	1.01133	1.01182
0.05975	0.4053	1.01343	1.01400
0.06649	0.3860	1.01524	1.01538

THALLOUS SULPHATE(Cont'd)

c/mol dm^{-3}	α	η/η_o	$(\eta/\eta_o)_{calc.}$
0.07702	0.3602	1.01822	1.01751
0.08581	0.3419	1.01922	1.01927
	THALLOUS HYDROXIDE		
0.02129	0.9457	1.00293	1.00289
0.03385	0.9193	1.00453	1.00445
0.03926	0.9088	1.00528	1.00513
0.05466	0.8815	1.00695	1.00702
0.06816	0.8600	1.00851	1.00867
0.13528	0.7769	1.01688	1.01683
0.19409	0.7240	1.02255	-
0.25998	0.6778	1.02938	-
0.52059	0.5614	1.05467	-

3.12 THALLOUS NITRATE

In the first interpretation, the salt was considered to be completely dissociated and the simple Jones - Dole equation was applied. The A- parameter of $TlNO_3$ was calculated to be 0.0052 dm$^{3/2}$mol$^{-\frac{1}{2}}$. Fitting the experimental data gave a B- coefficient of -0.060 dm^3 mol^{-1} and a standard deviation between experimental and calculated relative viscosities of 2.3×10^{-4}. While this salt was the most dissociated of the materials investigated it was only 86% dissociated at the highest concentration used.

Allowance was therefore made for ion pairing by using the equation

$$(\eta/\eta_o - 1) = A(\alpha c)^{\frac{1}{2}} + B_1 \alpha c + B_2 (1-\alpha)c \quad (3.23)$$

where the degree of dissociation is given by

$$\alpha = -K + (K^2 + 4K\gamma_{\pm}^2 \, c)^{\frac{1}{2}} / (2 \gamma_{\pm}^2 c) \qquad (3.24)$$

K is the dissociation constant of the ion pair, $\gamma_{\pm}$ is the mean ionic activity coefficient given by the Davies equation

$$- \log_{10} \gamma_{\pm} = 0.509 \left[I^{\frac{1}{2}} / (1 + I^{\frac{1}{2}}) - 0.3I \right] \qquad (3.25)$$

and I is the ionic strength of the solution expressed in mol dm^{-3}, equal in this instance to αc. The degree of dissociation was found by successive approximations, and the two parameters B_1, the viscosity coefficient of the fully dissociated salt, and B_2, the corresponding value for the ion pair $TlNO_3$ were then determined. Using this treatment the standard deviation dropped slightly compared with that of the simpler model. Values of the dissociation constant of $TlNO_3$ range from 0.3 to 0.6.[62] Using a value of 0.465,[63] B_1 was found to have a value of -0.062 dm^3 mol^{-1} while B_2 was -0.034 dm^3 mol^{-1}. To determine the sensitivity of these parameters to the value of the dissociation constant, the calculation was repeated using K_{diss} values ranging from 0.316 to 0.55. B_1 did not vary from -0.062 dm^3 mol^{-1} while B_2 varied from -0.039 to -0.031 dm^3 mol^{-1}.

3.13 THALLOUS SULPHATE

The experimental results were treated in a similar way to those of $TlNO_3$. The additional complication of the charge on the $TlSO_4^-$ ion pair was overcome by considering the solution to be a mixture of $Tl^+(TlSO_4^-)$ and $Tl_2^+SO_4^{2-}$.[54] The mixture rule was then used to determine the ion-ion interactions: i.e. the usual $Ac^{\frac{1}{2}}$ term was replaced by[64]

$$A_1 \quad (1-\alpha c)^{\frac{1}{2}} + A_2 \quad (\alpha c)^{\frac{1}{2}}$$

where A_1 refers to $Tl^+(TlSO_4^-)$ and A_2 refers to $Tl_2^+SO_4^{2-}$. Calculation of A_1 required a knowledge of the ionic equivalent conductance of the $TlSO_4^-$ ion pairs. A value of 0.0045 S m^2 mol^{-1} was taken,[65] giving A_1 = 0.0065 $dm^{3/2} mol^{-\frac{1}{2}}$. A_2 was found to be 0.0132 $dm^{3/2} mol^{-\frac{1}{2}}$.

For this salt,

$$\alpha = \left\{-(K+c\gamma_\pm)+\left[(K+c\gamma_\pm)^2+4Kc\gamma_\pm\right]^{\frac{1}{2}}\right\} \Big/ 2c\gamma_\pm \quad (3.26)$$

and $I = (1 + 2\alpha)c$. Thallous sulphate is considerably more associated than thallous nitrate. Published values of the equilibrium constant for ion pair formation are in good agreement[11] and a value of K_{diss} = 0.043 as determined by Bell and George[66] was taken. By fitting the experimental data to the extended Jones-Dole equation described above values of B_1 and B_2 of 0.173 dm^3 mol^{-1} and 0.184 dm^3 mol^{-1} respectively, were found.

3.14 THALLOUS HYDROXIDE

The relationship used to study the thallous nitrate solutions were again employed, but now over a larger concentration range. The ion-ion interaction term was calculated to be 0.0028 $(\alpha c)^{\frac{1}{2}}$.

There is some disagreement over the degree of ion pairing in thallous hydroxide solutions although a number of the published thermodynamic constants rely on a long extrapolation from high ionic strength.[62,67] The most recent value, derived by Lindsay[68] from conductance measurements, which gave a dissociation constant of 0.333 was chosen.

In the first analysis of the experimental data, values over the whole concentration range studied (up to 0.52 mol dm^{-3}) were fitted to equation (3.23) giving B_1 and B_2 values of 0.127 and 0.071 dm^3 mol^{-1} respectively.

When the concentration range was restricted to values below 0.135 mol dm^{-3} (i.e. comparable to the previous salts), B_1 and B_2 altered to 0.116 and 0.122 $dm^3 mol^{-1}$ respectively. At the same time, the standard deviation of the points from the calculated values fell by over 50% from that of the first analysis. As discussed above the simple Jones-Dole equation fails to represent adequately the viscosties of more concentrated solutions, and that an extended equation of the form of equation (3.12) must be used when considering higher concentration ranges. It may be concluded that some extension is required to describe the behaviour of TlOH solution up to 0.5 mol dm^{-3} and that by attempting to fit all the data to equation (3.23) an overemphasis is given to the ion pair/solvent interaction term. No attempt has been made here to introduce a third arbitrarily parameter, rather, the B_1 and B_2 values obtained from the lower concentration range have been used.
It should be noted that in none of the three cases did the introduction of the B_2 term into the Jones-Dole equation cause a significant reduction in the variance. Justification for using this ion pair analysis is based on the abundant evidence for the existence of such species in these systems from conductance, solubility and kinetic experiments.[62]

3.15 B- COEFFICIENT OF THE ION PAIRS

$B_{NO_3^-}$ and $B_{SO_4^{2-}}$ values have been well established as -0.046 $dm^3 mol^{-1}$ and + 0.2085 $dm^3 mol^{-1}$ at 25°C respectively. Then from the $TlNO_3$ results,

$$B_{Tl^+} = B_1 - B_{NO_3^-}$$

$$= -0.062 - (-0.046)$$
$$= -0.016 \text{ dm}^3 \text{ mol}^{-1}$$

From the Tl_2SO_4 results,

$$B_{Tl^+} = \tfrac{1}{2}\,(B_1 - B_{SO_4^{2-}})$$
$$= \tfrac{1}{2}\,(0.173 - 0.2085)$$
$$= -0.018\ dm^3\ mol^{-1}$$

There are less data available for B_{OH^-}. At 18°C Kaminsky[52] calculates a value of 0.109 $dm^3\ mol^{-1}$ while Gurney[55] quotes 0.12 $dm^3\ mol^{-1}$ at 25°C. A more recent value at the latter temperature is 0.119 $dm^3\ mol^{-1}$. If one takes the thallous ion to have the mean value from the $TlNO_3$ and Tl_2SO_4 experiments, namely $B_{Tl^+} = -0.017\ dm^3 mol^{-1}$ one has from the TlOH analysis

$$B_{OH^-} = B_1 - B_{Tl^+} = 0.116 - (-0.017) = 0.133\ dm^3 mol^{-1}$$

which is in fair agreement with the above values.

The crystal radius of Tl^+ is 0.147nm, which is exactly that of Rb^+. However, the B- coefficient of Tl^+ $-0.017\ dm^3 mol^{-1}$ is much closer to that of K^+, $-0.007\ dm^3 mol^{-1}$ than to that of Rb^+, $0.045\ dm^3 mol^{-1}$. On the other hand when $\bar{S}_h^o$ the ionic entropy, is plotted against B for a number of cations the Tl^+ values fall within the linear pattern discussed by Gurney fig. (3.6)[55]

B values for the ion pairs and the corresponding free ions are given in table (3.7). In each case the B- value of the ion pair is intermediate between that of the anion and that of the thallous ion, but dominated by that of the larger numerical value of the anion. Further, the difference in the coefficient for the ion pair and the free ions is of the same order as the experimental error in the B- values. For these compounds it may be concluded, perhaps surprisingly, that the formation of the ion pairs has little effect on the viscosity of the solution. This contrasts with the behaviour of the Na_2SO_4 and K_2SO_4 reported by Davies and Malpass where the ion pair B-

FIGURE (3.6)

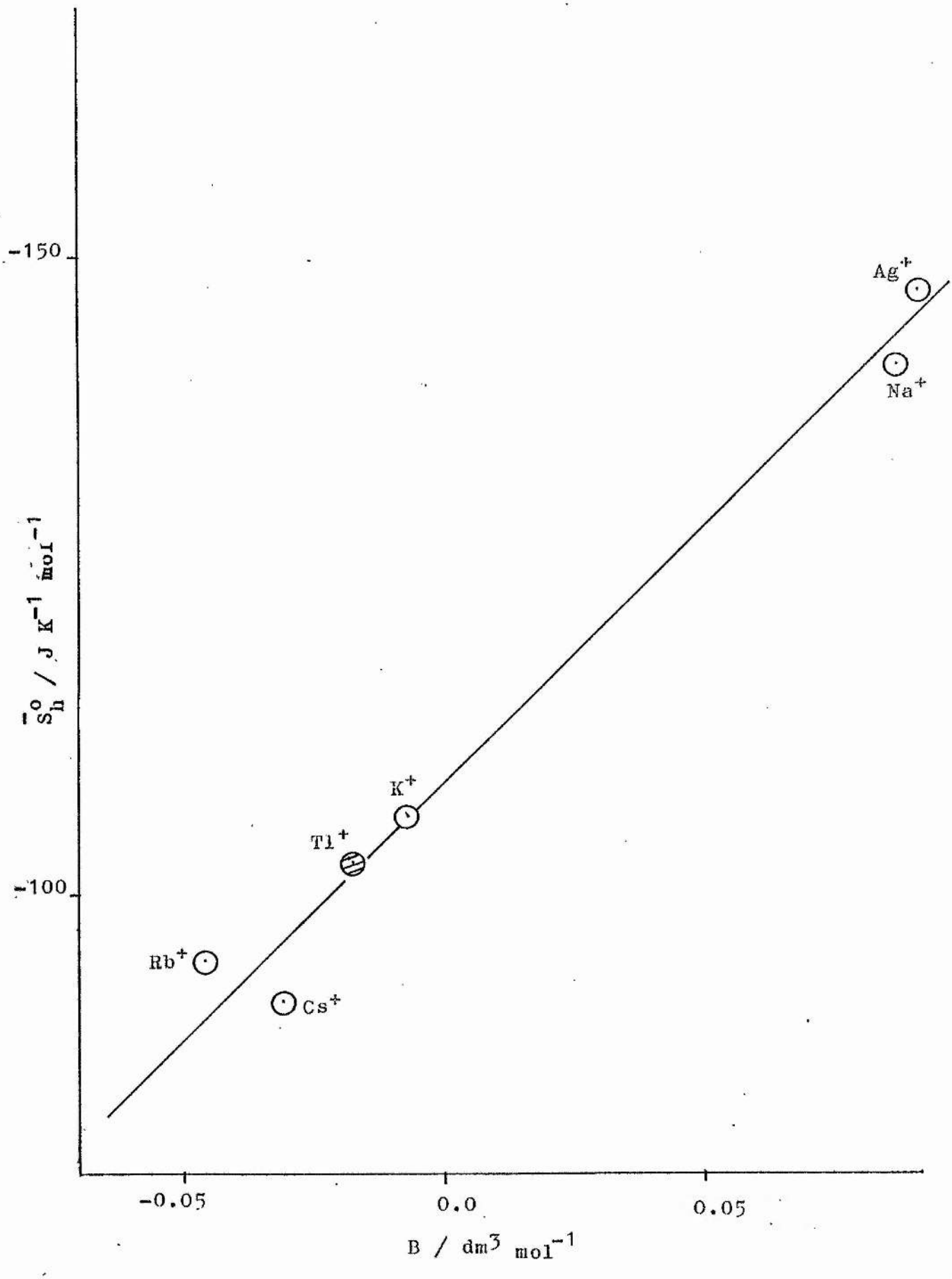

coefficients were approximately 0.03 $dm^3\ mol^{-1}$ lower than those of the free ions, but parallels the behaviour decribed by these workers for $LiSO_4^-$. For the $TlNO_3$ ion pair the B-coefficient (which is the least reliable of the three because of the relatively lower ion association) is apparently more positive than that for the dissociated salt. $CsNO_3$, a salt which has also an overall negative B- coefficient is also reported to behave in this way,[54] although the effect in $TlNO_3$ solution appears to be much larger.

TABLE 3.7 B- COEFFICIENTS FOR ION PAIRS AND FREE IONS

ion pairs/$dm^3 mol^{-1}$		Free ions/$dm^3 mol^{-1}$	
($TlNO_3$)	: -0.034 ± 0.017	$Tl^+ + NO_3^-$	-0.062 ± 0.005
($TlSO_4^-$)	: $+0.184 \pm 0.008$	$Tl^+ + SO_4^{2-}$	$+0.191 \pm 0.008$
(TlOH)	: $+0.122 \pm 0.008$	$Tl + OH^-$	$+0.116 \pm 0.008$

From the general similarity between B- coefficients of ion pairs of this type and their corresponding free ions, one may distinguish clearly between the effects on the solvent of the processes.

$$H^+ + CH_2(COO)^{2-} \rightarrow HOOCH_2COO^-$$

and

$$Tl^+ + SO_4^{2-} \rightarrow TlSO_4^-$$

In the former, charge is destroyed and the new species formed has a completely different B- coefficient compared with that of the free ions.[70] In the latter, an outer

complex may be formed in which the ionic charges still affect the surrounding solvent molecules in much the same way as the free ions. Formation of an ion pair of this outer type has been suggested for TlOH from the results of a Raman spectroscopy study.[71]

3.16 CONCLUSIONS

The foregoing work has shown that the viscosity of electrolyte solutions can be described by suitable forms of the Jones-Dole equation. For concentrations up to a maximum of 0.12 mol dm^{-3} in aqueous solution the simple Jones-Dole equation (3.4) is more suitable and the B-coefficient should be determined by either methods 2 or 3. For incompletely dissociated salts, the concentration terms of the Jones-Dole equation should be corrected for the degree of association of the ions.

CHAPTER FOUR

4.1 INTRODUCTION

B- coefficients have been measured in many non-aqueous solvents. With the exception of highly associated solvents such as glycerol, some dihydric alcohols and sulphuric acid, they have all been shown to be positive. In other associated solvents such as the alcohols and N-methylamides where only positive B- coefficients have been detected this has been attributed to the linear nature of the association of these molecules. Negative B- coefficients have only been found in solvents which are capable of forming three dimensional aggregates by hydrogen bonding.

Formamide which is known to be an associated solvent, has the ability to form three hydrogen bonds per molecule. It is a good electrolytic solvent with a larger dielectric constant than water and is therefore an interesting medium for the study of electrochemical processes. In view of the possibility of association in three dimensions it seemed possible that significant structure breaking effects might be present when salts are dissolved in formamide, and that these might lead to small or even negative B- coefficients. A study of the viscosity of electrolyte solutions in formamide was therefore undertaken.

4.2 PREVIOUS VISCOSITY STUDIES OF FORMAMIDE SOLUTIONS

Three previous studies of the viscosity of electrolyte solutions in formamide have been reported. Davies et al[72,73] studied a large number of salts in formamide and determined the viscosity, conductivity and

density of the solutions. However only three concentrations were studied for each electrolyte and the viscosity of the solvent varied between 0.003194 and 0.003388 J $m^{-3}s$. More recently, McDowall and Vincent[74] have reported B-coefficients for electrolytes in formamide. The present study is an extension of the latter work to obtain more information on solute-solvent interactions in formamide. Finally Bruno and Della Monica[75] have measured the viscosity of a number of salts in formamide. However, in this work concentrations ranged from 0.4 mol dm^{-3} to 6.0 mol dm^{-3} and were therefore unsuitable for determining Jones-Dole B- coefficients. In addition to these studied mentioned, both Davies[73] and Vincent[76] have reported viscosities of electrolytes in binary liquids containing formamide as one of the solvents.

4.3 EXPERIMENTAL RESULTS

The viscosities of lithium bromide, potassium chloride, rubidium iodide, caesium chloride, caesium bromide and caesium iodide in formamide have been determined. The viscosity of the caesium solutions were determined at 25,35,45 and 50°C . For lithium bromide solutions, viscosities were studied at 25,35 and 45°C while potassium chloride solutions were studied at 25 and 35°C. To obtain an ionic B- coefficient for Rb^+ at 25°C , the viscosity of rubidium iodide was determined at that temperature.

All the electrolyte solutions were prepared from concentrated (approximately 0.1 mol dm^{-3}) stock solutions. The latter were made up by weight and other solutions were prepared by dilution of the stock solution. After the

density of the solutions had been determined, the concentrations were converted to the molar concentration scale using the relationship

$$c = \frac{1000\ \rho_1\ m}{1000 + M_2\ m} \qquad (4.1)$$

where c is the concentration in moles per litre, m is the concentration in moles per kilogram of solvent (i.e. the molality), ρ_1 is the density of the solution and M_2 is the molecular weight of the solute.

The experimental information was analysed on the basis of the Jones-Dole equation[17]

$$\eta/\eta_o = 1 + Ac^{\frac{1}{2}} + Bc \qquad (4.2)$$

From the results of chapter III, a minimum of five concentrations were studied for each salt at each temperature. The concentrations studied, ranged between 0.005 mol dm^{-3} and 0.12 mol dm^{-3}. This restriction was necessary because at low concentrations, experimental errors increase rapidly with decreasing concentration and a theoretical A- coefficient provides a fixed origin at zero concentration. At concentrations higher than 0.12 mol dm^{-3} it was found necessary to use an extended form of the Jones-Dole equation[58] as described earlier. As there is no evidence of ion association in formamide at the concentrations studied all the electrolytes were assumed to be completely dissociated. Equation (4.2) can be re-arranged to give

$$(\eta/\eta_o - 1)/c^{\frac{1}{2}} = A + Bc^{\frac{1}{2}} \qquad (4.3)$$

and therefore plotting $(\eta/\eta_o - 1)/c^{\frac{1}{2}}$ against $c^{\frac{1}{2}}$ a straight line should be obtained giving A as the intercept and B

as the gradient.

This is shown for caesium iodide at 25°C fig. (4.1)

The data were analysed using a polynomial regression analysis, which permitted either the computation of A and B with both parameters allowed to vary, or with the A parameter held at the theoretical value. In general, the latter technique was used for reasons discussed in chapter III. Since ionic conductance data in formamide was available at 25°C only,[72] the theoretical value of A could be calculated for this temperature alone. Although Kaminsky has shown that $\frac{\partial A}{\partial T}$ for aqueous solutions was always positive, the experimental value of A for NaCl in aqueous solution between 12.5°C and 42.5°C differed by only 0.0013 $dm^{3/2}mol^{-\frac{1}{2}}$ and the theoretical values by 0.0006 $dm^{3/2}mol^{-\frac{1}{2}}$ over the same temperature range.[77] Thus it was decided that no appreciable error would be introduced by assuming that $\partial A/\partial T = 0$ for the salts studied in formamide. The value of A calculated for 25°C was therefore used at all temperatures. Table (4.1) shows the experimental and theoretical A values for the electrolytes studied in formamide.

These values demonstrate that the use of the theoretical A- coefficient over the entire temperature range studied does not impose a false origin on the system. The error in A is taken as the mean difference between the calculated and theoretical A values at 25°C and is considered to be $\pm$ 0.0032 $dm^{3/2}mol^{-\frac{1}{2}}$.

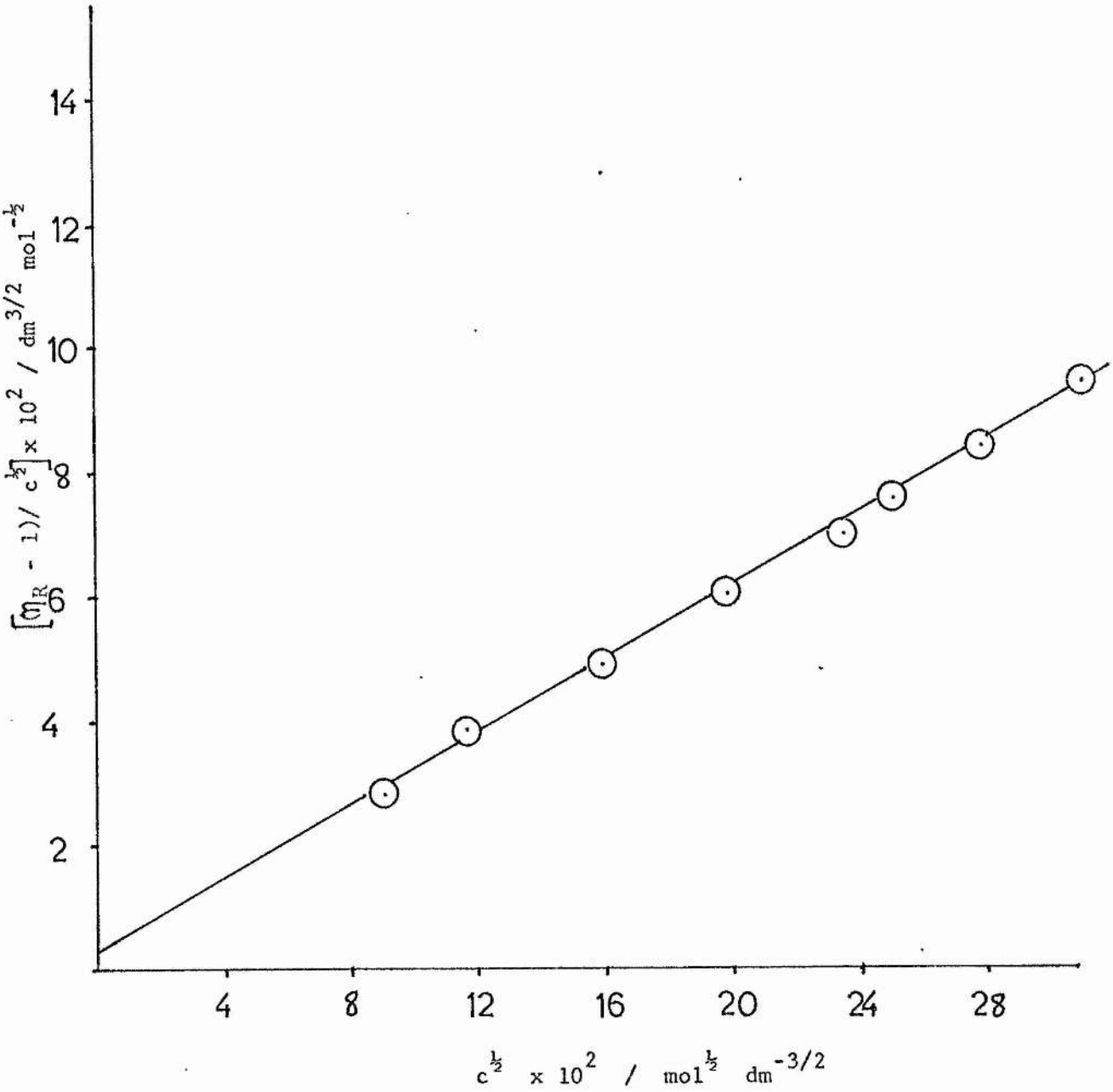
14
12
10
8
6
4
2
$[(\eta_R - 1)/c^{\frac{1}{2}}] \times 10^2$ / $dm^{3/2}$ $mol^{-\frac{1}{2}}$
4
8
12
16
20
24
28
$c^{\frac{1}{2}} \times 10^2$ / $mol^{\frac{1}{2}}$ $dm^{-3/2}$

FIG. 4·1

TABLE 4.1

Electrolyte	Theoretical A value 25°C / $dm^{3/2}\ mol^{-\frac{1}{2}}$	Experimental A Values/$dm^{3/2}mol^{-\frac{1}{2}}$ 25°C	35°C	45°C	50°C
LiBr	0.0068	0.0020	0.0000	0.0069	
KCl	0.0058	0.0106	0.0066		
RbI	0.0059	0.0073			
CsCl	0.0056	0.0018	0.0029	0.0044	0.0056
CsBr	0.0056	0.0035	0.0133	0.0013	0.0034
CsI	0.0057	0.0020	0.0055	0.0051	0.0098

The B- coefficients determined at the chosen temperatures are shown in table (4.2)

TABLE 4.2

EXPERIMENTAL B- COEFFICIENTS IN FORMAMIDE /$dm^3\ mol^{-1}$	25°C	35°C	45°C	50°C
LiBr	0.436 (±0.003)	0.407 (±0.010)	0.387 (±0.005)	
KCl	0.364 (±0.005)	0.345 (±0.003)		
RbI	0.269 (±0.005)			
CsCl	0.315 (±0.004)	0.303 (±0.004)	0.289 (±0.008)	0.284 (±0.006)
CsBr	0.273 (±0.002)	0.262 (±0.007)	0.249 (±0.006)	0.243 (±0.002)
CsI	0.243 (±0.008)	0.228 (±0.001)	0.228 (±0.003)	0.223 (±0.005)

The values in brackets in table (4.2) are the calculated standard error of the gradients given by

$$\left\{ \frac{\sum_{i=1}^{i=n} \left[y_c - (y_{calc})_i \right]^2}{n-2} \right\}^{1/2} \Big/ \left[\sum_{i=1}^{i=n} x_i \right]^{1/2}$$

where x is equal to $c^{\frac{1}{2}}$, y is equal to $(\eta/\eta_0 - 1)/c^{\frac{1}{2}}$ and n is the number of observations.

Lithium bromide was also studied at 50°C, but the results obtained showed too large a scatter for a reliable B- coefficient to be determined. Detailed experimental data on the above electrolytes in formamide is given in appendix III.

4.4 ADDITIVITY OF B- ION COEFFICIENTS

If the B- coefficients of electrolytes are dependent on the ion-solvent interactions only, then, as noted earlier, they should be additive in the values for the ionic constituents. Table (4.3) shows the differences in B- coefficients for cations with a common anion and anions with a common cation in formamide at 25°C. The B- coefficients for LiCl, NaBr and KBr have been taken from reference 74 and converted to units of $dm^3 mol^{-1}$ where appropriate

TABLE 4.3

B- COEFFICIENT DIFFERENCES / $dm^3 mol^{-1}$ AT 25°C		
NaCl - NaBr	KCl - KBr	CsCl - CsBr
0.030 (±0.006)	0.028 (±0.006)	0.042 (±0.006)

TABLE 4.3 Contd.

LiCl - CsCl	LiBr - CsBr
0.172 (±0.008)	0.163 (±0.008)

It is seen that within experimental error the B ion values are additive.

4.5 RESOLUTION OF B- COEFFICIENTS INTO IONIC COMPONENTS

The first attempt to resolve B- coefficients into ionic components was undertaken by Cox and Wolfenden[78] for aqueous solutions at 18°C and 25°C. They argued, since Li^+ has a mobility less than 3% larger than $(IO_3)^-$, then on the basis of Stokes' Law and assuming the hydrated ions to be spherical, the volume of the hydrated Li^+ ion would be almost 10% larger than the volume of the $(IO_3)^-$ ion. Since the Einstein equation[49] (3.2) is derived from Stokes' Law, the arguement leads directly to the prediction that B_{Li^+} is approximately 10% greater than $B_{(IO_3)^-}$. Cox and Wolfenden thus assigned the value of 0.146 $dm^3 mol^{-1}$ to Li^+ and 0.136 $dm^3 mol^{-1}$ to $(IO_3)^-$ from the $LiIO_3$ value at 18°C. They further assumed that B_{Li^+} 18°C = B_{Li^+} 25°C. From the additivity principle, the B values for the other ions followed.

A different approach to the division of B-coefficients was taken by Gurney.[55] He pointed out that, the mobility and its temperature coefficient are almost the only quantities for which experimental values can be obtained for anions and cations sperately. Gurney considered two factors in dividing B- coefficients. Firstly

the B value for KCl was very close to zero (-0.014 $dm^3 mol^{-1}$). This suggested that either both K^+ and Cl^- had large opposite effects on the viscosity of water, or that both ions had very little effect on the structure and therefore the viscosity of water. The second factor considered was a plot of the temperature coefficient of mobility defined as $C^{T_2}_{T_1} = \frac{\eta_2 \lambda_2}{\eta_1 \lambda_1}$ against the equivalent conductivity of the ions λ_o at 18°C. fig.(4.2) This showed that K^+ and Cl^- lie very close together and therefore have a similar effect on the structure of water

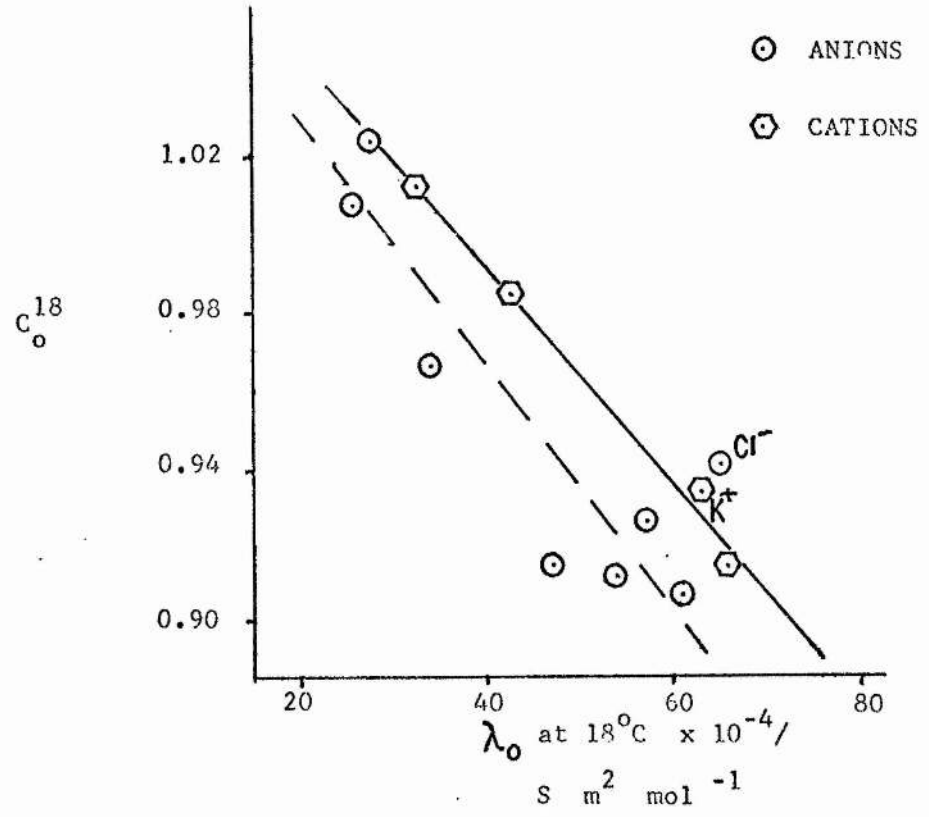

FIG. 4·2

From this Gurney concluded that K^+ and Cl^- had very little effect on the viscosity of water and that $B_{K^+} = B_{Cl^-} = \frac{B_{KCl}}{2}$ at 25°C. B_{K^+} and B_{Cl^-} were therefore given the value $-0.007\ dm^3mol^{-1}$. Kaminsky[77] has extended this method and assumed that $B_{K^+} = B_{Cl^-}$ at all temperatures between 15 - 45°C. Nightingale[79] has criticised this method, since on the basis of mobility data alone, other salts such as RbCl or CsCl would be more suitable. Krumgal'z,[80] in agreement with Nightingale suggested that KNO_3, NH_4NO_3, RbCl, RbI, CsBr and CsI are also more suitable than KCl for the resolution of B in aqueous solution since for all these salts $\lambda_o^+ \simeq \lambda_o^-(25°C)$. The above methods used by both Cox and Wolfenden and Gurney yield B values which agree within the limits of experimental error in aqueous solutions.

In addition to these methods of resolution of B- coefficients in aqueous solutions discussed above, many attempts have been made to resolve the B- coefficients in non-aqueous solutions. Gillespie,[81] who investigated the viscosities of solutions of the type $MHSO_4$ in sulphuric acid where $M^+ = Li^+$, Na^+, K^+, NH_4^+ and $\frac{1}{2}Ba^{2+}$ attributed the total B value for the salt to the cation alone, assuming that the HSO_4^- anions, which had the same dimensions as the solvent molecules, would have very little disturbing effect on the solution structure. He thus completely ignored the effect of the electrostatic field of the anion, and the B- values obtained are of comparative value only. Criss and Mastroianni[82] studied the viscosity of electrolytes in methanol solution and used the method of Gurney to

resolve their B- coefficients. Since $\lambda_o^{25}K^+ = \lambda_o^{25}Cl^-$, B_{K^+} was assumed to be equal to B_{Cl^-}. Tuan and Foss[83] proposed the equality $B_{Bu_4N^+} = B_{Ph_4B^-}$ for acetonitrile solutions, since according to the results of Kunze and Fuoss[84] these ions have similar mobilities at least in methanol solution. Yao and Bennion[85] used a similar assumption to divide their B- coefficients in dimethyl sulphoxide solution. They considered the B- coefficients for $(i\text{-amyl})_3$ Bu N^+ and $B(Ph)_4^-$ ions to be equal because of their very similar size and shape and low surface charge density. Ionic $B_\pm$ coefficients for electrolytes in formamide were first estimated by Notely and Spiro[86] using the viscosity data of Davies et al.[73] These workers do not state how the division was made. However inspection of their $B_\pm$ values suggests that they assumed similar contributions from Cs^+ and Cl^- and assigned values of $B_{Cs^+} = 0.21$ dm^3mol^{-1} and $B_{Cl^-} = 0.20$ dm^3mol^{-1}. These B- coefficients are of comparative value only since the original viscosity work contained only two concentrations suitable for valid application of the Jones-Dole equation. More recently, McDowall and Vincent[74] have applied the method of Cox and Wolfenden to obtain $B_\pm$ coefficients in formamide.

4.6 KRUMGAL'Z METHOD FOR DIVISION OF B- COEFFICIENTS

In 1973 Krumgal'z proposed a general method for the resolution of B- coefficients in organic solvents.[80] Earlier he had shown[87] that tetra-alkylammonium salts R_4N^+, where R was equal to C_4 and above, and other complex organic ions e.g. iso-Am_3BuN^+, Ph_4B^- and Ph_4As^+ are not solvated in

organic solvents. Their dimensions in such solvents could be considered unchanged and therefore constant. Krumgal'z argued that B- coefficients could be resolved into ionic components on the assumption that the B± coefficients for these ions in organic solvents were proportional to their volumes. From this assumption, and the additivity of the B- coefficients with respect to the constituent ions, the B± coefficients could be calculated from the relationship

$$\frac{B_{R_4N^+}}{B_{R_4^1N^+}} = \frac{r^3_{R_4N^+}}{r^3_{R_4^1N^+}} \qquad (4.4)$$

AND

$$B_{R_4N^+} - B_{R_4^1N^+} = B_{R_4NX} - B_{R_4^1NX} \qquad (4.5)$$

Krumgal'z calculated and tabulated B± coefficients for seven organic solvents by this method. Sacco and co-workers,[88] have used the equality of $B_{TAB^+} = B_{BPh_4^-} = B(TABBPh_4)/2$ to obtain ionic B- coefficients in sulpholane, although they incorrectly state that they use the above method of Krumgal'z.

The Krumgal'z method was used in this project to determine the B- coefficients for the electrolytes studied in formamide at 25°C. Relative viscosities were determined for tetrabutylammonium iodide $(C_4H_9)_4NI$ and tetrapentylammonium iodide $(C_5H_{11})_4NI$ at 25°C. The B- values found for the salts were:

$$B_{(C_4H_9)_4NI} = 0.602 \ (\pm 0.01) \ dm^3mol^{-1}$$

TAB^+ = Triisoamylbutyl ion BPH_4^- = Tetraphenyl boride ion

AND

$$B_{(C_5H_{11})_4NI} = 0.801 \text{ dm}^3\text{mol}^{-1} \quad (\pm 0.01)$$

The effective ionic radius of the $(C_4H_9)_4N^+$ ion was taken as 0.385 nm as determined by Krumgal'z[87]. Data from the same source, on the variation of the radii of tetra-alkylammonium ions with the number of carbon atoms, was used to calculate the radii of $(C_5H_{11})_4N^+$, which was found to be 0.430 nm. Application of equations (4.4) and (4.5) gives

$$B_{(C_4H_9)_4N^+} / B_{(C_5H_{11})_4N^+} = \frac{0.0571}{0.0795}$$

AND

$$B_{(C_4H_9)_4N^+} - B_{(C_5H_{11})_4N^+} = 0.602 - 0.801$$

solving these two equations gives $B_{(C_4H_9)_4N^+} = 0.507 \text{ dm}^3\text{mol}^{-1}$

$B_{(C_5H_{11})_4N^+} = 0.706 \text{ dm}^3\text{mol}^{-1}$ and I^- therefore has the value $B_{I^-} = 0.095 \text{ dm}^3\text{mol}^{-1}$. The additivity principle now enables the remaining ions studied to be assigned $B_{\pm}$ values

It should be noted that the Krumgal'z method and that of Cox and Wolfenden require ionic radii values to be known very accurately. The function in r^3 used in both methods yields the ionic B- coefficient calculated sensitive to small changes in the ionic radius r.

The ionic radii used were calculated by Krumgal'z using Stokes' law at 25°C only. No information on transport numbers or ionic equivalent conductances in formamide at temperatures other than 25°C are available in the literature, this method of determining B- coefficient therefore could

not be extended to the higher temperatures studied.

4.7 B- COEFFICIENTS DIVISION BY THE CORRESPONDENCE PLOT TECHNIQUE

The linear relationship between ionic viscosity B- coefficients and ionic entropy was first demonstrated by Gurney[55]. By plotting $B_{\pm}$ against $\bar{S}^{o}_{2}$ he obtained two almost parallel straight lines. When the partial molal ionic entropies were split using the convention $\bar{S}^{o}_{2}H$ = 0.0 J $K^{-1}mol^{-1}$, his plot showed that the points for the positive ions lay along one straight line while those for negative ions lay on an almost parallel line fig (4.3). Gurney found that if he assigned a value of -23.01 J K^{-1} mol^{-1} to the absolute ionic entropy of H^{+} then both the positive and negative ions produced a single straight line. fig (4. 3)

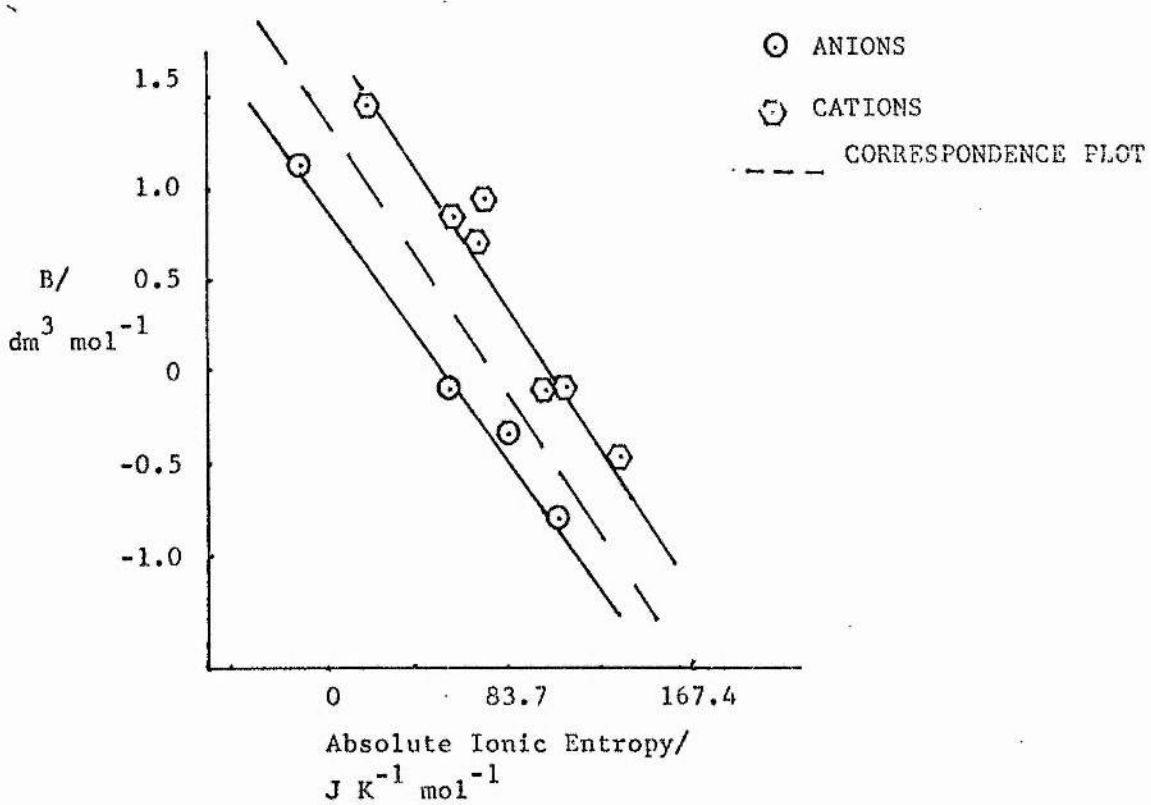

The broken line is the correspondence plot for the positive and negative ions obtained by making H = -23.01 J $K^{-1}mol^{-1}$

Since Gurney effectively made use of the ionic B- coefficients to obtain a more satisfactory division of partial molal entropies of electrolytes, it seemed that this correspondence technique could be employed in reverse to obtain ionic B- coefficients. Partial molal entropies of electrolytes in formamide have been divided into their ionic contributions by means of a correspondence plot by Criss,Held and Luksha[89] . They divided the published partial molal entropies of the electrolytes in formamide by an arbitrary process. They then plotted these values against the partial molal entropies of the ions in aqueous solution and in the same manner as Gurney, they adjusted the ionic partial molal entropies in formamide to give a single straight line for both the positive and negative ions. The values obtained by Criss and co-workers are shown in table (4.4) converted to $J\ K^{-1}mol^{-1}$.

TABLE 4.4

ION	$\bar{S}^o_m$ $J\ K^{-1}\ mol^{-1}$	$\bar{S}^o_n$ $J\ K^{-1}mol^{-1}$	$\bar{S}^o_g$ $J\ K^{-1}mol^{-1}$	$\bar{S}^o_h$ $J\ K^{-1}mol^{-1}$
Li^+	5.8	-20.0	133.1	-153.1
Na^+	10.5	-15.3	147.7	-163.0
K^+	47.3	21.5	154.4	-132.9
Rb^+	62.3	36.5	164.4	-127.9
Cs^+	71.5	45.7	169.9	-124.2
Cl^-	42.3	16.5	153.1	-136.6
Br^-	63.6	37.8	163.6	-125.8
I^-	72.3	46.5	169.0	-122.5

The values in column one are taken from the latest published data by Criss and Salomon[90] and converted to the appropriate SI units. These values are the absolute ionic entropies $\bar{S}^o_m$ expressed in the hypothetical 1 molal standard state. Column two contains the $\bar{S}^o_n$ values converted to the mole fraction standard state using the relationship

$$\bar{S}^o_n = \bar{S}^o_m - R \ln (1000/M_1) \qquad (4.6)$$

where M_1 is the molecular weight of the solvent and the subscripts n and m refer to mole fraction and molality, respectively. The intrinsic entropy of the hypothetical ideal gas for the solute $\bar{S}^o_g$ is listed in column three and the values were determined using the Sackur-Tetrode equation[11]

$$\bar{S}^o_g = 4.184\ (6.864 \log_{10} W + 26.00)\ J\ K^{-1} mol^{-1} \qquad (4.7)$$

where W is the atomic weight of the gas.

Equation (4.7) is the reduced Sackur-Tetrode equation applicable to atoms or ions with inert gas structure at a temperature of 25°C and a pressure of 1.013×10^5 N m^{-2}. The single ionic entropies $\bar{S}^o_h$ listed in column four were obtained from the relationship

$$\bar{S}^o_h = \bar{S}^o_n - \bar{S}^o_g \qquad (4.8)$$

In this final conversion, subtraction of the intrinsic entropy of such an ideal gas $\bar{S}^o_g$ causes the entropy value calculated to represent only the entropy change in the solvent due to the presence of the ion. To apply the correspondence technique, the B- coefficients were divided assuming B_{I^-} = 0.0 $dm^3\ mol^{-1}$ and the resulting ionic B- coefficients were plotted against $\bar{S}^o_h$ values, fig. (4.4).

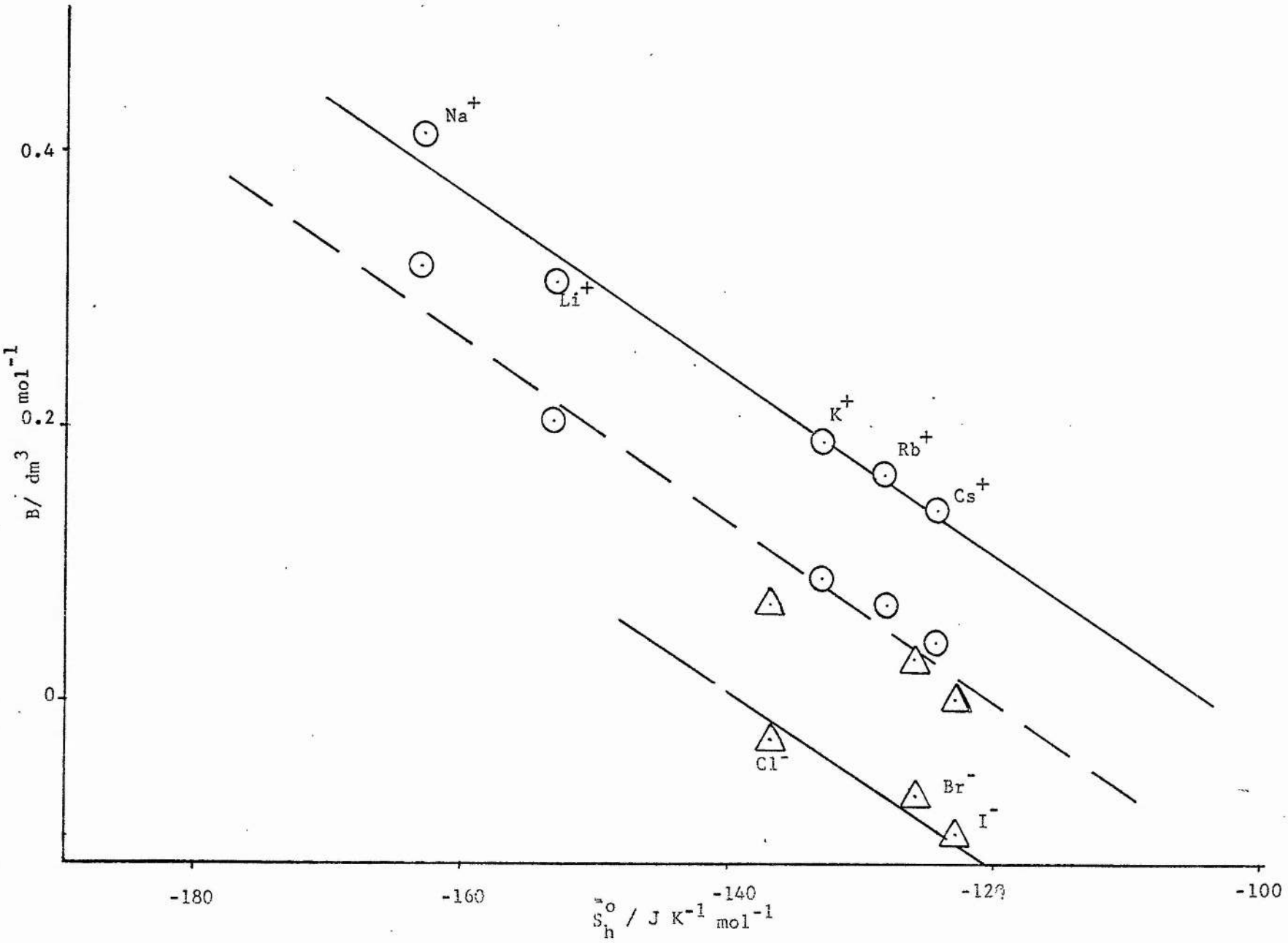
Na+
Li+
K+
Rb+
Cs+
Cl-
Br-
I-
0.4
0.2
0
B/ dm3 mol-1
-180
-160
-140
-120
-100
S°h / J K-1 mol-1

FIG. 4-4

The B- coefficient for sodium was determined previously in a study of the viscosity of NaCl in formamide/water[76] Fig. (4.4) shows two almost parallel lines. Adjustment of the B ion values to produce a single straight line for both positive and negative ions resulted in the B ion values in column two of table (4.5) and the central plot in fig (4.4)

TABLE 4.5

	B ion coefficients at 25°C / $dm^3\ mol^{-1}$			
	(1)	(2)	(3)	(4)
Li^+	0.311	0.307	0.378	0.150
Na^+	0.423	0.419	0.490	0.086
K^+	0.197	0.193	0.264	-0.007
Rb^+	0.174	0.171	0.241	-0.030
Cs^+	0.148	0.144	0.215	-0.045
Cl^-	0.167	0.171	0.100	-0.007
Br^-	0.125	0.129	0.058	-0.032
I^-	0.095	0.099	0.028	-0.070

(1) B ion values obtained by the method of Krumgal'z

(2) B ion values obtained by the correspondence plot method

(3) B ion values determined by the method of Cox and Wolfenden.

(4) B ion values in aqueous solution for comparison.[16]

The $B_{\pm}$ coefficients obtained by methods (1) and (2) are seen to agree within the limits of experimental error.

4.8 COMPARISON OF THE METHODS AVAILABLE FOR THE DIVISION B- COEFFICIENTS

The original method of division adopted by Cox and Wolfenden[78] has been criticised by Gurney[55] and by Krumgal'z[80] because of the assumption that particles as small as the hydrated Li^+ion obey Stokes' Law. Gurney considered the problem without recourse to this postulate. His method of division and the extension of it by Kaminsky are probably the most satisfactory methods of obtaining ionic B- coefficients in aqueous solution. Gurney was able to show by other means, namely studies of $\partial(\eta_o\lambda_o)/\partial T$ values that both K^+ and Cl^- demonstrated similar ion-solvent behaviour in aqueous solution. Although this method did not extend to temperatures higher than 18°C, Kaminsky had some justification for assuming that the ions behave in a similar way between 0 and 45°C. Since individual ionic conductances at different temperatures were not available in formamide, this method could not be used directly in this work.

The ionic B- coefficients obtained by correspondence techniques are dependent on the absolute ionic entropies in aqueous solution since these values are used to determine the absolute ionic entropies in formamide. However, Criss et al[91] have determined the absolute ionic entropies in D.M.F. from solubility measurements and known ionic enthalpies and they have shown that the $\bar{S}^o_h$ values obtained by the correspondence plot method are in agreement with $\bar{S}^o_h$ values obtained by a more conventional manner. They have therefore, justified the correspondence plot method of obtaining absolute ionic entropies in non-aqueous solvents.

The values used in determining $\bar{S}^o_h$ - coefficients

for the ions in formamide were calculated on the basis of $H^+ = -20.92\ J\ K^{-1}mol^{-1}$ in water. This numerical value of H^+ is the average obtained by the various methods used to determine H^+ in aqueous solutions[90]. This method of division of B- coefficients is, like other methods, somewhat arbitrary. However, excellent agreement is obtained with the method of Krumgal'z table (4.5) This agreement obtained by two completely different approaches gives confidence in the ionic B- coefficients so determined.

Ionic B- coefficients have been determined previously by correspondence methods in methanol and N-methylformamide at 25°C[90]. It might be noted that the B ion values obtained in these two solvents were consistent with setting $B_{K^+} = B_{Cl^-}$ at 25°C. In formamide at this temperature however, the ionic B- coefficients obtained are more consistent with the equivalence $B_{Rb^+} = B_{Cl^-}$.

4.9 IONIC B- COEFFICIENTS ABOVE 25°C

In attempting to divide the B- coefficients of salts determined in formamide at 35°C, 45°C and 50°C three approaches were considered. First, the conductance data of Davies et al[73] was studied to determine if a relationship existed between the temperature coefficient of mobility and the ionic conductances in formamide similar to that shown for aqueous solutions by Gurney[55]. This study was hampered by the lack of information on transport numbers in formamide at temperatures other than 25°C. The conductance data was split into contributions by assuming that different cations and anion had the same value at the temperature considered. However no satisfactory relationship

was observed when the data was plotted in an analagous manner to fig (4.2). A second attempt to divide B- coefficients into ionic contributions was made by applying the method of correspondence plots used by Criss at al[89] to obtain non-aqueous ionic entropies. As this method yields ionic entropies in non-aqueous solutions, and since B_T and $\bar{S}^o_T$ measure similar properties, it was assumed that ionic B- coefficients at any temperature could be obtained by plotting the ionic B- coefficient at the chosen temperature against the standard ionic entropies at the same temperature in formamide. As in the method of Criss, the ionic B- coefficients in formamide would be adjusted to yield a single straight line for both anions and cations. A careful search of the literature failed to produce sufficient data on entropies in formamide to permit the adoption of this technique.

The third method was also a correspondence plot method. Fig. (4.5) shows the ionic B- coefficients at 25°C plotted against the ionic B- coefficients at 35°C and 42.5°C in aqueous solution. Both plots give excellent linear relationships. It was thus assumed that a similar relationship might exist between the ionic B- coefficients at 25°C and those at other temperatures in formamide. Figs. (4.6) and (4.7) show these plots for formamide at 35°C and 45°C. The initial division of B- coefficients at the three higher temperatures was made assuming B_{Cl^-} = 0.00. This yielded two parallel lines for the cations and anions in both cases. The ionic B- coefficients at the higher temperatures were then adjusted to produce a single line to represent both the cations and the anions. The ionic B- coefficients obtained by this method are shown

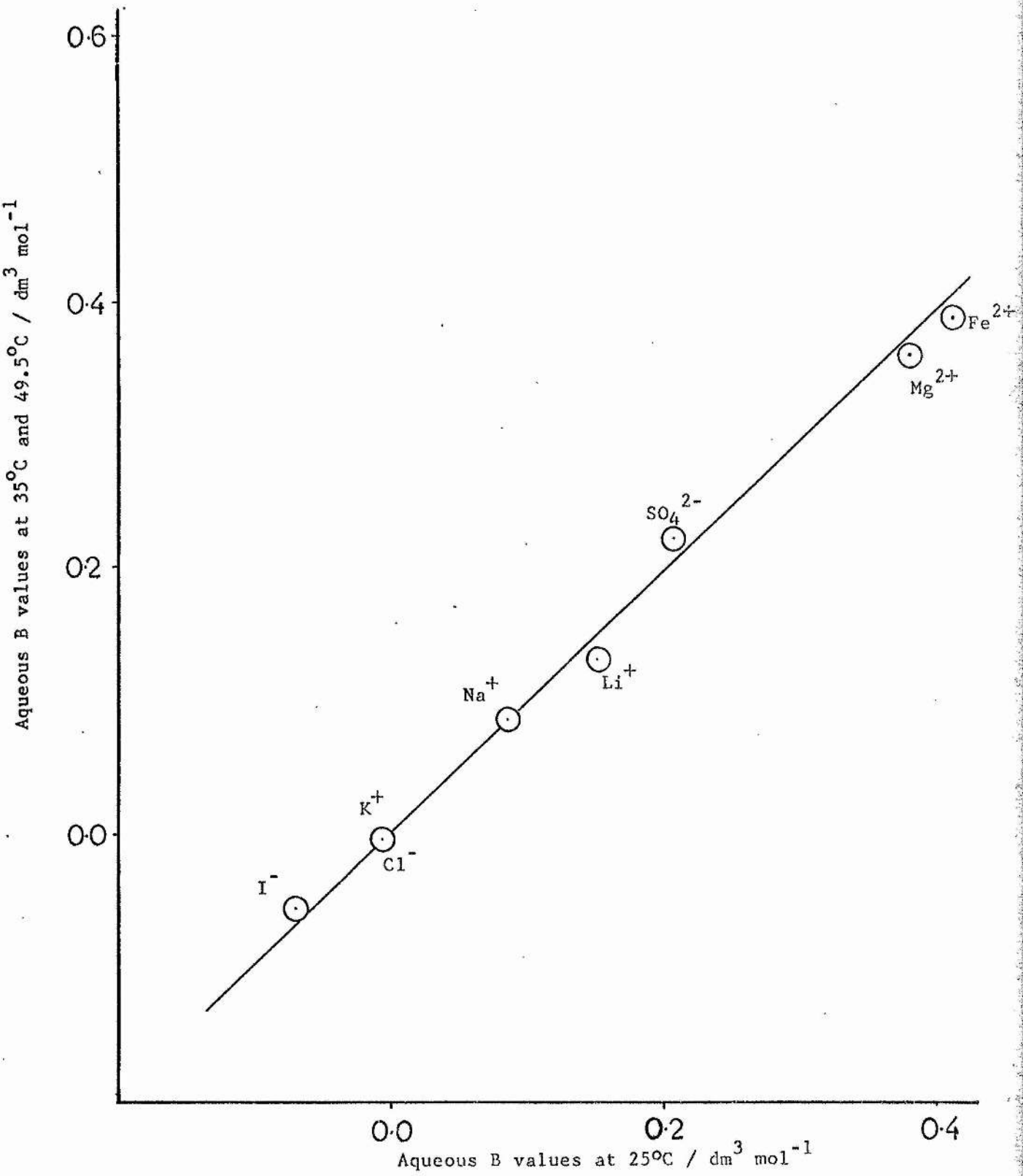
0·6
0·4
0·2
0·0
Aqueous B values at 35°C and 49.5°C / dm³ mol⁻¹
I⁻
K⁺
Cl⁻
Na⁺
Li⁺
SO₄²⁻
Mg²⁺
Fe²⁺
0·0
0·2
0·4
Aqueous B values at 25°C / dm³ mol⁻¹

FIG. 4·5

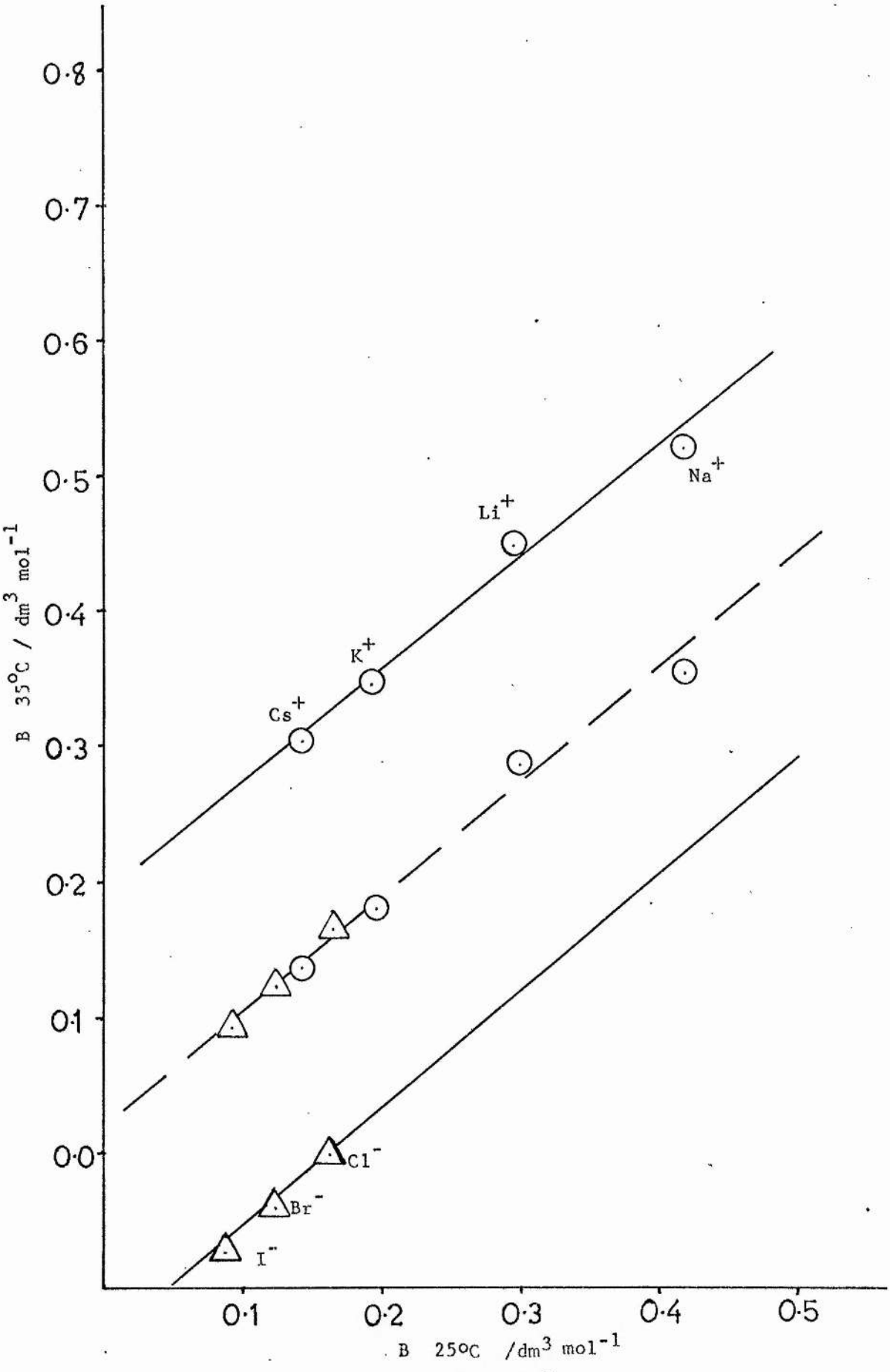
0·8
0·7
0·6
0·5
0·4
0·3
0·2
0·1
0·0
B 35°C / dm³ mol⁻¹
Li⁺
Na⁺
K⁺
Cs⁺
Cl⁻
Br⁻
I⁻
0·1
0·2
0·3
0·4
0·5
B 25°C /dm³ mol⁻¹

FIG. 4·6

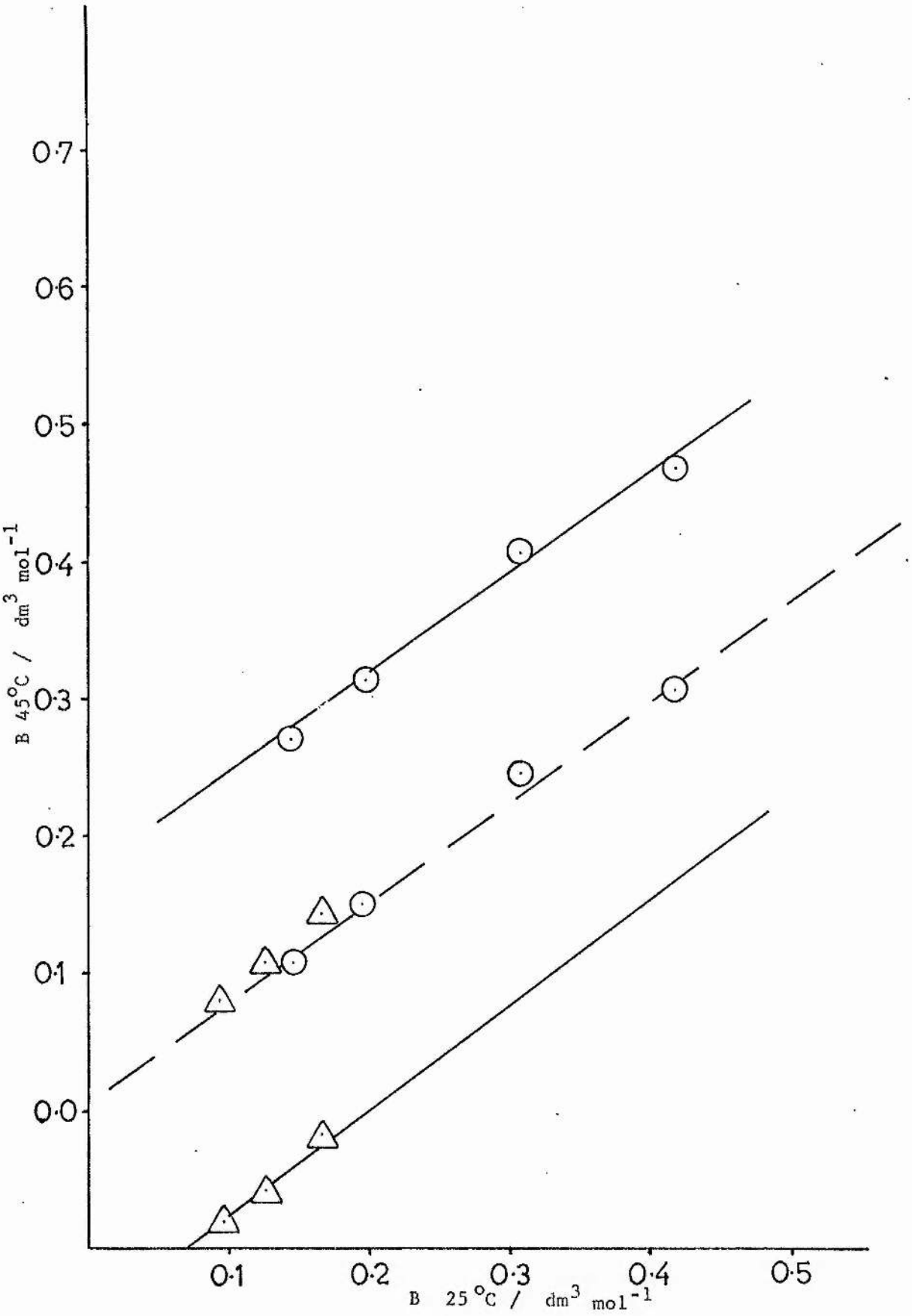

FIG. 4·7

in table (4.6). This method was not applied at 50°C due to the fact that too few salts were studied at this temperature.

TABLE 4.6

IONIC B- COEFFICIENTS/ $dm^3\ mol^{-1}$			
	25°C	35°C	45°C
Li^+	0.311	0.284	0.265
Na^+	0.423	0.356	0.328
K^+	0.197	0.181	0.170
Cs^+	0.148	0.139	0.127
Cl^-	0.167	0.164	0.162
Br^-	0.125	0.123	0.122
I^-	0.095	0.089	0.101

The ionic B- coefficients in formamide determined at all temperatures investigated were positive. With the exception of Li^+ and Na^+ the B- coefficients decreased with increasing ionic radii within a group of the periodic table. Na^+ which has a larger ionic radius than Li^+ also has a larger B- coefficient. This reversal in the general trend within a group of the periodic table for formamide is also observed for Li^+ and Na^+ in the absolute ionic entropies values for these ions in this solvent. In aqueous solution, the B- coefficients decrease with increasing ionic radii within a group of the periodic table with no exceptions. Since few lithium salts have been studied in non-aqueous

solvents then no comparison between the ionic radii and the B- coefficients of Li^+ and Na^+ could be obtained. The Li^+/ Na^+ reversal agrees with the ionic B- coefficients found by McDowall and Vincent[74] in formamide and also those of Notely and Spiro[86] in the same solvent. It would seem therefore that this phenomena may be peculiar to formamide solutions. From the B- values alone it would appear that structure-breaking is absent in this solvent. This agrees with the opinion of Criss[82] who considers that structure breaking is peculiar to aqueous solutions alone. However, further information is available when $\partial B/\partial T$ plots for the ions are studied as shown later.

4.10 TEMPERATURE COEFFICIENT OF B

The ionic B- coefficients have been plotted against temperature for the ions investigated. figs (4.8) and (4.9). The $\partial B/\partial T$ values for Li^+, Na^+, K^+ and Cs^+ are negative and this is strong evidence that these ions are structure-making ions in formamide. The $\partial B/\partial T$ values for Cl^- and Br^- are practically zero within the limits of experimental error. These ions therefore have very little effect on the solvent structure. The $\partial B/\partial T$ value for I^- is small but significantly positive and I^- is therefore a weak structure-breaking ion in formamide. All the salts investigated were overall structure-ordering salts. Thus while CsI has a negative temperature coefficient of B the structure-ordering properties of the Cs^+ ion overcome the structure-disordering properties of the I^-ion.

4.11 DISCUSSION OF B-COEFFICIENTS AND $\partial B/\partial T$ VALUES

Although all the ions studied at all four

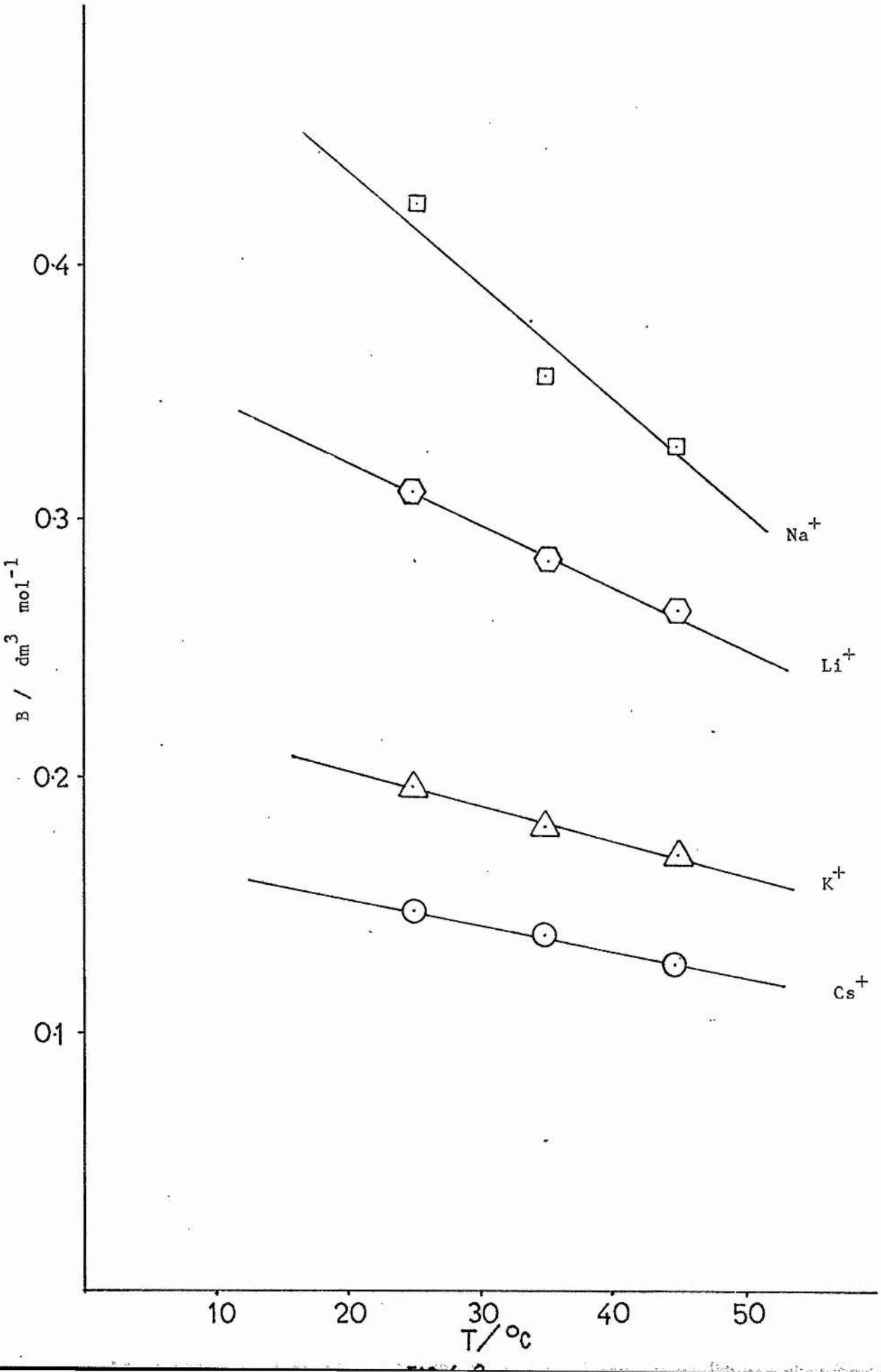
0·4
0·3
0·2
0·1
B / dm^3 mol^{-1}
Na$^+$
Li$^+$
K$^+$
Cs$^+$
10
20
30
40
50
T/ °C

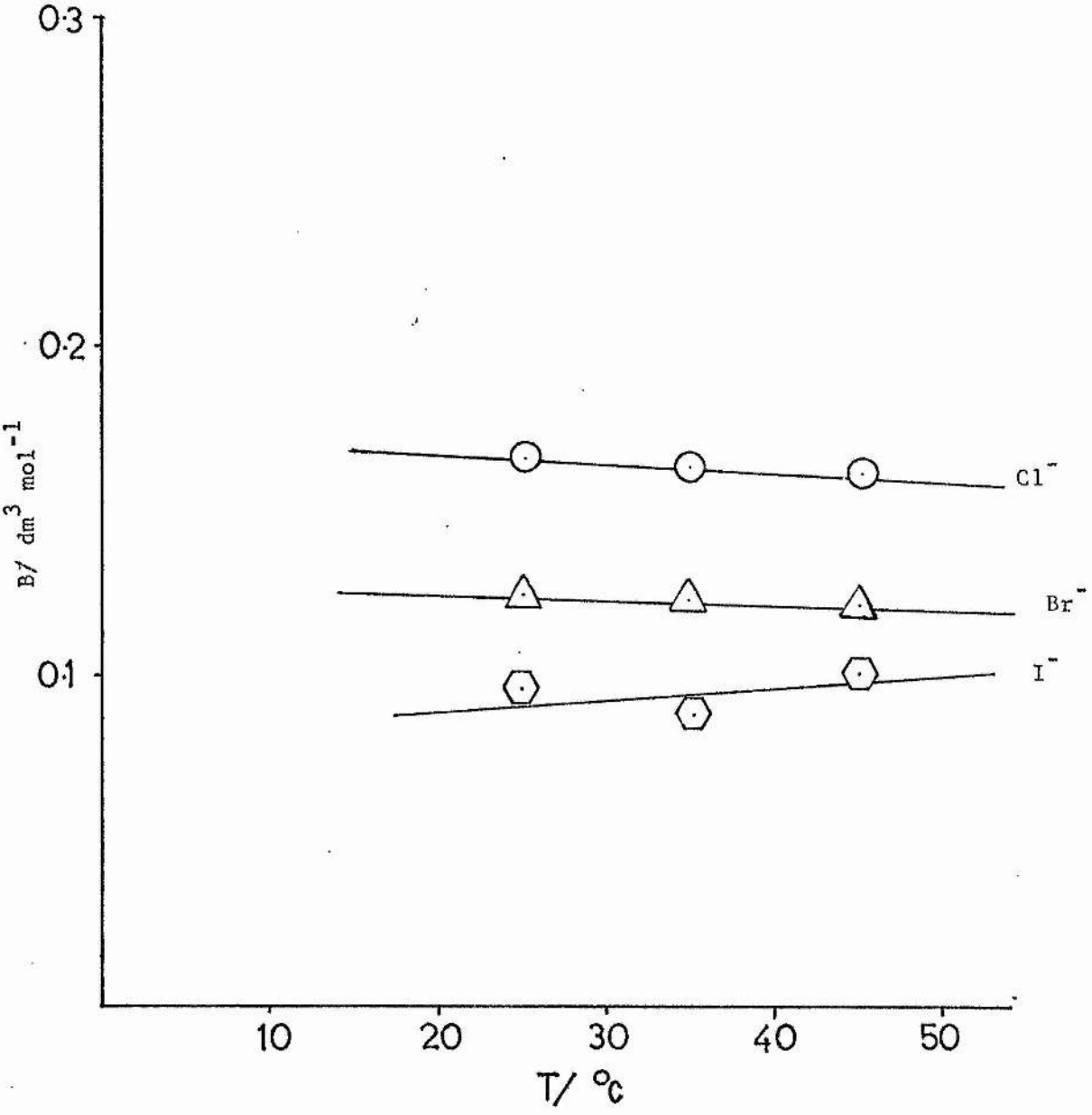

FIG. 4·9

temperatures have positive B- coefficients, the $\partial B/\partial T$ plots have shown that I^- is a structure-breaking ion in formamide. The criterion, that negative B- coefficients indicate structure-breakers, in aqueous solution is therefore invalid in formamide solution. To explain the disturbance of the solvent structure by the presence of the ion, various models have been proposed. Frank and Wen[19] proposed a model whereby three regions of solvent molecules were present in solution. Region A was considered to be a region in which solvent molecules, which were nearest neighbours to the ions themselves, were immobilised. This region could be called the solvation sheath of the ion. The second region of solvent structure, region B, was a region of structural- disruption proposed by the authors to explain negative B- ceofficients. Region C the third region was an area of undisturbed solvent structure unaffected by the presence of the ions. Experimental justification for region A was taken as the increase in solvent viscosity on the addition of certain electrolytes. Region B was considered to arise because of the approximate balance between the two orientating influences acting on any given solvent molecule. One, the normal structure orientating influence of neighbouring solvent molecules and two the orientating influence of the spherically symmetrical ionic field on the solvent dipoles. In region A the latter effect persists, and the former influence persists in region C. Large positive B- coefficients were explained by assuming that small or multiply charged ions e.g. Li^+,F^-, Mg^{2+} could promote additional structuring beyond the first region and overlap into region B

thus tending towards a net structure-making influence as observed for these ions in most solvents. The necessity for region B was supported by Frank and Evans[92] who argued that the outward orientation of like dipoles in region A should always produce at least some disorder in region B but that large monovalent ions e.g. I^- exhibit more net structure-breaking than this alone could account for. Gurney[55] who used the term co-sphere to define the area of solvent called region A by Frank and Wen, explained negative B- coefficients by assuming that for net structure-breakers region B coalesced with region A, perhaps to the extent of extinguishing it altogether. Application of this model to the present results indicates that for cations in formamide, region B is extremely small or non-existent. The cations are solvated in formamide and the solvation shell extends into the structure-breaking region eclipsing it. For Cl^- and Br^- regions A and B would appear to be in balance and no overall structure-making or breaking is observed. The effect of I^- on the other hand would seem to be the expansion of region B into region A thus disordering the solvent molecules and causing structure-breaking.

Frank and Wen's region A, Gurney's co-sphere and Nightingale's[79] solvated radius are all based on the postulate that around an ion there exists a region of modified solvent differing from the bulk solvent in structure and properties. Attempts have been made by various workers[93] to determine the number of solvent molecules bound to the ions in this modified solvent zone.

The solvation number of ions have been determined from various different measurements i.e. density, viscosity, mobility, compressibility etc. Unfortunately the solvation numbers obtained from the various methods differ, sometimes quite markedly. Bockris[94] has explained this discrepancy by pointing out that in some cases different parts of solvation were being determined. He proposed that the total effect of the solvation of ions could be divided into two parts; "primary" solvation consisting of solvent molecules firmly bound to the ions and "secondary" solvation which amounts to the polarisation of the solvent not included in the primary solvation. This partition of solvation effects has been supported by Samoilov[4] who preferred the terms "close and "far" solvation to the terms used by Bockris. Samoilov however rejects the interpretation that close solvation consists chiefly in the firm binding of the solvent molecules by the ion.

If the exchange of solvent molecules closest to the ion is relatively small then solvation is strong and as the frequency of the exchange increases, the solvation weakens. This approach to ion solvation considers only the interaction of the ion with the closest solvent molecules i.e. close solvation. Samoilov has pointed out that the whole specific nature of the interaction of an ion with solvent molecules is connected precisely with close solvation. He has explained positive and negative B- coefficients in aqueous solution by consideration of the mobility of the ions, the self-diffusion coefficient of the solvent and the temperature coefficient of these two properties. This treatment has been extended by Darmois[96] who pointed

out that for structure-making ions

$$\frac{1}{\mu_i}\frac{\partial \mu_i}{\partial T} > -\frac{1}{\eta}\frac{\partial \eta}{\partial T}$$

where μ_i is the mobility of the ions and η is the viscosity of the solvent. For structure-breaking ions this relationship is reversed. The Samoilov approach indicates that negative hydration corresponds to distortion of short range order in solution in agreement with Gurney.

A more recent analysis of B- coefficients and $\partial B/\partial T$ values has been given by Stokes and Mills [16]. They have equated the viscosity of a dilute electrolyte solution to that of the solvent plus the contributions from four other sources thus

$$\eta = \eta^{o} + \eta^{*} + \eta^{E} + \eta^{A} + \eta^{D} \qquad (4.9)$$

Here η^{*} is a positive coefficient due to the ion-ion interaction in solution and accounted for in the Jones-Dole equation by the term $Ac^{\frac{1}{2}}$. η^{E} is the viscosity increment arising from the size and shape of the ion and is closely related to the Einstein effect. η^{E} is always positive and normally increases with increasing ionic radii. η^{A} is defined as the increment due to the alignment or orientation of polar molecules by the ionic field. Since this causes an entropy reduction, the solution will be more ordered and therefore η^{A} will be a positive increment. η^{D} is the viscosity change associated with the distortion of the solvent structure leading to a decrease in viscosity. This distortion has been described as being due to competing forces from the solvent structure in the bulk and from the ionic field or the orientated molecules associated with the ion. η^{D} is therefore

analogous to Region B in the Frank and Wen model. Stokes and Mills then substitute equation (4.9) into the simple Jones-Dole equation and by eliminating the ionic interaction contributions from both sides they obtain

$$\eta^E + \eta^A + \eta^D = \eta^o \text{ Bc} \qquad (4.10)$$

The B- coefficient can now be interpreted in terms of η^E, η^A and η^D at a given concentration . In this scheme, structure-making ions are believed to have large positive η^E values since such ions e.g. Li^+ are envisaged as having a primary sheath of firmly bound solvent molecules which move as a single kinetic unit. Solvent molecules beyond the inner layer are also considered to be ordered to some extent by these highly charged ions producing positive η^A values. The sum of $\eta^E + \eta^A$ will therefore more than cancel the negative value due to η^D. For structure-making ions therefore $\eta^E + \eta^A \gg \eta^D$ and B is large and positive. Structure-breaking ions are normally large with small surface densities e.g. I^-. This small charge density leaves the ion unable to orient solvent molecules beyond the first layer,and only weakly in the first layer. η^E and η^A are therefore very small. η^D however is large due to the competition between the ionic field and the bulk structure. In this class of ions then $\eta^E + \eta^A < \eta^D$ and B is negative.

In this treatment of the B- coefficients therefore negative B- coefficients indicate structure-breaking ions. Earlier however Kaminsky investigated the temperature coefficient of B and concluded that ions which have negative $\partial B/\partial T$ values are structure-making and those which have

positive $\partial B/\partial T$ values are structure-breaking ions. He showed, in agreement with other workers, that the main points to be considered in explaining B- coefficients were the solvation of the ion, the structure-breaking contribution of the ion and the long range ordering by the ionic field.

The present results obtained in formamide indicate that solvation is dominant for cations. The negative values found for the cations in formamide can be correlated with long range ordering effects. As the temperature increases, this ordering of the solvent molecules by the ionic field is disturbed by thermal motion. The close solvation observed is almost temperature independent in the temperature range studied, η decreases therefore more rapidly than η_o. The structure-breaking I^- ion categorised by its positive $\partial B/\partial T$ value has disrupted the solvent structure initially due to its presence. An increase in temperature therefore cannot disrupt the solution to any greater extent. However η_o decreases more rapidly than η since the thermal energy provided has a disordering effect on the solvent structure. The B- coefficient therefore increases i.e. $\eta/\eta_o >$ with increasing temperature. The Cl^- and Br^- ions appear to have little structural effect on the solvent. Thus as the temperature is increased both η and η_o decrease at the same rate and the B- coefficients vary little with temperature.

These findings can be explained using the Stokes and Mills postulate. For the structure-making cations, η^E will be large and positive and η^A will also be positive. As structure-breaking is minimal for these ions then η^D will be

negative but small. Therefore $\eta^E + \eta^A > \eta^D$ and large positive B values will result. The negative $\partial B/\partial T$ values can be explained by assuming that η^A decreases as the temperature increases . η^E and η^D would change little with temperature. This gives B- coefficients which become smaller as the temperature increases. For Cl^- and Br^- η^E and η^D are approximately equal. The small surface charge densities are unable to produce a high degree of long range order and η^A is therefore small but positive. The overall effect is that $\eta^E + \eta^A > \eta^D$ and positive B- values result. This model changes very little with temperature and therefore the B- coefficients are approximately independent of temperature. For structure -breaking ions η^E will be small and η^D is also small for I^- in formamide. Again η^A holds the balance between positive and negative B- coefficients. From this approach it would seem that η^D is always small in formamide and even for ions which can be shown to be structure-breakers in formamide positive B- coefficients are obtained. As the temperature is raised η^D becomes smaller and η^E and η^A remain the same. The B-coefficents would then become positive as the temperature increased.

The two salts studied at 25°C to enable the Krumgal'z method of B- coefficient division to be used are worthy of note. The B- coefficients of $(C_4H_9)_4N$ I and $(C_5H_{11})_4$ NI were large and positive and exhibited similar values to those obtained for tetra-alkylammonium salts in most other solvents. At first glance the very

large ions would appear to disturb the solvent structure and cause some structure-breaking. However the size of the ions gives very large η^E values and η^A is small as also is η^D resulting in large B- coefficients for the tetra-alkylammonium ions.

The foregoing discussion indicates that in formamide an ion may be a net structure-breaker, whilst still having a positive B- coefficient. The criterion that structure-breakers have negative B- coefficients as in aqueous solution is invalid in formamide. Perhaps in this solvent the border between structure-ordering and structure-disordering ions should be taken as a B- coefficient of 0.100 $dm^3\ mol^{-1}$. A quantitative theory to explain B- coefficients must therefore take into account the different criteria to be considered for each solvent system. Solvents such as water and formamide which are capable of associating in three dimensions are extremely complex media, and the straightforward treatment outlined above to explain the observations may therefore be too simple.

4.12 VISCOSITY AS A RATE PROCESS

In the theory of the viscosity of liquids, Eyring[2] considered that molecules displaced relative to one another in the course of viscous flow had to overcome an energy barrier between the adjacent positions. He argued that since the flow of a liquid is a rate process, in as much as it takes place with a definite velocity under given conditions, then the theory of absolute reaction rates could be reasonably applied to the problem of viscosity. He considered a lattice model with a certain proportion

of the lattice points consisting of holes. If two layers of molecules in a liquid at a distance λ_1 apart are considered to be sliding past one another under the influence of an applied force, then the coefficient of viscosity of the liquid η is by definition

$$\eta = \frac{f \lambda_1}{\Delta u} \qquad (4.11)$$

where λ_1 is the distance between the two liquid layers of unit surface area, f is the shear force tending to displace one layer with respect to the other and Δu is the relative velocity of the two layers. In this model, it is assumed that the motion of one layer with respect to the other involves the passage of a molecule from one equilibrium position to another in the same layer. For this to occur, a suitable vacancy or hole must be formed by pushing away the molecules in the liquid and this requires a certain amount of energy. The jump of the molecule from its equilibrium position to an adjacent one can therefore be regarded as equivalent to overcoming a potential energy barrier. Figure (4.10) shows the lattice model considered. λ is the distance between two adjacent positions in the direction of the flow and whereas it is not necessarily identical with λ_1 it is assumed to be so. It is further assumed, that if no external shearing force acts on the liquid, the potential energy barrier is symmetrical, fig(4.11) and the distance between the initial position and the maximum potential energy is $\lambda/2$. The activated state corresponding to the top of the potential energy barrier is therefore midway between the two equilibrium positions. By considering the rate constant for viscous flow from

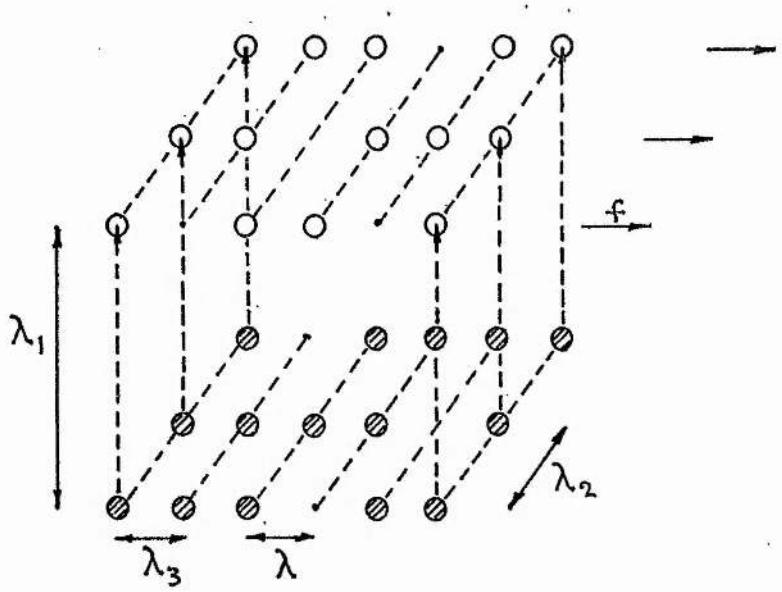

FIG. 4·10

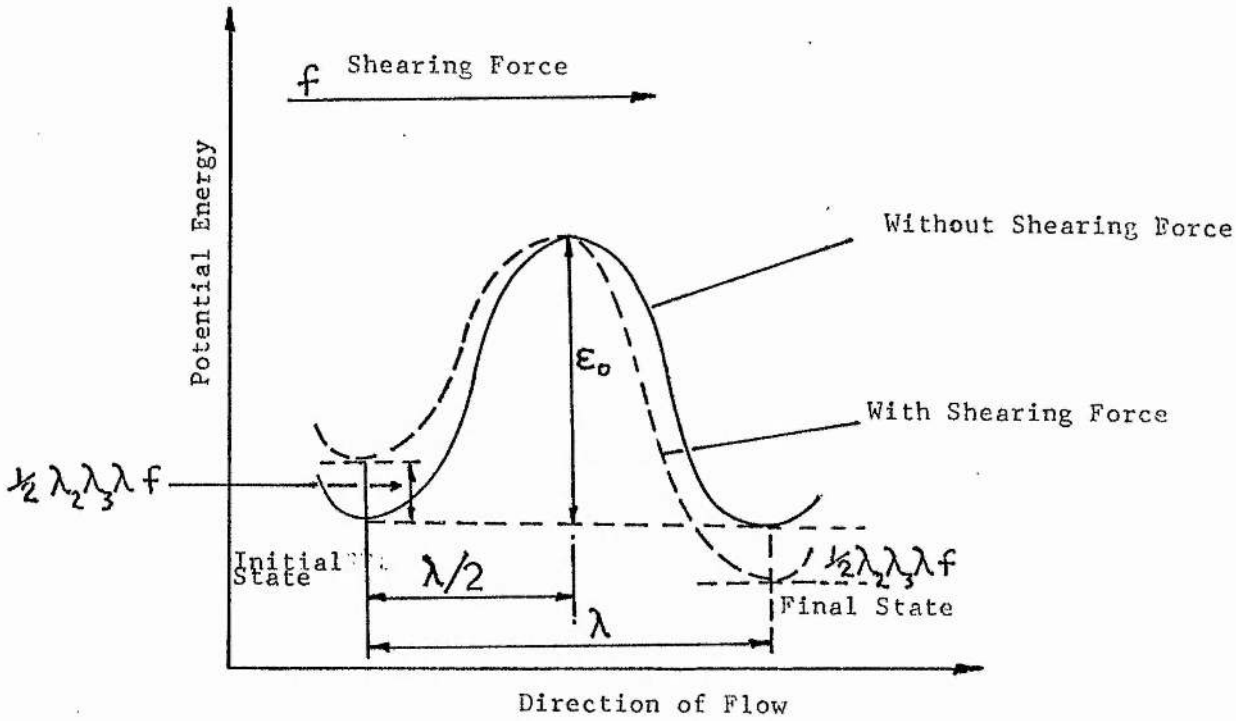

FIG. 4·11

the absolute reaction rate theory and the specific rate of the forward and backward movements Eyring obtained the relationship

$$1/\eta = \frac{hN}{V} e^{-\Delta G^*/RT} \qquad (4.12)$$

where ΔG^* is the standard free energy of activation per mole, h is Planck's constant, N is Avogadro's number, V is the molar volume of the liquid and R is the gas constant.
Since $\Delta G^* = \Delta H^* - T\Delta S^*$
equation (4.12) can be written as

$$\eta = \frac{hN}{V} e^{-\Delta S^*/R} e^{\Delta H^*/RT} \qquad (4.13)$$

assuming ΔS^* is constant and the molar volume of the liquid does not change over the temperature range considered, equation (4.13) can be represented as

$$\eta = A e^{\Delta H^*/RT} \qquad (4.14)$$

where ΔH^* is the energy of activation for viscous flow.
Both Anrade and Arrhenius [101,102] obtained empirical relationships of this form.
Rewriting equation (4.14) gives

$$\Delta H^* = R \, d\ln \eta / d(1/T) \qquad (4.15)$$

4.13 PODOLSKY MODEL

Podolsky [3] also used a lattice model to study transport processes in liquids. He defined the rate of a generalised transport process as

$$\Pi = k_\pi \lambda^2 e^{(-\Delta G^*/RT)} \qquad (4.16)$$

where Π was equal to D, the self diffusion coefficient

of the pure liquid, or ϕ the fluidity of the solution, or U the absolute mobility of an ion. λ was the distance between the lattice sites , and k was the factor in the absolute reaction rate expression. This treatment was equivalent to assigning different activation energies to sets of particles distributed simultaneously among lattice sites of equal spacing. Podolsky assumed that perturbed and unperturbed solvent molecules and ions used the same mechanism for transport, and that λ was constant. From the application of this theory to the viscosity of aqueous solution, he showed that log U was linear with the Jones-Dole B- coefficient for the ions. This relationship was not obeyed for formamide solution.

4.14 NIGHTINGALE AND BENCK MODEL

In 1959, Nightingale and Benck[97] suggested that the effect of a strong electrolyte on the viscosity of a solvent could also be treated as a rate process. By substitution of the Jones-Dole equation (1,8) for the viscosity of a dilute electrolyte solution into equation (4.15) they obtained

$$\Delta H^{*} = \frac{R \, d\ln \left[\eta_o(1 + Ac^{\frac{1}{2}} + Bc)\right]}{d(1/T)} \qquad (4.17)$$

For dilute electrolytes, the influence of the interionic attraction on the viscosity of the solution can be considered negligible

$$\therefore \quad \Delta H^{*} \simeq R \, \frac{d\ln \left[\eta_o(1 + Bc)\right]}{d(1/T)} \qquad (4.18)$$

equation (4.18) may be rewritten as

$$\Delta H^* = R \, d\ln \eta_o / d(1/T) + \left[R/(1+Bc) \times d(1+Bc)/d(1/T) \right] \quad (4.19)$$

In a similar manner to the Eyring approach, the free energy of activation for viscous flow is given by

$$\Delta G^* = RT \ln \frac{\eta V}{hN} \quad (4.20)$$

In equation (4.19) the left hand term can be identified as the total activation enthalpy of the solution and the first term on the right hand side can be identified as the activation enthalpy of the solvent. Therefore

$$\Delta H^*_{\eta} = \Delta H^*_{\eta_o} + \Delta H^*_{\eta_s} \quad (4.21)$$

where $\Delta H^*_{\eta s}$ may be considered as representing the increase or decrease in the activation enthalpy of the pure solvent due to the presence of the solute ions. Since $\Delta H^*_{\eta_s}$ is considered to represent the total ionic effects equation (4.21) may be rewritten

$$\Delta H^*_{\eta} - \Delta H^*_{\eta_o} = \nu^+ \Delta H^*_+ + \nu^- \Delta H^*_- \quad (4.22)$$

where ΔH^*_+ and ΔH^*_- represent the effect on the activation enthalpy due to each individual cation and anion and ν^+ ν^- are the number of cations and anions respectively per molecule of solute. Nightingale has divided aqueous $\Delta H^*_{\eta_s}$ values assuming that $\Delta H^*_{\eta\, K^+} = \Delta H^*_{\eta\, Cl^-}$. From the ionic $\Delta H^*_{\eta_\pm}$ values obtained he showed that a qualitative relationship existed between ionic $\Delta H^*_{\eta_\pm}$ values and ionic B- coefficients in aqueous solution.

Structure-making ions having positive B- ceofficients have

positive enthalpies of activation and structure-breaking ions with negative B- coefficients have negative enthalpies of activation. McDowall [38] has applied the Nightingale method to his viscosity measurements in formamide. He concluded that although his data was insufficiently precise to calculate reliable ionic enthalpies the above qualitative relationship was obeyed for the total enthalpies of activation of the electrolytes.

4.15 FEAKINS MODEL

More recently Feakins et al [98] have applied transition state theory with a slightly different approach. From Eyring's theory

$$\eta_R = \eta / \eta_o = V_o/V \; e^{(\Delta G^{\ddagger} - \Delta G^{\ddagger}_o)\, RT} \qquad (4.23)$$

Expanding the Jones-Dole equation

$$\eta_R = 1 + Ac^{\frac{1}{2}} + Bc \qquad (4.24)$$

As $\ln \eta_R = (Ac^{\frac{1}{2}} + Bc) - \frac{1}{2}(Ac^{\frac{1}{2}} + Bc)^2 + \text{----}$ (4.25)

i.e. $\ln \eta_R = Ac^{\frac{1}{2}} + (B - A^2/2)\, c + \text{------}$ (4.26)

and omitting $A^2/2$ and higher terms which are normally outwith the precision of the measurements gives

$$\ln \eta_R \doteq Ac^{\frac{1}{2}} + Bc \qquad (4.27)$$

Combining equation (4.23) and (4.27) gives

$$Ac^{\frac{1}{2}} + Bc = \ln V_o/V + (\Delta G^{\ddagger} - \Delta G^{\ddagger}_o)/RT \qquad (4.28)$$

where the subscript zero refers to the solvent, and the parameters without subscript refer to the solution. Ignoring ion-ion effects equation (4.28) can be written as

$$Bc = \ln V_o/V + (\Delta G^{\ddagger} - \Delta G_o^{\ddagger})/RT \qquad (4.29)$$

V, the average molar volume of the solution is given by

$$V = X_o \bar{V}_o + X_1 \bar{V}_1 = \bar{V}_o - X_1(\bar{V}_o - \bar{V}_1) \qquad (4.30)$$

where $\bar{V}_o^o$ and $\bar{V}_1^o$ are the partial molar volumes of the solvent and solute respectively.

$$\bar{V}_o^o = V_o = M_o/\rho_o \qquad (4.31)$$

where M_o is the molecular weight of the solvent and ρ_o its density. As X_1 tends to zero

$$X_1 = M_o\, c/1000\,\rho_o \qquad (4.32)$$

$$\text{and } \ln (V_o/V) = X_1(\bar{V}_o^o - \bar{V}_1^o)/\bar{V}_o^o \qquad (4.33)$$

$$\therefore \ln (V_o/V) = c(\bar{V}_o^o - \bar{V}_1^o)/1000 \qquad (4.34)$$

Now

$$\Delta G^{\ddagger} = X_1 \Delta\mu_1^{o\ddagger} + (1 - X_1)\Delta\mu_o^{o\ddagger} \qquad (4.35)$$

where $\Delta\mu_o^{o\ddagger} = \Delta G_o^{\ddagger}$, the free energy of activation per mole for the pure solvent and $\Delta\mu_1^{o\ddagger}$ is the contribution per mole of the solute to the free energy of activation for viscous flow of the solution.

$$\therefore (\Delta G^{\ddagger} - \Delta G_o^{\ddagger}) = X_1 (\Delta\mu_1^{o\ddagger} - \Delta\mu_o^{o\ddagger}) \qquad (4.36)$$

combining equations (4.29), (4.34) and (4.36) gives

$$B = (\bar{V}_o^o - \bar{V}_1^o)/1000 + (M_o/1000\,\rho_o)(\Delta\mu_1^{o\ddagger} - \Delta\mu_o^{o\ddagger})/RT \qquad (4.37)$$

or

$$B = (\bar{V}_o^o - \bar{V}_1^o)/1000 + (\bar{V}_o^o/1000)(\Delta\mu_1^{o\ddagger} - \Delta\mu_o^{o\ddagger})/RT \qquad (4.38)$$

Feakins[98] has calculated $\Delta\mu_1^{o\ddagger}$ values for salts in both aqueous and non-aqueous solutions from equation (4.37)

Equation (4.38) was used to calculate the contribution per mole of solute $\Delta\mu_i^{o\neq}$ to the free energy of activation for viscous flow of the formamide solutions and the results are shown in table (4.7). The free energy of activation per mole for the solvent $\Delta\mu_o^{o\neq}$ was calculated from the Eyring equation[2] (4.20).

$$\Delta\mu_o^{o\neq} = \Delta G_o^{\neq} = RT \cdot \ln (\eta_o \cdot \bar{V}_o^o / hN) \qquad (4.39)$$

TABLE 4.7

	$\Delta\mu_i^{o\neq}$ / kJ mol^{-1}				$\Delta H_i^{o\neq}$ / kJ mol^{-1}	$\Delta S_i^{o\neq}$ / J k^{-1}mol^{-1}
	25°C	35°C	45°C	50°C	25°C	25°C
LiBr	40.8 (±0.2)	39.5 (±0.6)	38.7 (±0.3)		71.9 (±2.4)	104.6 (± 8)
NaCl	47.4* (±0.3)	46.3 (±0.3)	45.0 (±0.3)	44.7 (±0.3)	80.2 (±3.0)	110.1 (±10)
NaBr	44.1 (±0.4)	43.5 (±0.4)	42.1 (±0.4)	41.1 (±0.4)	79.8 (±3.9)	119.8 (±13)
KCl	36.5 (±0.3)	35.7 (±0.2)	35.0 (±0.3)	34.5 (±0.3)	60.0 (±0.6)	78.8 (± 2)
RbI	32.0 (±0.3)					
CsCl	34.1 (±0.3)	33.7 (±0.3)	33.2 (±0.5)	33.0 (±0.4)	47.6 (±0.6)	45.2 (± 2)
CsBr	31.9 (±0.2)	31.6 (±0.5)	31.0 (±0.4)	30.8 (±0.2)	45.9 (±0.6)	46.9 (± 2)
CsI	30.8 (±0.2)	30.6 (±0.2)	30.4 (±0.2)	30.2 (±0.3)	37.1 (±0.6)	21.3 (± 2)
	Activation parameters for formamide					
	14.4 (±0.01)	14.3 (±0.01)	14.2 (±0.01)	14.2 (±0.01)	17.1 (±0.3)	9.0 (± 1)

* Extrapolated Value

The $\bar{V}_1^o$ values in the above calculation were taken from the data by Gopal[99] and by Bruno and Della Monica[100] which are shown in table (4.8).

TABLE 4.8

SALT	$\bar{V}_1^o$	Ref.	SALT	$\bar{V}_1^o$	Ref.
LiBr	28.3	100	RbI	54.65	99
NaCl	21.1	99	CsCl	42.3	99
NaBr	28.0	99	CsBr	49.3	99
KCl	32.0	99	CsI	61.05	99

By measuring B- coefficients as a function of temperature, the activation entropy and enthalpy contributions due to the solute were evaluated from equations (4.40) and (4.41).

$$\Delta S_1^{o\neq} = -d(\Delta\mu_1^{o\neq})/d\,T \qquad (4.40)$$

$$\Delta H_1^{o\neq} = \Delta\mu_1^{o\neq} + T\Delta S_1^{o\neq} \qquad (4.41)$$

Table (4.7) also contains the $\Delta S_1^{o\neq}$ and $\Delta H_1^{o\neq}$ values for the salts investigated. The activation parameters for NaCl and NaBr were calculated from B- coefficients taken from reference (38).

Table (4.9) compares the $\Delta\mu_1^{o\neq}$ values for anions with a common cation and cations with a common anion.

TABLE 4.9

			kJ mol^{-1}
$(\Delta\mu_1^{o\neq})_{NaCl}$	-	$(\Delta\mu_1^{o\neq})_{NaBr}$	= 3.3
$(\Delta\mu_1^{o\neq})_{CsCl}$	-	$(\Delta\mu_1^{o\neq})_{CsBr}$	= 2.2
$(\Delta\mu_1^{o\neq})_{NaCl}$	-	$(\Delta\mu_1^{o\neq})_{CsCl}$	= 13.3
$(\Delta\mu_1^{o\neq})_{NaBr}$	-	$(\Delta\mu_1^{o\neq})_{CsBr}$	= 12.2

4.16 DISCUSSION OF ACTIVATION PARAMETERS

$\Delta S_1^{o\neq}$ and $\Delta H_1^{o\neq}$ for all electrolytes investigated were found to be large and positive, as also reported for dimethyl sulphoxide solutions.[60] In aqueous solutions on the other hand NaCl, KCl, RbCl and CsCl have negative values for these parameters.[98] LiCl which is considered a net structure-maker in water has a positive $\Delta H_1^{o\neq}$ value but a negative $\Delta S_1^{o\neq}$ value. In formamide as in aqueous solutions, the activation parameters decrease with increasing crystal radius of the cations. This trend is reversed for Li^+ and Na^+.

Feakins et al [98] have shown that for net structure-makers $\Delta\mu_1^{o\neq} > \Delta\mu_o^{o\neq}$, and $\Delta\mu_1^{o\neq} < \Delta\mu_o^{o\neq}$ for net structure-breakers. All electrolytes investigated in formamide therefore are net structure-makers. The contributions of the solutes to the molar free energy of activation of the solutions $\Delta\mu_1^{o\neq}$ are between two and three times that of the pure solvent. The formation of the transition state is therefore less favourable in the presence of these electrolytes.

Inspection of equation (4.38) indicates that activation parameters for the salts cannot readily be divided into ionic contributions, thus equation (4.38) can be rewritten as

$$B_+ + B_- = \frac{\bar{V}^\circ_o}{1000}\left(1-\frac{\Delta\mu^{\circ\neq}_o}{RT}\right) - \frac{\bar{V}^\circ_+}{1000} - \frac{\bar{V}^\circ_-}{1000} + \frac{\bar{V}^\circ_o}{1000RT}\left(\Delta\mu^{\circ\neq}_+ + \Delta\mu^{\circ\neq}_-\right) \quad (4.42)$$

Let $\phi = \bar{V}^\circ_o\left(1-\frac{\Delta\mu^{\circ\neq}_o}{RT}\right)$ and $\vartheta = \bar{V}^\circ_o/RT$

Then

$$(1000\,B_+ + \bar{V}^\circ_+) = \phi X + \vartheta\,\Delta\mu^{\circ\neq}_+ \quad (4.43)$$

and

$$(1000\,B_- + \bar{V}^\circ_-) = \phi\,(1-X) + \vartheta\,\Delta\mu^{\circ\neq}_- \quad (4.44)$$

The crucial factor in determining ionic activation values therefore is the division of ϕ between the cation and the anion. Calculation of ionic activation values for aqueous solutions by this method indicates that ϕ is not divided equally between the cation and the anion when the values are correlated with the ionic values of Feakins[98] obtained assuming equal contributions for K^+ and Cl^-. However, as knowledge of ionic activation parameter values would provide a useful insight into ion-solvent interactions, and since the consistency of differences in the $\Delta\mu_1^{\circ\neq}$ values has been shown above (Table 4.9) it was decided to split the electrolyte activation parameters using an assumption similar to Feakins.[98] The cation and the anion with the most similar B- coefficients in formamide for which activation parameters have been determined are Cs^+ and Cl^-. The $\Delta\mu_1^{\circ\neq}$, $\Delta H_1^{\circ\neq}$, and $\Delta S_1^{\circ\neq}$ values therefore have been divided into ionic contributions assuming equal values for Cs^+ and Cl^- and are shown in table (4.10).

TABLE 4.10

Ion	$\Delta\mu_1^{o\neq}$ / kJ mol^{-1} 25°C	$\Delta H_1^{o\neq}$ / kJ mol^{-1} 25°C	$\Delta S_1^{o\neq}$ / J K^{-1}mol^{-1} 25°C	$T\Delta S_1^{o\neq}$ / kJ mol^{-1}
Li^+	25.95	49.8	80.3	23.9
Na^+	30.35	56.4	87.5	26.1
K^+	19.45	36.2	56.2	16.7
Rb^+	18.25			
Cs^+	17.05	23.8	22.6	6.7
Cl^-	17.05	23.8	22.6	6.7
Br^-	14.85	22.10	24.3	7.2
I^-	13.75	13.3	-1.3	-0.4
		Formamide Parameters		
	14.4	17.08	9.0	

For the ions Li^+, Na^+, K^+, Cs^+, Cl^- and Br^- both $\Delta H_1^{o\neq}$ and $\Delta S_1^{o\neq}$ values are positive indicating that formation of the transition state is associated with bond-breaking and a decrease in order. The positive $\Delta H_1^{o\neq}$ and negative $\Delta S_1^{o\neq}$ values for I^- suggest that for this ion formation of the transition state is associated with an increase in order. Consideration of the $\Delta\mu_1^{o\neq}$ values shows that only the I^- contribution is less than the free energy of activation for the pure solvent. The formation of the transistion state is therefore more favourable in the presence of the I^- ion than in the pure solvent alone.

This in the Feakins[98] classification is evidence for I^- as a structure-breaker in formamide.

Taking into consideration B- coefficients $\partial B/\partial T$ values and activation parameters for the ions, it can be concluded that cations enhance the structure of formamide, decreasing in the order $Na^+ > Li^+ > K^+ \geqslant Rb^+ > Cs^+$. The anions Cl^- and Br^- show neither definite structure- making nor structure-breaking properties in this solvent. Similar conclusions for Br^- in formamide were reached by Somsen[103] from the partial molar heat capacities of CsBr in formamide. Only I^- shows definite structure- disrupting properties in formamide. These trends in the order of ion-solvent interactions in formamide : are in close agreement with those found from solvation numbers in formamide[93]. These observations can be understood in terms of the mechanisms of solvation of protic solvents. Parker[104] has classified solvents under two headings. Protic solvents e.g. water, formamide and methanol are characterised as having protons available for hydrogen-bond formation, whilst dipolar aprotic solvents such as N, N- dimethyl- formamide are only very weak proton donors.

The solvation of cations in protic solvents has been investigated by Parker et al[12] by measuring the free energies of transfer of K^+ from water to formamide. This study demonstrated that K^+ and formamide interacted through the oxygen atom of the amide. The C - O bond of the formamide molecules in the first solvation sphere around a K^+ ion was considered as having less than full double bond character. The bonding in these molecules was thought to be more like structure (4.12) than the normal structure (4.13)

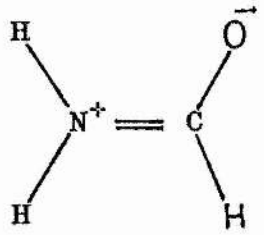

(4.12)

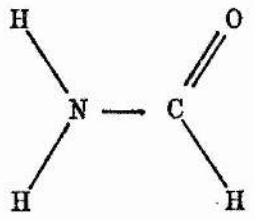

(4.13)

and alkali metal ions such as K^+ were considered to show purely electrostatic ion-solvent interactions in this solvent.

It has been shown [104] that the solvation of anions in protic solvents decreases strongly in the series OH^-, $F^- \gg Cl^- > Br^- > N_3^- > I^-$. Anions are solvated by ion-dipole interactions, on which is superimposed a strong hydrogen-bond which is greatest for small anions e.g.

Small anions e.g. F^- and Cl^- are strong hydrogen-bond acceptors and therefore in protic solvents they show strong hydrogen-bonding interactions rather than specific 1:1 ion-dipole interactions. For large anions such as I^- localisation of the charge occurs resulting in weak hydrogen-bond acceptors. As these anions have small charge densities their ion-dipole interactions are weak. Large anions therefore show only weak ion-solvent interactions in formamide.

CHAPTER FIVE

5.A BINARY LIQUID MIXTURES

5.1 INTRODUCTION

The study of binary liquid mixtures provides a method of investigating the physical forces acting between two molecules of different species. Initial predictive attempts to explain the properties of liquid mixtures were based on the assumption that the A - B forces between two molecules A and B were always determinable from the strengths of the forces A -A and B - B. If the A-B forces were always some average of the A - A and B - B forces, then the properties of binary mixtures would be predictable , in principle, from a knowledge of the pure components alone. However, such averaging is not universally valid and is unsatisfactory for many classes of substances and inadequate for detailed interpretation of even the simplest mixtures. The observed properties of a binary mixture should be used as a source of information about the A-B forces. In recent years, the emphasis has changed from attempts to explain the properties of liquid mixtures solely from a knowledge of those of the pure components to attempts to derive the observed properties by statistical mechanical theory[105] and group solution models[106]. The term complex formation is often used when strong specific interactions exist between the molecules of the mixture. However, the general situation involves the correlated motion of two or more molecules over a time which may last from picoseconds to many seconds. Thus very weak interactions will also alter the time averaged behaviour of the system and lead to thermodynamic quantities which are

not the averages of the properties of the pure components.

In an analogous manner to the study of ion-solvent interactions in electrolyte solutions, viscosity measurements have been widely used[107,108] to investigate solute-solvent interactions in binary liquid mixtures. Since formamide and the first four members of the n-alcohol homologous series are all associated liquids, it was considered that strong specific interactions might exist in binary mixtures of these components and that such interactions could be monitored by measuring the viscosity of the mixtures. The viscosity of binary mixtures of formamide in methanol, ethanol, propan-1-ol and butan-1-ol was therefore determined over a range of temperature between 20°C - 50°C. The formamide/methanol system has been studied by Merry and Turner[109], Kozlowski[110] and also McDowall[38] at a series of temperatures, but no evidence for complex formation between these two components has been found. Merry and Turner also investigated ethanol /formamide binary liquid mixtures and again concluded that no strong specific interactions were present[109].

5.2 EXPERIMENTAL

Binary liquid mixtures were prepared by weight and all solutions were stored in flasks with ground glass joints, and sealed with a paraffin film. The viscosity and density of the prepared solutions were determined by the procedures described in chapter II.

5.3 RESULTS AND DISCUSSION

The absolute viscosities for the binary liquids, calculated from the viscometer constants, the efflux times

and the densities of the solutions are shown in graphical form for the four systems at the chosen temperatures in figs. (5.1)-(5.4). The numerical results are tabulated in Appendix 4.

In the following discussion, methanol/formamide will be termed system 1, ethanol/formamide system 2, propan-1-ol/formamide system 3 and butan-1-ol/formamide system 4. From figs. (5.1) and (5.2) the viscosity of systems 1 and 2 decrease constantly from formamide to alcohol. The shapes of these isotherms are characteristic of systems in which no addition compounds or addition compounds of low stability are formed[111]. The negative deviations from additivity of the viscosity of these systems does not necessarily mean that the alcohols do not interact with formamide in the sense of hydrogen-bond formation. However, the main factor producing a viscosity isotherm of this shape is probably the disruption of the hydrogen-bonded formamide structure. The solute-solvent interactions occuring in these systems are insufficiently strong to exceed this negative influence and therefore no viscosity maximum is observed.

The propan-1-ol/formamide system displays S-shaped viscosity isotherms. At 20°C the curve has a point of inflection but no viscosity maximum. However, of the fifteen solutions studied for this system, a solution of composition $X_f = 0.0486$ had a viscosity at 20°C less than that for pure propan-1-ol. This type of isotherm is considered to be the result of the formation of a compound of low stability[111]. In this system the contribution of the compound to the viscosity of the mixture is insufficient

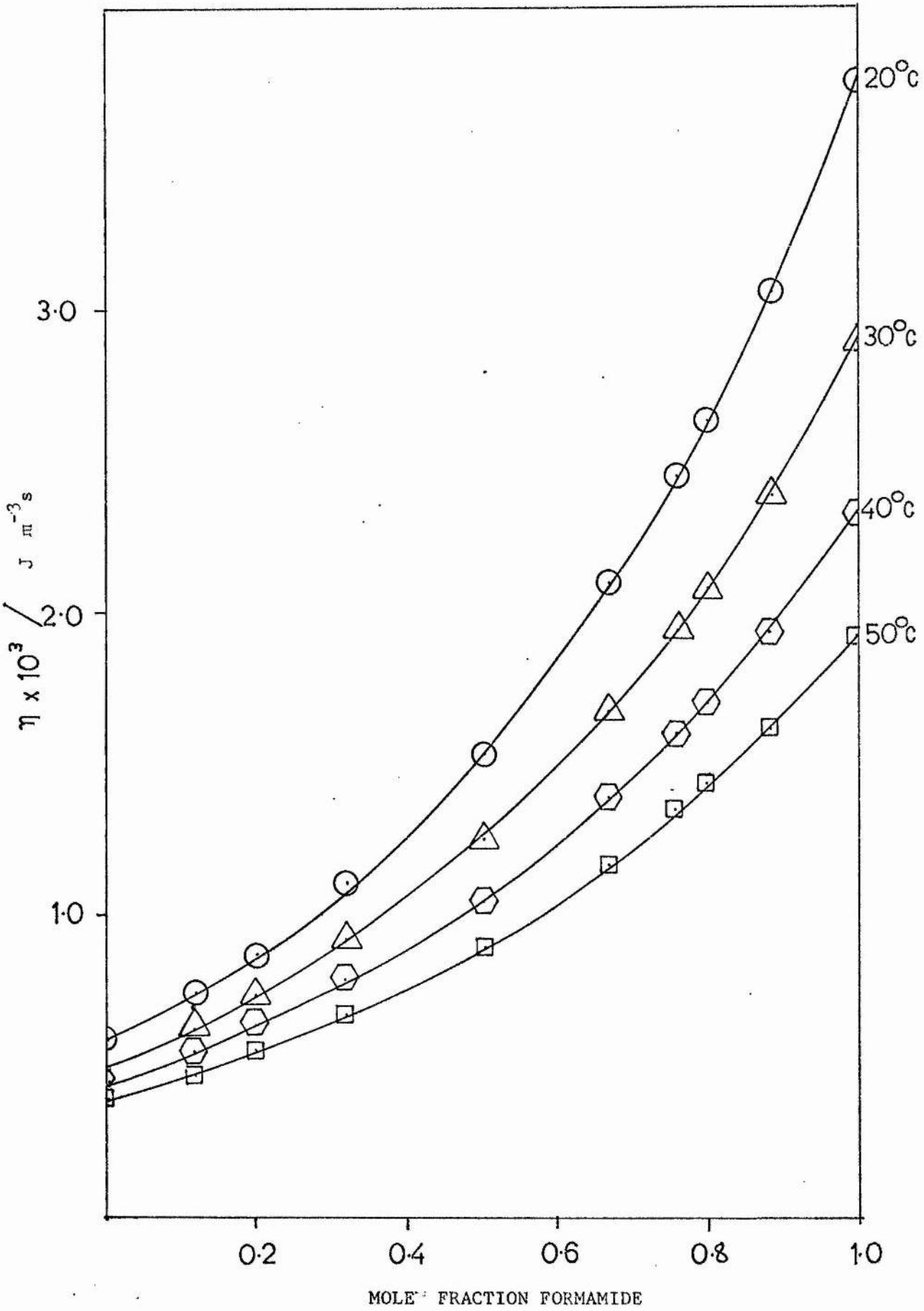
20°c
30°c
40°c
50°c
3·0
2·0
1·0
η x 10³ / J m⁻³s
0·2
0·4
0·6
0·8
1·0
MOLE FRACTION FORMAMIDE

FIG. 5·1

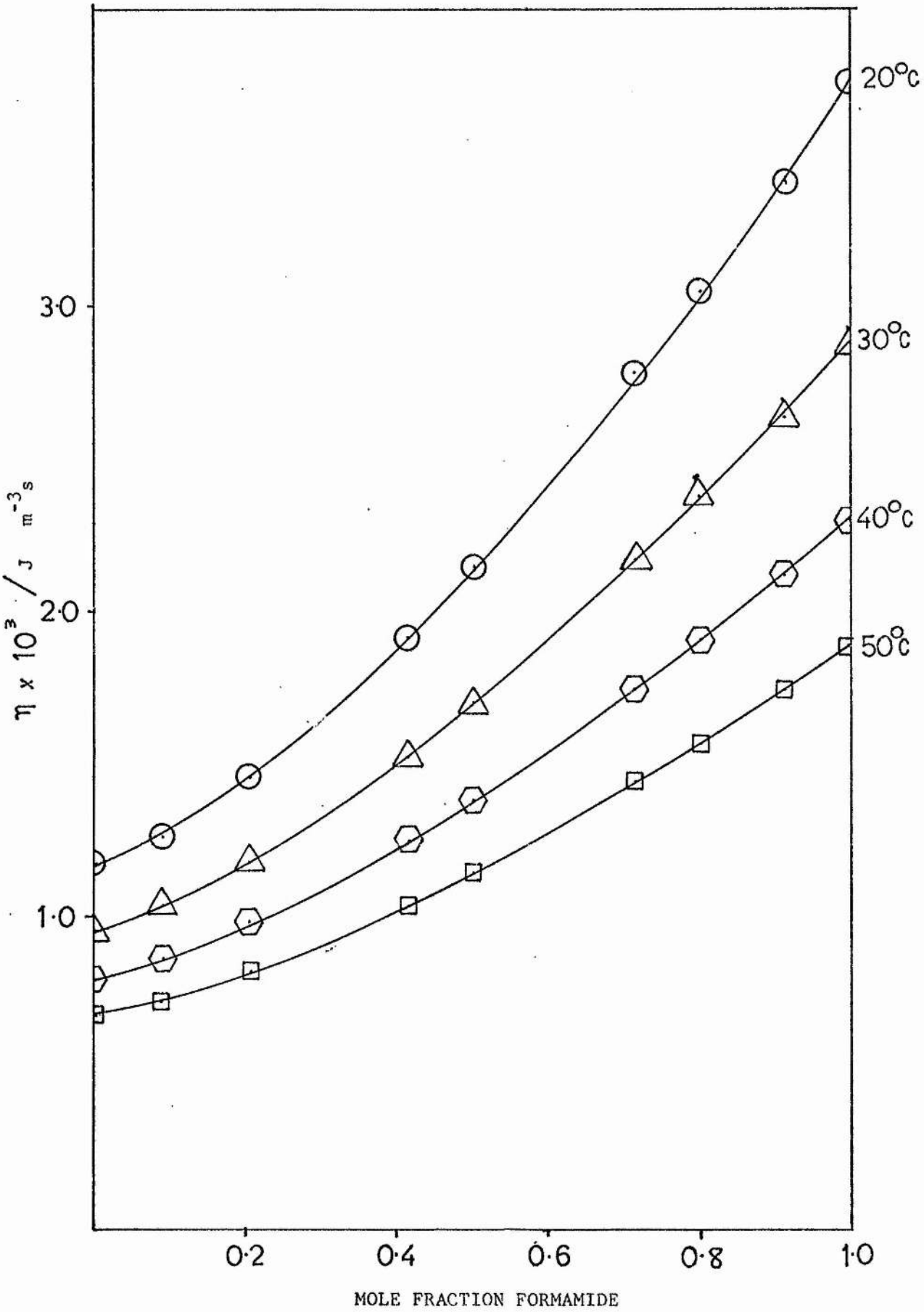
20°c
30°c
40°c
50°c
3·0
2·0
1·0
η x 10³ / J m⁻³s
0·2
0·4
0·6
0·8
1·0
MOLE FRACTION FORMAMIDE

FIG. 5·2

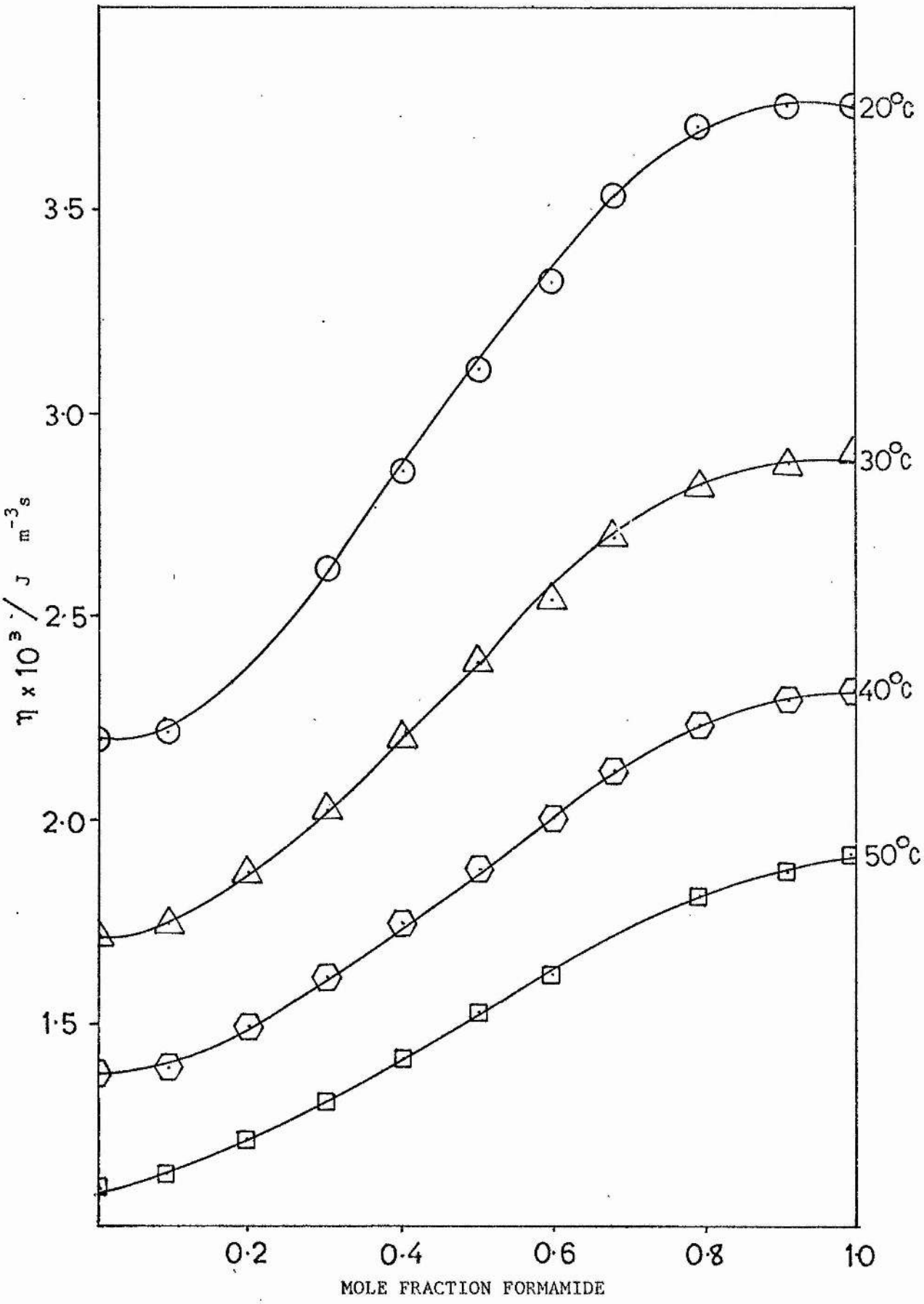
20°c
30°c
40°c
50°c
3·5
3·0
2·5
2·0
1·5
η x 10³ / J m⁻³s
0·2
0·4
0·6
0·8
1·0
MOLE FRACTION FORMAMIDE

FIG. 5·3

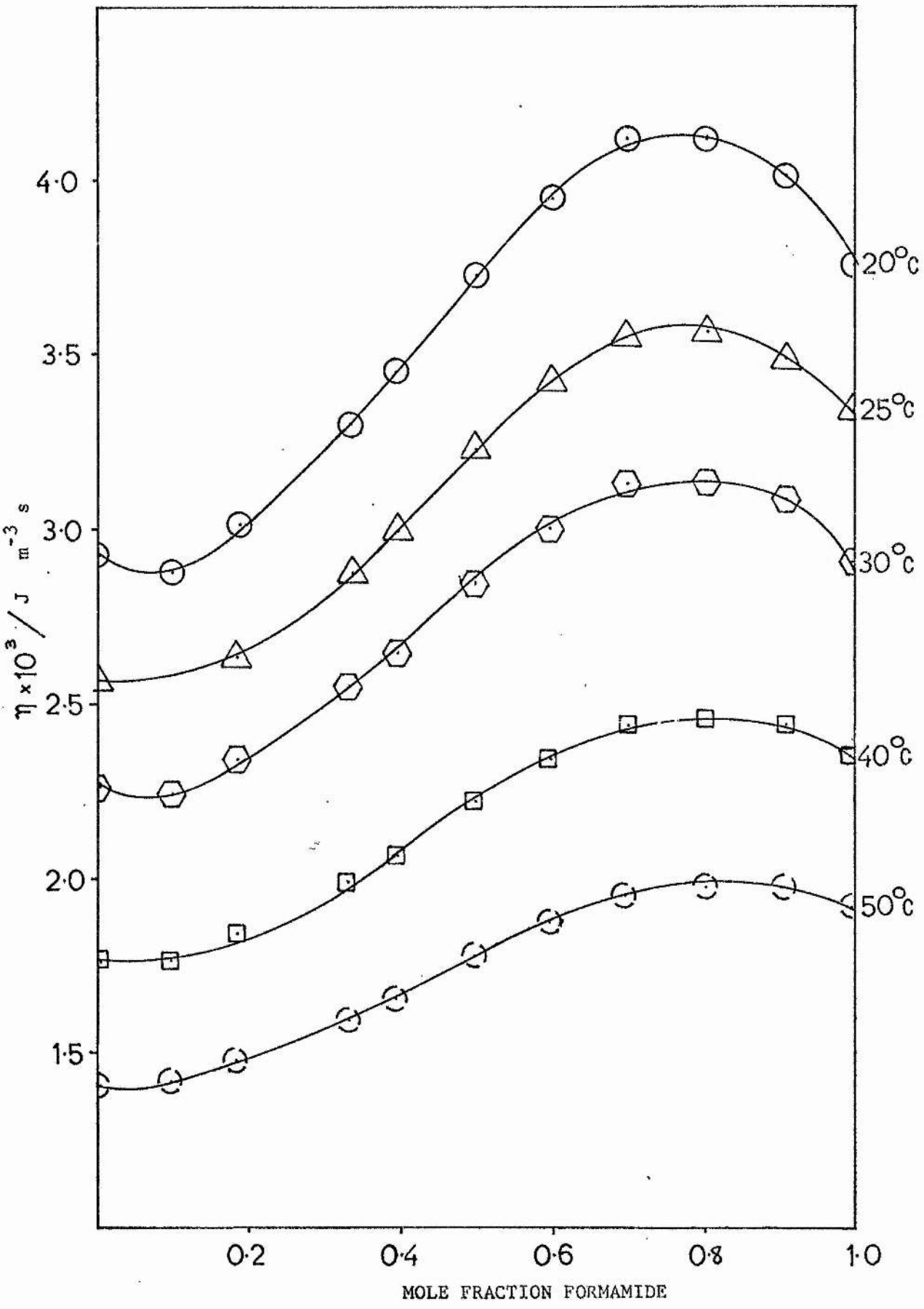
4·0
3·5
3·0
2·5
2·0
1·5
η x10³ / J m⁻³ s
0·2
0·4
0·6
0·8
1·0
MOLE FRACTION FORMAMIDE
20°c
25°c
30°c
40°c
50°c

FIG. 5·4

to produce a viscosity maximum.

The butan-1-ol/formamide binary liquids are characterised by, more pronounced S-shaped isotherms than the propan-1-ol system at the four temperatures investigated, suggesting that a compound is formed which is more stable than that between propan-1-ol and formamide. Both minima and maxima occur in this system. The minimum is found towards the lower viscosity component and is probably due to the disruption of the hydrogen-bonded liquids, while the maximum, which is displaced towards the more viscous component, may result form the large contribution of the compound to the viscosity of the mixture.

For the first two systems discussed above, as the temperature increased, the negative deviation from additivity became less pronounced. The latter two systems showed less obvious S-shaped isotherms with increase in temperature. The solute-solvent interactions therefore are more easily observed at lower temperatures. The temperature coefficient of viscosity however is an extremely important parameter and is used in a subsequent section to calculate the activation parameters for viscous flow. The reduction in the observed interactions as the temperature is increased is due to the rise in thermal energy of the system, the weak interactions and low stability compounds formed at low temperatures become less stable as the temperature rises. The viscosity of the mixture therefore receives smaller contributions from the compound with the decreasing stability of the latter.

5.4 EXCESS VISCOSITY

The calculation of excess viscosities provides a more quantitative estimate of complex formation in binary liquid mixtures. An excess viscosity η^E is normally defined as[107]

$$\eta^E = \eta - x_1 \eta_1 - x_2 \eta_2 \qquad (5.1)$$

where η is the viscosity of the mixture and the subscripts 1 and 2 refer to the two components. Fort and Moore[107] have correlated the excess viscosity with the maximum heat of mixing of the solutions and have shown that η^E is linear with ΔH^M. From this they concluded that η^E is related to the strength of the interaction between the liquids since ΔH^M is an approximate measure of the strength of the interaction.

The excess viscosities for the four systems studied in formamide were calculated from equation (5.1). Since complex formation is most evident at the lowest temperature, η^E was determined at 20°C only. The results obtained are shown in figs (5.5) and (5.6). Negative excess functions are normally interpretated as indicating no specific interaction between the molecules of the mixture, while positive excess functions are taken to suggest strong interactions and complex formation. Fig (5.5) indicates clearly that both methanol and ethanol/formamide solutions have large negative excess viscosities over the complete concentration range. Propan-1-ol on the other hand shows positive excess viscosities when mixed with formamide at concentrations $x_f \geqslant 0.4$ and above. When small concentrations of formamide are added to propan-1-ol negative excess viscosities are obtained. The maximum negative excess viscosity was

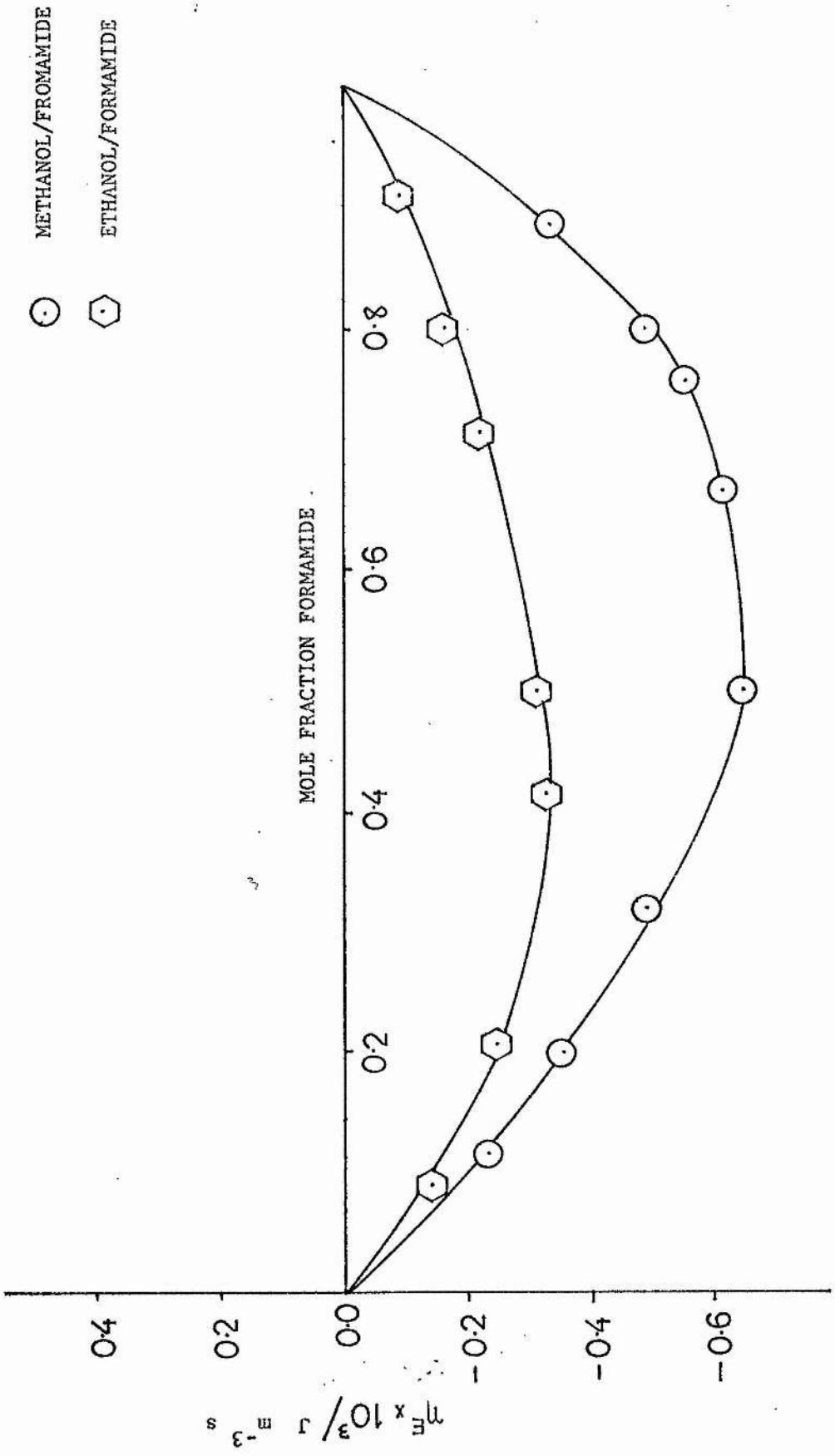
METHANOL/FROMAMIDE
ETHANOL/FORMAMIDE
MOLE FRACTION FORMAMIDE
0·0
0·2
0·4
0·6
0·8
0·4
0·2
-0·2
-0·4
-0·6
$\eta^E \times 10^3$/ J m^{-3} s

FIG. 5·5

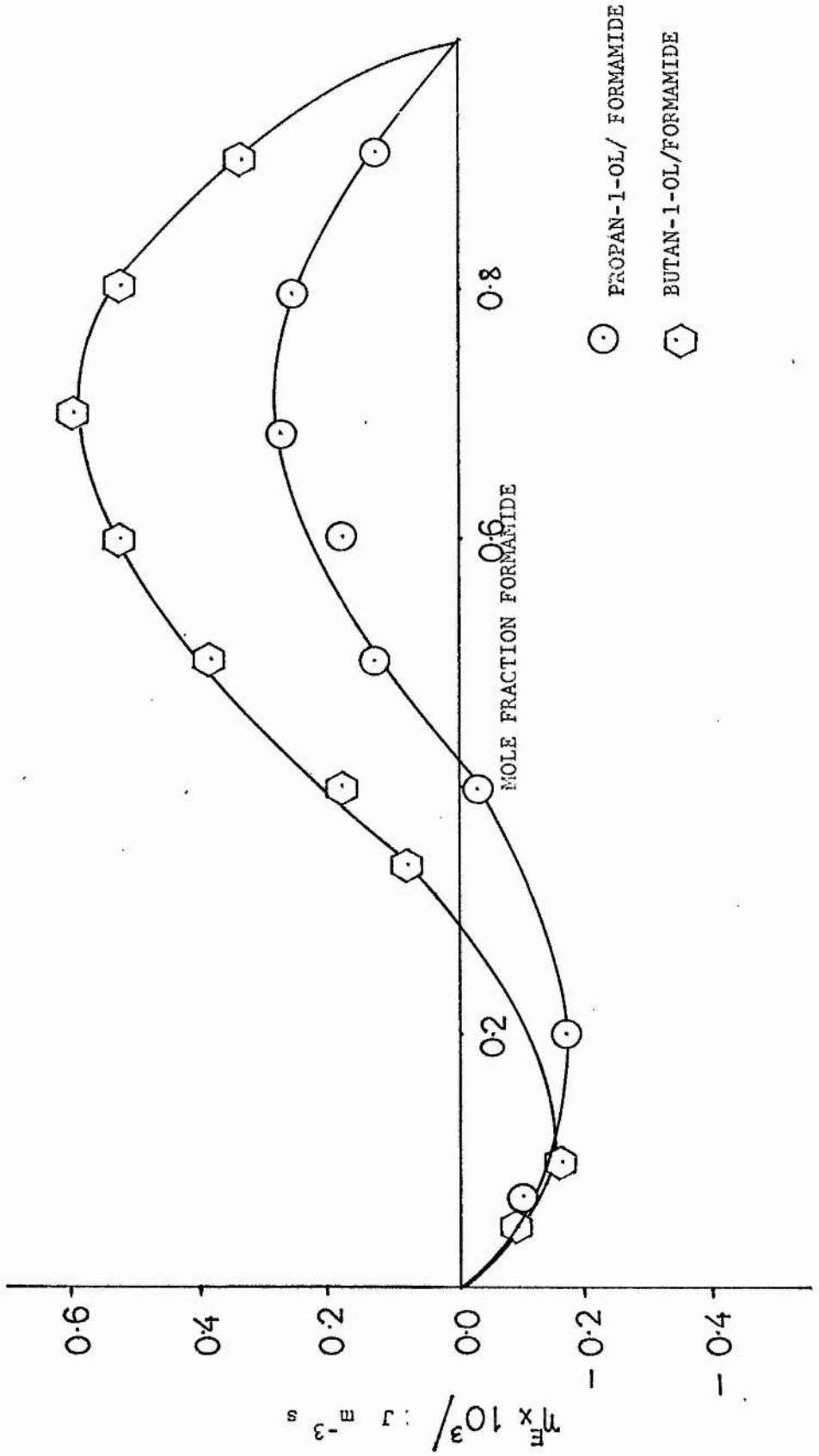
$\eta^E x\ 10^3$ / J m^{-3} s
0·6
0·4
0·2
0·0
− 0·2
− 0·4
0·2
0·6
0·8
MOLE FRACTION FORMAMIDE
PROPAN-1-OL/ FORMAMIDE
BUTAN-1-OL/FORMAMIDE

FIG. 5·6

obtained at $X_f = 0.7$. The butan-1-ol formamide system is also characterised by minimum and maximum turning points in the η^E /mole fraction plot fig. (5.6). The lowest excess viscosity in this system appears at $X_f=0.1$ but the maximum excess viscosity appears at the same concentration as in the propan-1-ol/formamide system, viz. $X_f = 0.7$.

These results confirm that although weak interactions inevitably occur in systems 1 and 2 there is no strong specific interactions and no evidence of complex formation. Systems 3 and 4 on the other hand show signs of strong specific interactions at a concentration of $X_f = 0.7$. With a much higher η^E maximum, system 4 would appear to form a more stable complex than system 3.

5.5 ACTIVATION PARAMETERS FOR VISCOUS FLOW

In chapter 4 (p.110) it was shown that if the variation of molar volume and entropy of activation with temperature is ignored, the viscosity of a liquid can be represented by equation (4.12)

$$\eta = \frac{hN}{V} e^{\Delta G^*/RT} \qquad (5.2)$$

or

$$\eta = \frac{hN}{V} e^{(\Delta H^*/RT - \Delta S^*/R)} \qquad (5.3)$$

so that a plot of $\ln\eta$ against $1/T$ should be linear with a slope of $(\Delta G/2.303R)$. This was found to be true, for the present results and values of ΔH^*, ΔG^* and ΔS^* are shown in appendix 4 for the four systems and illustrated in figs. (5.7 to 5.9)

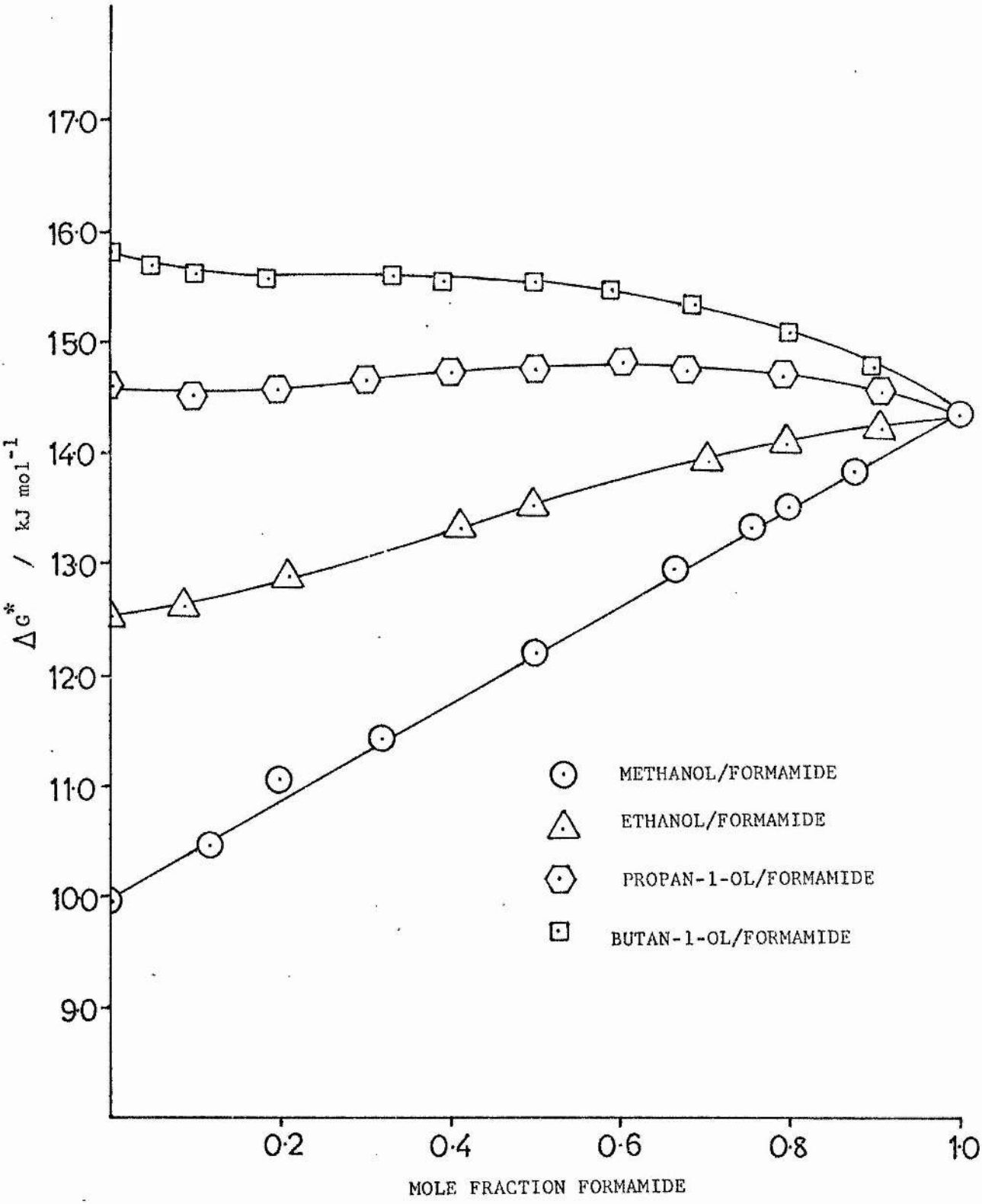
17·0
16·0
15·0
14·0
13·0
12·0
11·0
10·0
9·0
ΔG^* / kJ mol^{-1}
0·2
0·4
0·6
0·8
1·0
MOLE FRACTION FORMAMIDE
METHANOL/FORMAMIDE
ETHANOL/FORMAMIDE
PROPAN-1-OL/FORMAMIDE
BUTAN-1-OL/FORMAMIDE

FIG. 5·7

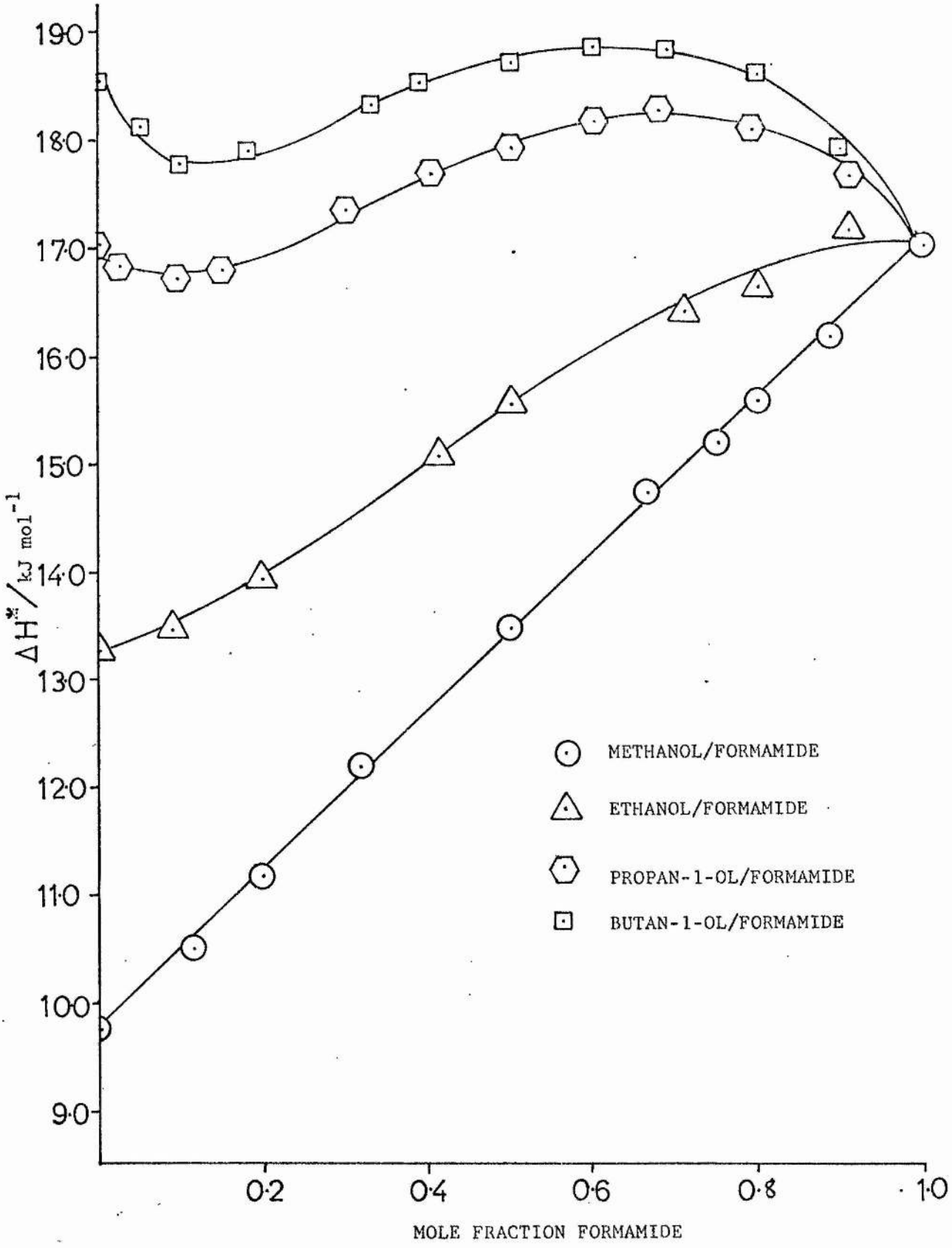
190
180
170
160
150
140
130
120
110
100
90
ΔH^{E} / kJ mol^{-1}
0·2
0·4
0·6
0·8
1·0
MOLE FRACTION FORMAMIDE
METHANOL/FORMAMIDE
ETHANOL/FORMAMIDE
PROPAN-1-OL/FORMAMIDE
BUTAN-1-OL/FORMAMIDE

FIG. 5·8

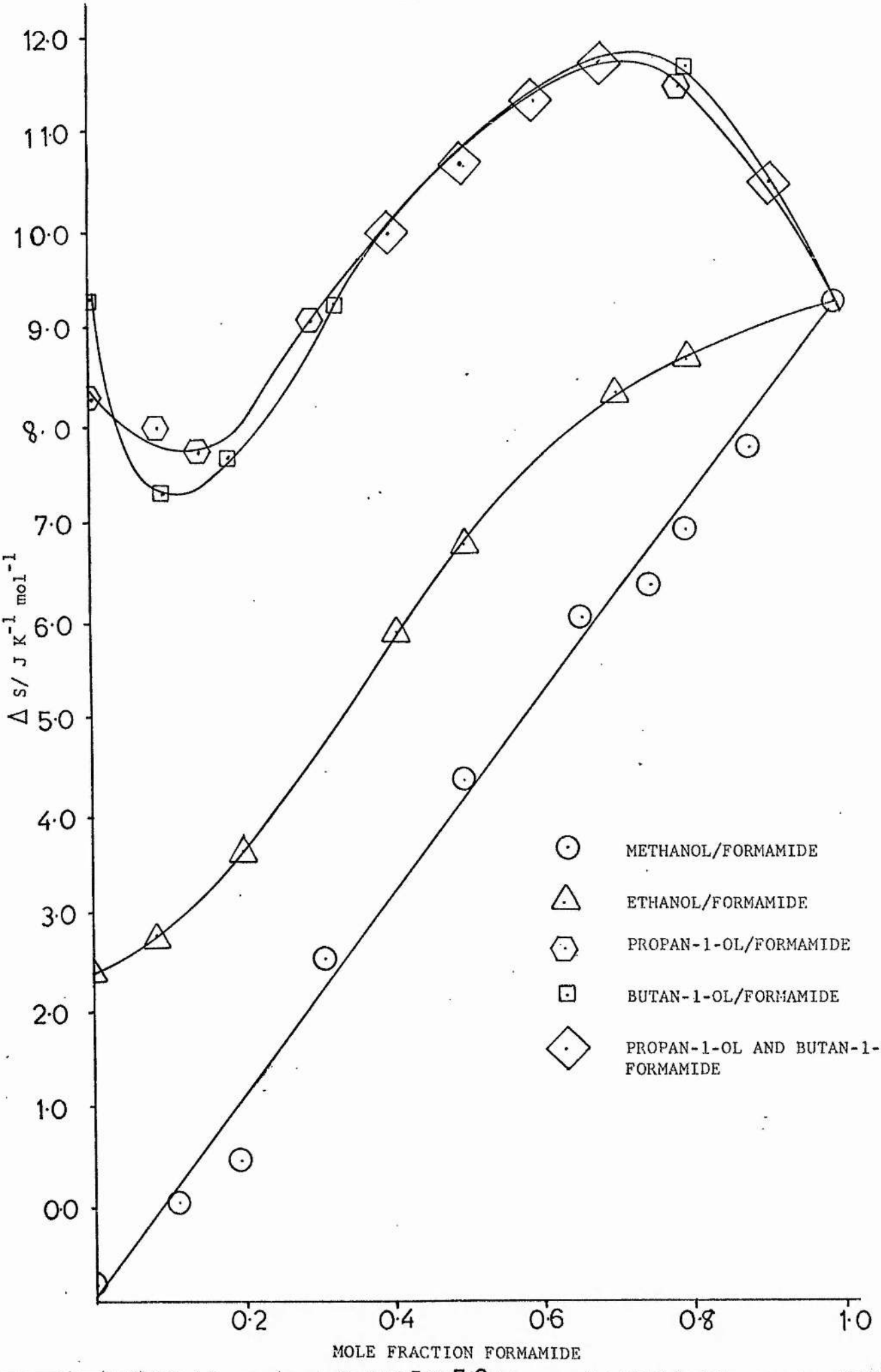
12·0
11·0
10·0
9·0
8·0
7·0
6·0
5·0
4·0
3·0
2·0
1·0
0·0
Δ S/ J K⁻¹ mol⁻¹
0·2
0·4
0·6
0·8
1·0
MOLE FRACTION FORMAMIDE
METHANOL/FORMAMIDE
ETHANOL/FORMAMIDE
PROPAN-1-OL/FORMAMIDE
BUTAN-1-OL/FORMAMIDE
PROPAN-1-OL AND BUTAN-1-OL
FORMAMIDE

FIG 5.9

The results of ΔG^*, ΔH^* and ΔS^* for the pure components compare favourably with available literature values[112]. The most striking feature of the plot is the negative sign of ΔS^* for methanol since Eyring[2] suggested that ΔS^* will be large and positive for all associated liquids. The other pure components have indeed large and positive ΔS^* values. For systems 1 and 2 the activation parameters for viscous flow increase in an almost linear manner from pure alcohol to pure formamide, again indicating no strong interactions between the components. This conclusion is in agreement with that of Merry and Turner[109], Kozlowski[110] and McDowall[38], for the methanol/formamide system. Kozlowski considers water /formamide and methanol/formamide binary liquid systems to be 'perfect' liquids from viscosity measurements. A cryoscopic study of the methanol/formamide system by Joukovsky[113] showed that no complex formation occurs. It might be concluded that the following type of species has a similar free energy of formation to simple amide or simple alcohol clusters fig (5.10)

fig 5.10

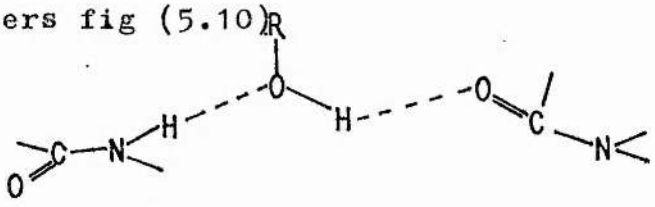

With system 3 the ΔH^* and ΔS^* versus composition plots have both maxima and minima figs.(5.8)and(5.9) The maximum in ΔH^* plot is probably due to a loosening of the associated propan-1-ol molecules on the addition of formamide. As $X_f \geqslant 0.1$ the enthalpy of activation for viscous flow increases to a maximum value at a concentration of $X_f = 0.7$ suggesting a more tightly packed structure i.e. a tendency towards

compound formation. From fig (5.8) the maximum in the ΔH^* value for system 3 indicates the formation of a compound $X_f = 0.7$. Figure (5.9) is a plot of the entropy of activation of viscous flow ΔS^* against composition. This term is associated with the entropy change occuring when a molecule in a position of minimum free energy in a solution frees itself, perhaps by severing some hydrogen bonds, in order to be activated to the transition state for viscous flow. Although the ΔG^* parameters for the four systems are plotted on the same graph and likewise for the ΔH^* and ΔS^* values, these parameters cannot be compared directly for the four systems because of the pre-exponential volume term in equation(5.2)

System 4 shows plots for ΔH^* and ΔS^* similar to those of system 3. The ΔG^* plot shows no maximum or minimum for this system. As the concentration of formamide increases the free energy of activation for viscous flow decreases and levels off betwen $X_f = 0.2$ and $X_f = 0.5$. Above this latter concentration the ΔG^* value decreases steadily. The ΔH^* against composition plot for this system indicates a compound of $X_f = 0.7$ as for system 3.

Erdey-Grúz et al [114] have studied the viscosity of mixtures of methanol, ethanol and propan-1-ol in water. Like formamide, water is a protic solvent, associates by hydrogen-bonding and causes an exchange of hydrogen-bonds when mixed with formamide. These workers showed that the three alcohols when mixed with water, exhibited viscosity maximums at about 20-25 mole % alcohol concentration. As noted in this project for propan-1-ol and butan-1-ol in formamide, the water/alcohol systems also showed greater viscosity maximum at lower

temperatures and with increasing length in the carbon chain of the alcohol. The authors concluded that the viscosity maximum was a consequence of a specific interaction between water and alcohol in which hydrogen-bonds formed between the alcohol and water molecules play an important role . Methanol and ethanol are both capable of forming compounds with water but are unable to do so with formamide at the temperatures studied. The formation of complexes between water and monovalent alcohols is considered to take place by hydrogen bonding and by the occupation of the structural cavities of water. At lower concentrations, the molecules of the alcohol occupy these cavities and deform but do not destroy the water structure. As the concentration increases however, there is insufficient cavities for all the solute molecules and a new type of hydrogen-bonded liquid structure is formed. In formamide/alcohol solutions it is possible that the size of the methanol and ethanol molecules is sufficiently small to fit into structural cavities in formamide. With the higher alcohols, propan-1-ol and butan-1-ol, the molecules may be too large to enter the cavities and hydrogen bonded complexes are formed.

5.6 PREDICTION OF THE VISCOSITY OF LIQUID MIXTURES

A number of relationships have been proposed to predict the viscosity of liquid mixtures, most of which are empirical while the remainder are based on the free volume or similar models.

For ideal liquids, Arrhenius[9] proposed the empirical equation for viscosity of a binary mixture:

$$\ln \eta = \phi_A \ln \eta_A + \phi_B \ln \eta_B \qquad (5.4)$$

where ϕ_A and ϕ_B are the volume fractions and η_A and η_B are the viscosities of the pure components A and B respectively. An equation which introduced a term to take account specifically of molecular interactions A --- B was introduced by Dolezalek[115] and later by Hind et al[116];

$$\eta = x_A^2 \eta_A + x_B^2 \eta_B + 2x_A x_B \eta_{AB} \qquad (5.5)$$

where η_{AB} was termed the 'mutual viscosity'coefficient'. In 1960 Bearman and Jones[105] derived an equation similar to the above from statistical mechanics. Their basic assumption was that the mean frictional forces acting on the molecules of a binary system were related to the gradients of the local thermodynamic properties and to the relative mean velocities of the components. They showed that the viscosity could be represented by the sum of three integrals representing the interactions of like and unlike pairs of molecules. On the basis of the statistical mechanical theory of Frenkel[117] and the rate theory of Eyring[2], Tamura and Kurata [118] derived a semi-empirical relationship similar to that of Dolezalek and Hind.

5.7 TAMURA AND KURATA EQUATION

Frenkel[117] and Eyring[2] have shown that the viscosity of a pure liquid is given by

$$\eta_A = (kT/v_A)\, \tau_A \qquad (5.6)$$

where k is the Boltzmann constant, T the absolute temperature and v_A the volume occupied by one molecule of the liquid. τ_A represents the relaxation time of flow and is given by

$$\tau_A = (h/kT)\, e^{\Delta G_A^*/RT} \qquad (5.7)$$

where h is the Planck constant and ΔG_A^* is the free energy of activation for viscous flow relating to A --- A contact of molecules. Tamura and Kurata applied the same procedure to describe a mixture of liquids A and B and introduced the term "mutual activation free energy of viscous flow". ΔG_{AB}^*, relating to A --- B molecular contacts. τ_{AB} was taken to be the relaxation time of flow of a molecule A in liquid B where

$$\tau_{AB} = (h/kT)\, e^{\Delta G_{AB}^*/RT} \qquad (5.8)$$

If x_A and x_B were the mole fractions of A and B and the probabilities of the molecular contacts A --- A, B --- B and A --- B under the condition of random mixing were then given by x_A^2, x_B^2 and $2x_Ax_B$ respectively, τ was then assumed to be given by the weighted mean of the individual relaxation times:

$$\tau = x_A^2\tau_A + x_B^2\tau_B + 2x_Ax_B\tau_{AB} \qquad (5.9)$$

$$\therefore \quad \eta_{AB} = \left[\frac{kT}{(v_A v_B)^{\frac{1}{2}}}\right] \tau_{AB} \qquad (5.10)$$

Thus

$$\eta = x_A^2\left(\frac{v_A}{v}\right)\eta_A + x_B^2\left(\frac{v_B}{v}\right)\eta_B + 2x_Ax_B\left(\frac{v_Av_B}{v^2}\right)^{\frac{1}{2}}\eta_{AB} \qquad (5.11)$$

where the parameters with no subscript refer to the mixture. The volume fraction of liquid A is obtained from

$$\frac{x_Av_A}{v} = \frac{W_A\rho}{\rho_A} = \phi_A \qquad (5.12)$$

where ρ is the density of the mixture, ρ_A is the density of component A and W_A is the weight fraction of component A hence

$$\eta = x_A \phi_A \eta_A + x_B \phi_B \eta_B + 2(x_A x_B \phi_A \phi_B)^{\frac{1}{2}} \eta_{AB} \qquad (5.13)$$

This equation is similar to that of Dolezalek but introduces a degree of dependence of the viscosity on the volume. It was shown by Tamura and Kurata[118] that the agreement between their equation and the experimental results for a number of systems was considerably better than that for the Dolezalek model.

5.8 MATO AND HERNANDEZ EQUATION

These workers pursued a similar argument to the above but considered that the probability of molecular interactions A---A, would be given by the product of the mole fraction and the volume fraction of the particular species and suggested the relationship [119]

$$\eta = \phi_A^2 \eta_A + \phi_B^2 \eta_B + 2\phi_A \phi_B \eta_{AB} \qquad (5.14)$$

This is of the same form as equation (5.13) with the mole fraction replaced by the volume fraction.

The foregoing equations for the viscosity of a binary mixture are derived from Eyring's activation state theory[2] which has been criticised by Rice et al[120]. The latter workers suggested that it is merely a parametric representation rather than a molecular theory, since the parameters from it cannot be related to the intermolecular potential or the radial distribution function. Rice and coworkers admit however that the Eyring model is easily visualised and that if the resulting formulae are considered to be parametric representations, the adjustment of the parameters often leads to useful representation of the experimental data.

5.9 APPLICATION OF THE DOLEZALEK, TAMURA-KURATA AND MATO-.HERNANDEZ EQUATIONS

The experimentally determined viscosities for the four binary liquids have been compared with viscosities calculated from the Dolezalek, Tamura-Kurata and Mato-Hernandez equations. The predicted values of the absolute viscosities, together with the magnitude of error were calculated for each system at different compositions by polynomial regression analysis. The percentage error between the calculated and experimental viscosities was determined for each composition and an average percentage error calculated for each binary liquid system. This average percentage error was the criterion used to determine the model best suited to a particular binary liquid system. Table (5.1) shows the average percentage error and the mutual viscosity coefficient η_{AB} calculated for each system from all the compositions investigated.

From Table (5.1) it can be seen that all three equations provided an adequate description ($\pm$4%) of the binary mixture methanol/formamide. The Dolezalek equation however was slightly better than the other two models for this system. As the solute-solvent interactions decrease with increasing temperature, all the equations provide a better description of the four systems at higher temperatures.

The three equations were able to describe the ethanol/formamide system more precisely thatn the methanol / formamide system. This is possibly due to the similarity in molecular weights of ethanol and formamide (46.07 and 45.04 respectively). Since the Tamura-Kurata equation introduces

TABLE 5.1

METHANOL/FORMAMIDE

MODEL		20°C	30°C	40°C	50°C
1	%Error	3.66	2.93	2.43	1.87
	η_{AB}/J m^{-3}s	0.00086	0.00078	0.00070	0.00063
2	%Error	3.85	3.11	2.61	2.08
	η_{AB}/J m^{-3}s	0.00082	0.00075	0.00068	0.00060
3	%Error	3.80	3.29	2.77	2.29
	η_{AB}/J m^{-3}s	0.00079	0.00072	0.00065	0.00058

ETHANOL/FORMAMIDE

1	%Error	1.41	1.26	1.04	0.79
	η_{AB}/J m^{-3}s	0.00184	0.00149	0.00122	0.00101
2	%Error	2.03	1.82	1.53	1.40
	η_{AB}/J m^{-3}s	0.00210	0.00168	0.00137	0.00113
3	%Error	2.17	1.92	1.59	1.45
	η_{AB}/J m^{-3}s	0.00227	0.00181	0.00146	0.00121

TABLE 5.1 Cont.

PROPAN-1-OL/FORMAMIDE

MODEL		20°C	30°C	40°C	50°C
1	%Error	5.08	4.25	3.59	3.06
	$\eta_{AB/J\ m^{-3}s}$	0.00311	0.00235	0.00184	0.00148
2	%Error	4.93	4.24	3.66	3.18
	$\eta_{AB/J\ m^{-3}s}$	0.00356	0.00268	0.00210	0.00169
3	%Error	4.08	3.53	3.01	2.56
	$\eta_{AB/J\ m^{-3}s}$	0.00369	0.00278	0.00218	0.00176

BUTAN-1-OL/FORMAMIDE

1	%Error	6.26	5.47	4.76	4.06
	$\eta_{AB/J\ m^{-3}s}$	0.00408	0.00309	0.00238	0.00188
2	%Error	5.17	4.49	3.91	3.36
	$\eta_{AB/J\ m^{-3}s}$	0.00466	0.00353	0.00273	0.00217
3	%Error	3.49	2.93	2.50	2.04
	$\eta_{AB/J\ m^{-3}s}$	0.00459	0.00347	0.00268	0.00214

MODEL 1 DOLEZALEK
2 TAMURA/KURATA
3 MATO/HERNANDEZ

a dependence on volume it might be considered that this equation should have defined the methanol/formamide system better than the ethanol/formamide as the molar volumes of methanol and formamide are very similar (40.5 and 39.7 $cm^3 mol^{-1}$ respectively). As noted for the methanol/formamide system, the simplest of the predictive models, the Dolezalek equation, defines the system best. This fact that the simple model gives a better description of methanol and ethanol/formamide mixtures than the more complex models may be a further indication that no strong interactions are present in these systems.

For the propan-1-ol/formamide system the Mato-Hernandez equation provides the best description at all four temperatures. With the probability of compound formation in this system, the Dolezalek approach appears to be too simple and is the least successful. The estimated viscosities however were still within 5% of the experimental measurements for all models.

The butan-1-ol system was also best described by the Mato- Hernandez equation which appears to provide a better estimate of the viscosity of solutions which have strong A - B interactions. This equation has been criticised by Irving[108] who considered that it could not be validly applied to sytems with both maxima and minima in their viscosity isotherm. In this work however, the predictive ability of equation (5.14) has improved as the maxima and minima in the viscosity isotherms become more apparent from propan-1-ol to butan-1-ol/formamide, figs. (5.3 and 5.4).

It is instructive to determine the activation parameters for viscous flow from η_{AB} values obtained by

the various models. Associated liquids have been divided into two classes by Tyuzyo [112] according to the variation of ΔH^* with temperature. Liquids which have ΔH^* values independent of temperature as high as their boiling points are classed as associated liquids of the first kind, whereas liquids demonstrating ΔH^* values which decrease with increasing temperature are termed as associated liquids of the second kind. In this interpretation saturated alcohols and formamide were classed as associated liquids of the first type, a classification supported by this present work and demonstrated by fig. (5.10). $\ln \eta_{AB}$ values determined by the predictive models have been plotted against 1/T and the η_{AB} values obtained from the most successful model were used to determine the activation parameters ΔG^*_{AB}, ΔH^*_{AB} and ΔS^*_{AB} for the systems. These parameters are compared with those for the pure components in table (5.2).

TABLE 5.2

System Formamide in	Model	ΔG^*_{AB}/ kJ mol^{-1}	ΔH^*_{AB}/ kJ mol^{-1}	ΔS^*_{AB}/ J K^{-1} mol^{-1}
Methanol	Dolezalek	10.92	9.98	-3.14
Ethanol	Dolezalek	13.19	14.98	6.02
propan-1-ol	Mato-Hernandez	15.22	19.39	14.01
butan-1-ol	Mato-Hernandez	16.09	19.37	11.01
Pure Components		ΔG^*	ΔH^*	ΔS^*
Methanol		9.97	9.72	-0.84
Ethanol		12.58	13.29	2.39
propan-1-ol		14.62	17.08	8.25
butan-1-ol		15..83	18 .58	9 .23
Formamide		14.37	17.04	8.97

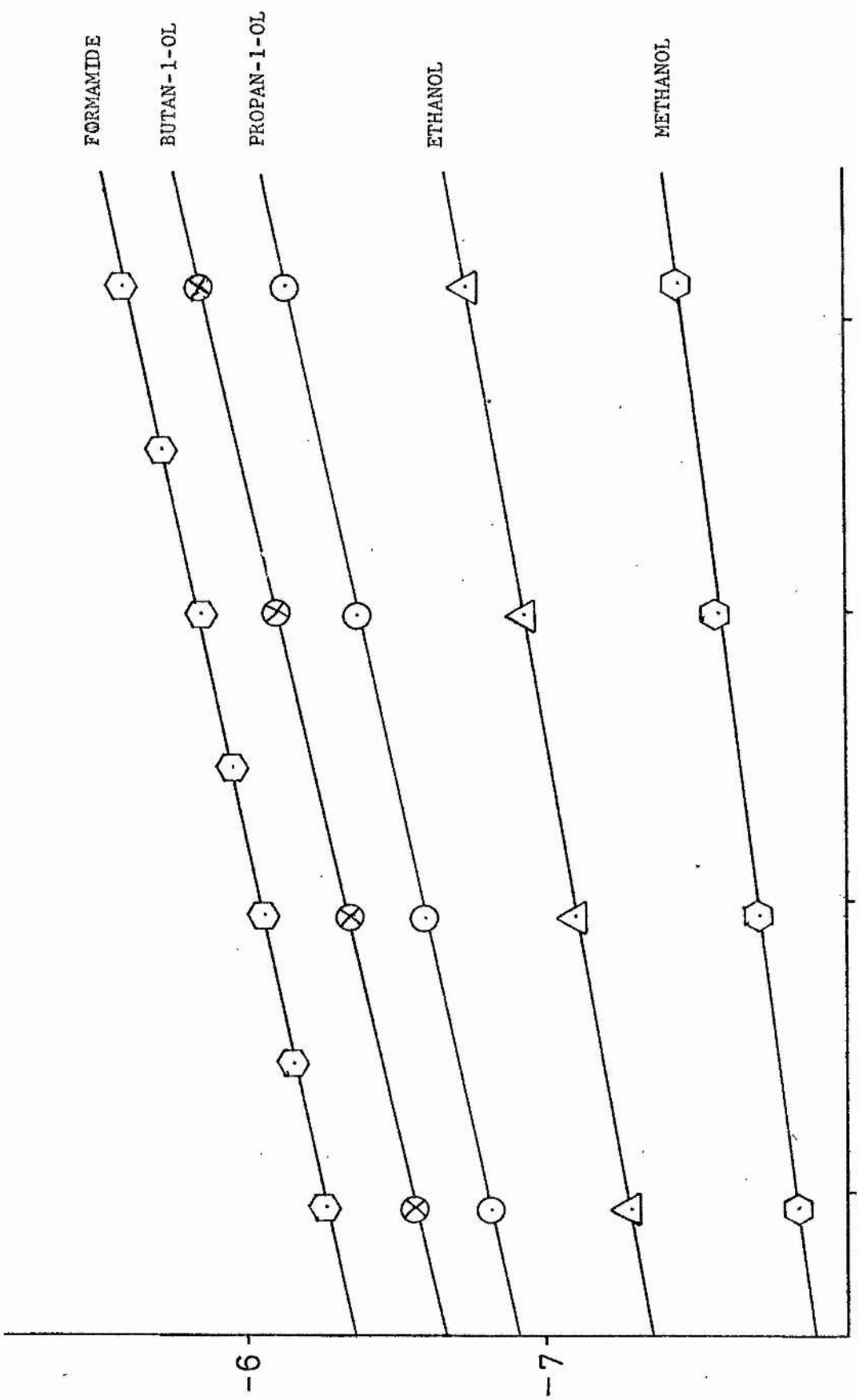
FORMAMIDE
BUTAN-1-OL
PROPAN-1-OL
ETHANOL
METHANOL
-6
-7
ln η
31
32
33
34
1/T x 10⁴ / K⁻¹

FIG 5.10

METHANOL/FORMAMIDE

The graphs of $\ln \eta_{ab}$ against 1/T for all three models showed some curvature. The Dolezalek model produced the most linear plot and the activation parameters were calculated from this model. From table (5.2) ΔS^*_{AB} is smaller than that for either of the pure components. ΔH^*_{AB} is almost equal to that for pure methanol suggesting that a similar number of bonds must be broken for viscous flow in the mixture as in pure methanol. The ΔS^*_{AB} and ΔH^*_{AB} values combine to give a ΔG^*_{AB} value which lies between those of the pure components. This could imply that the association of unlike molecules in this system is less than that between like molecules. The negative ΔS^*_{AB} value for this system may indicate that the extent of ordering in the transition states for η_A, η_B and η_{AB} is not the same.

ETHANOL/FORMAMIDE

All three models gave excellent linear plots of $\ln \eta_{AB}$ against 1/T and the Dolezalek model was again used to determine the activation parameters. These values suggest , in a similar manner to the above, that like molcules associate to a greater extent than unlike molecules. ΔG^*_{AB}, ΔH^*_{AB}, and ΔS^*_{AB} all lie between the values for the pure components.

PROPAN-1-OL/FORMAMIDE

The η_{AB} values calculated by the Mato-Hernandez model were used to calculate the ΔG^*_{AB}, ΔH^*_{AB} and ΔS^*_{AB} parameters for this system. As shown in table (5.2) all three activation parameters are greater than the values for the pure components. The larger ΔH^*_{AB} value suggests that a greater number of bonds have to be broken for a molecule of propan-1-ol in the neighbourhood of a molecule of

formamide to move to the next equilibrium position than are required for a molecule to reach the next equilibrium position in either of the pure solvents. The activation parameters for this system suggest that propan-1-ol molecules associate with formamide molecules to a greater extent than with each other.

BUTAN-1-OL/FORMAMIDE

The Mato-Hernandez model gave the most linear relationship between $\ln \eta_{AB}$ and 1/T. In general the model which provided the best predictions for a given system also yielded the most linear plot for $\ln \eta_{AB}$ versus 1/T. As in the propan-1-ol/formamide system the activation parameters are larger than those for the pure components. Unlike molecules therefore would appear to associate to a greater extent than like molecules.

5.10 PARTIAL MOLAL VOLUME

Densities of the binary mixtures studied were fitted to equation (5.16)[121]

$$\frac{1}{\rho} = \frac{\bar{V}_2^o}{M_2} + \left\{ \frac{1}{M_1} (\bar{V}_1^o + h + k) - \frac{\bar{V}_2^o}{M_2} \right\} \omega_1 - \frac{1}{M_1} (h + 3/2k) \omega_1^2 + \frac{k\omega_1^3}{2M_1} \qquad (5.16)$$

where ρ is the density of the mixture, M_1 and M_2 are the molecular weights of components 1 and 2 respectively and $\bar{V}_1^o$ and $\bar{V}_2^o$ are the molar volume of the components, ω_1 is the weight fraction of component 1 in the mixture and h and k are constants. The initial results indicated that the number of mixtures studied was too low to permit evaluation of accurate $\bar{V}_1^o$ data. To overcome this problem, the data of McDowall[38] for methanol/formamide was used as an additional source of experimental observations. This provided fourteen observations over the entire composition

range and enabled the calculation of the partial molal volume of formamide in formamide/methanol solution and methanol in methanol/formamide solution at the temperature studied. A plot of partial molal volume against mole fraction at four temperatures is shown in fig. (5.11). The partial molal expansibility of methanol in methanol/formamide solution,

$$C_2 = \left(\frac{\partial V_2}{\partial T}\right)_P \qquad (5.17)$$

is shown as a function of mole fraction of methanol in the mixture fig.(5.12).

The plots are smooth curves from pure formamide to pure methanol. This is further evidence therefore that this binary liquid system shows no tendancy towards complex formation.

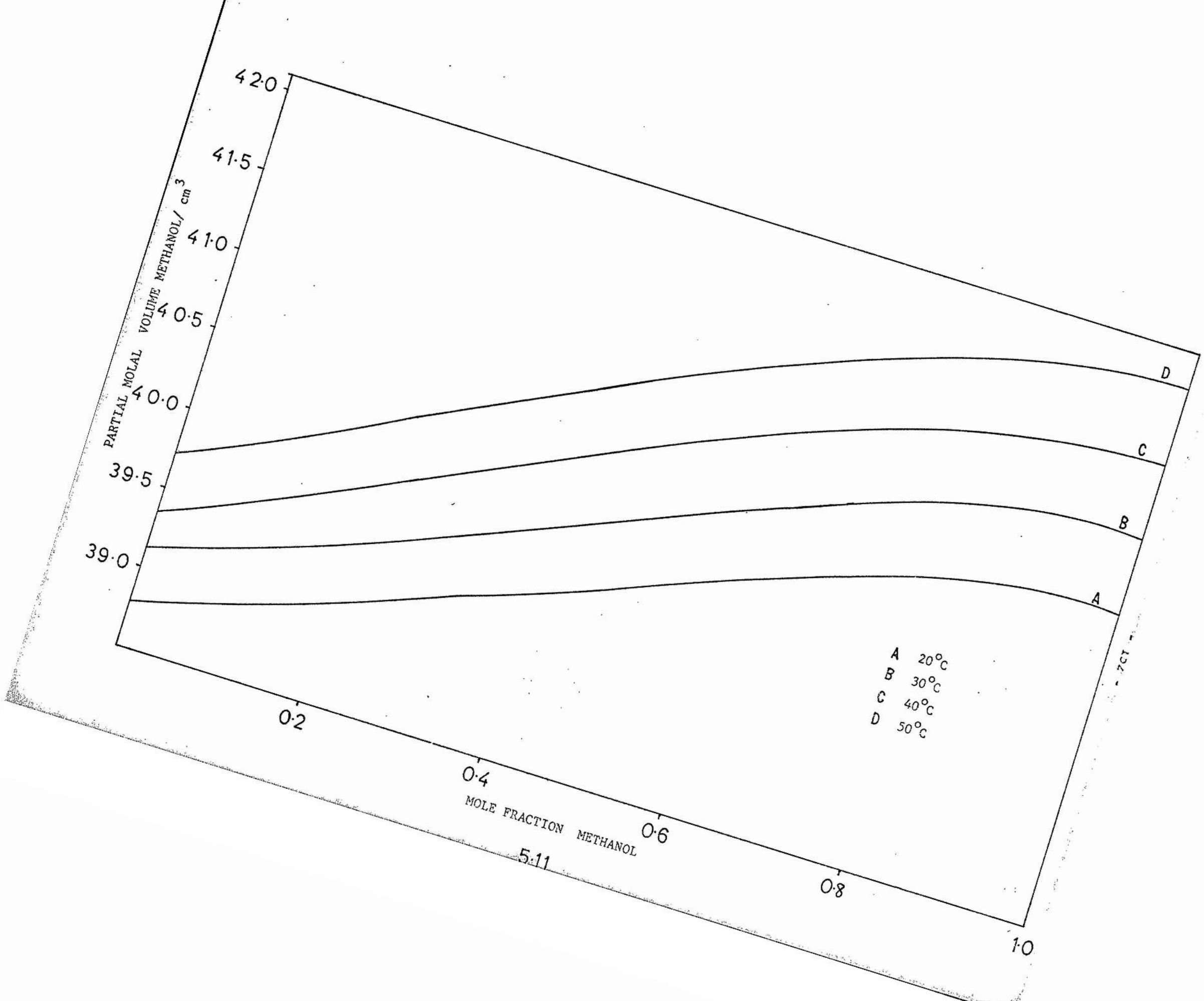
PARTIAL MOLAL VOLUME METHANOL/ cm3
42·0
41·5
41·0
40·5
40·0
39·5
39·0
0·2
0·4
0·6
0·8
1·0
MOLE FRACTION METHANOL
A
B
C
D
A 20°C
B 30°C
C 40°C
D 50°C
5·11

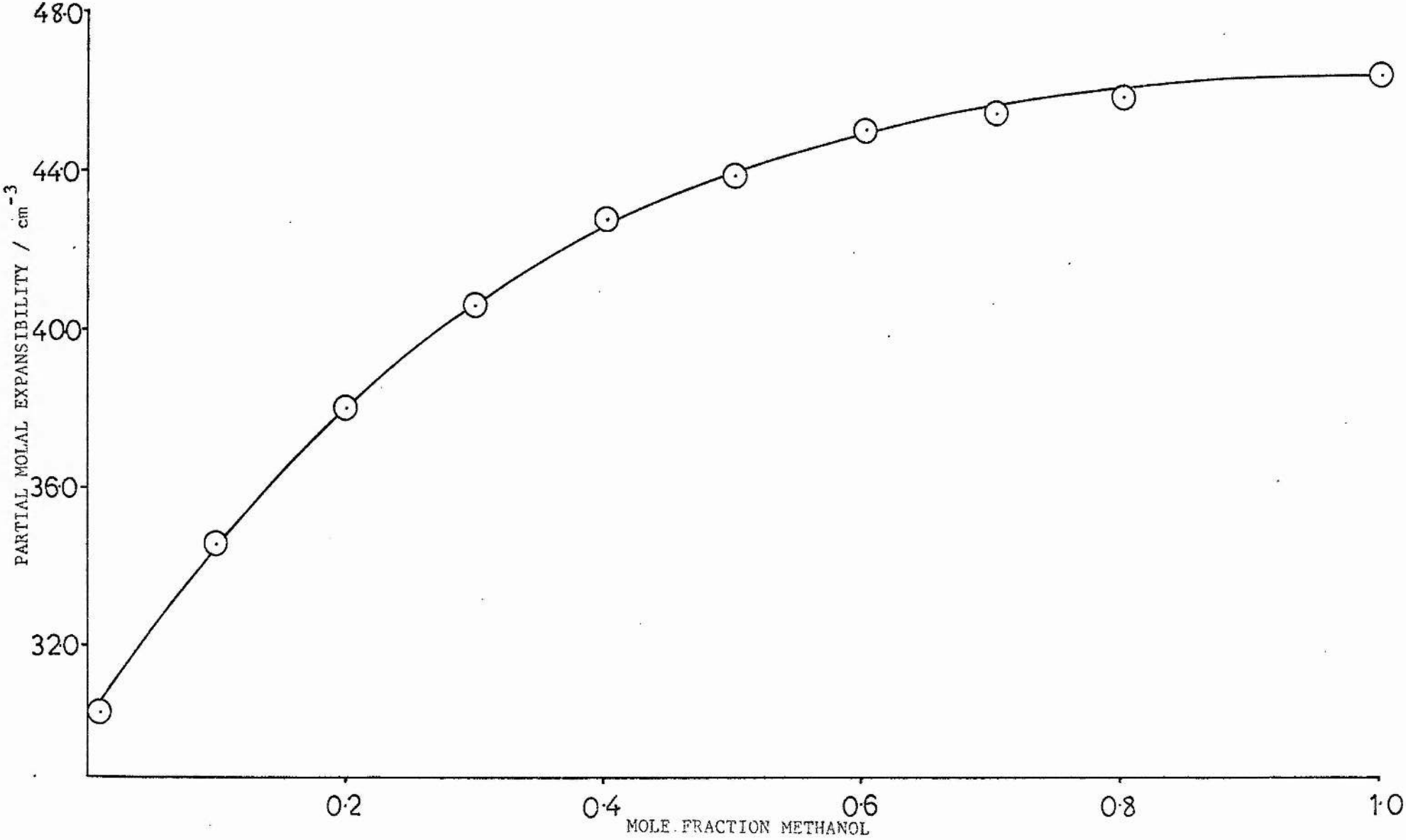
48·0
44·0
40·0
36·0
32·0
PARTIAL MOLAL EXPANSIBILITY / cm^{-3}
0·2
0·4
0·6
0·8
1·0
MOLE FRACTION METHANOL

FIG. 5·12

5.B TIME DOMAIN SPECTROSCOPY

5.11 INTRODUCTION

Dielectric-spectroscopy methods have been used for a considerable time to study the molecular behaviour of polar systems. Historically the behaviour of polar molecules is studied experimentally by measuring the complex dielectric permittivity

$$\varepsilon(i\omega) = \varepsilon'(\omega) - i\varepsilon''(\omega) \qquad (5.18)$$

over the necessary frequency range. As the whole field of dielectric spectroscopy covers an unusually wide range of frequencies, from about 10^{-4} to 10^{11} Hz, a large number of time-consuming frequency domain techniques were required.

In principle, the application of transient methods is an alternative to this point-by-point approach in the frequency domain. A single time domain pulse, applied to the dielectric sample, yields a time domain response. When the Fourier spectra from the signal is calculated it is possible by selecting the components at some fixed frequency to simulate the frequency domain response. Methods to analyse the experimental data, developed for frequency domain measurements, can then be used e.g. Debye plots[122] and Cole-Cole Argand diagrams[123]. Since the time domain signal usually covers a large frequency spectrum, a pulse or transient method is less time-consuming than frequency domain methods.

While transient methods have been used for a number of years for the study of slow relaxation processes, such as those in polymeric materials, much faster relaxations have come within the scope of the method since the late 1960's. These transient methods all originate from a technique known

as time domain reflectrometry (TDR) developed for finding breaks or faults in transmission lines. A fast voltage step, with a rise time of approximately 35×10^{12}s, is propagated in a low-loss coaxial line. If a discontinuity is present in the line, such as a section filled with a polar material, reflection and transmission will occur at the interface. From the time taken for the reflected step to reach the origin, the location of the discontinuity can be found while the change in the shape of the step voltage is a measure of the dynamic behaviour of the discontinuity. At present both reflection and transmission methods are used in the study of dielectrics and the transient high frequency methods are collectively known as time domain spectroscopy (TDS) methods.

In physical chemistry, development was started by Fellner - Feldegg[124] who demonstrated the advantages of the TDR method over standard frequency domain techniques. Suggett et al[125] were then able to improve the original method leading to higher accuracies and to an increase in the frequency range to about 15×10^9 Hz. The extension to lower frequencies was then carried out by Fellner-Feldegg[126] and De Loor et al[127].

At present a number of TDS techniques exist to evaluate the dielectric permittivites of polar meterials. The accuracy of these methods are at least comparable to that of the standard frequency domain methods. The advantages of the TDS system are the relatively simple equipment required and the very short time taken to carry out the measurements.

It was considered that it might be instructive to carry out these measurements on some associated liquids and correlate these with viscosity studies. Binary liquids with strong intermolecular interactions would be particularly interesting to investigate by this technique.

5.12 THEORY

In a coaxial line, of negligible series resistance filled with dielectric, the characteristic impedance is given by

$$Z = \frac{Z_o}{\left[\varepsilon(\omega)\right]^{1/2}} \qquad (5.19)$$

where

$$\varepsilon = \varepsilon' - i\varepsilon'' - \frac{i\vartheta}{\omega\varepsilon_o} \qquad (5.20)$$

represents the complex permittivity, ϑ the specific conductance of the dielectric, Z_o the characteristic impedance of the air filled line, ω the angular frequency and ε the permittivity of free space. The propagation constant υ, which governs the attentuation and phase shift per unit length of a signal travelling along the line is given by

$$\upsilon = \upsilon_o\left[\varepsilon(\omega)\right]^{1/2} \qquad (5.21)$$

and υ_o the propagation of the air filled line, is given by

$$\upsilon_o = \frac{i\omega}{c} = \frac{2i\pi}{\lambda} \qquad (5.22)$$

Consider a wave propagated in a coaxial line of characteristic impedence Z_o. For the transition to a region of impedence Z the voltage reflection and transmission coefficients ρ_{12}, τ_{12} are given by

$$\rho_{12} = \frac{Z - Z_o}{Z + Z_o} \qquad (5.23)$$

$$\tau_{12} = \frac{2Z}{Z + Z_0} \qquad (5.24)$$

As indicated by equation (5.23 and 5.24) for a dielectric system, Z , and hence ρ and τ will be complex, frequency dependent quantities. Their frequency dependence will be reflected in differences between the time domain waveform of the incident signal and of the responses i.e. the reflected and transmitted signals. The measurements in the time domain can be transformed into equivalent information in the frequency domain. The basis of this transformation is that any physically realisable pulse in the time domain f(t) is related to a complex spectrum $F(\omega)$ in the frequency domain by the Fourier transform and its inverse i.e.

$$F(\omega) = \int_{-\infty}^{+\infty} f(t) \exp\left(-i\omega t\right) dt \qquad (5.25)$$

and

$$f(t) = \frac{1}{2\pi} \int_{-\infty}^{+\infty} F(\omega) \exp\left(i\omega t\right) d\omega \qquad (5.26)$$

any pulse therefore can be considered as an infinite sum of frequency contributions, the Fourier transform giving the amplitude and phase of the contributions as a function of frequency.

The response of a dielectric sample in the frequency domain may be found by measuring a suitable incident pulse and the corresponding responded pulse, and calculating the ratio of the Fourier transforms. This is exactly the equivalent of performing the response measurements in the frequency domain. If $G(\omega)$ is the frequency response of the dielectric system and $f_i(t)$ and $f_r(t)$ the incident and responded pulses then

$$G(\omega) = \frac{F_r(\omega)}{F_i(\omega)} \qquad \frac{\int_{-\infty}^{+\infty} f_r(t) \exp\left(-i\omega t\right) dt}{\int_{-\infty}^{+\infty} f_i(t) \exp\left(-i\omega t\right) dt} \qquad (5.27)$$

$G(\omega)$ is therefore defined for all frequencies contained in the incident pulse.

5.13 EXPERIMENTAL

Equipment:

Measurements were made using a Hewlett Packard 180 Time Domain Reflectometry system (12.4GHz) set up for total reflection TDS.fig.(5.13) Data from this was collected and averaged in a Northern Scientific NS-575 Digital Signal Analyser, which was used to store signals from the dielectric sample and the short and to subtract the blank cell signal. The corrected signals which were displayed on the NS-575 oscilloscope were fed into a Data Dynamics teletype where a paper tape was prepared for computer analysis of the data. The NS-575 could also be used to add or subtract constants to the signals and could output the signals in a form suitable for x - y recorders, tape cassettes or directly into a computer.

Coaxial lines and connectors fig,(5.14) were of the Amphenol APC 7 type. The dielectric cells were APC 7 gold plated coaxial lines modified to the required lengths according to the method of Fellner-Feldegg[128] fig. (5.15). Two cells were constructed using machined Kel-F beads which made a tight seal between the inner and outer conductors. The Kel-F bead was placed the required distance along the coaxial line to produce sample cells of 0.984 cm and 0.096 cm in length. The cell lengths were accurately measured using a centering light with the cell held on the moving platform of a universal milling machine. With the centering light clamped the cell was raised or lowered by means of the

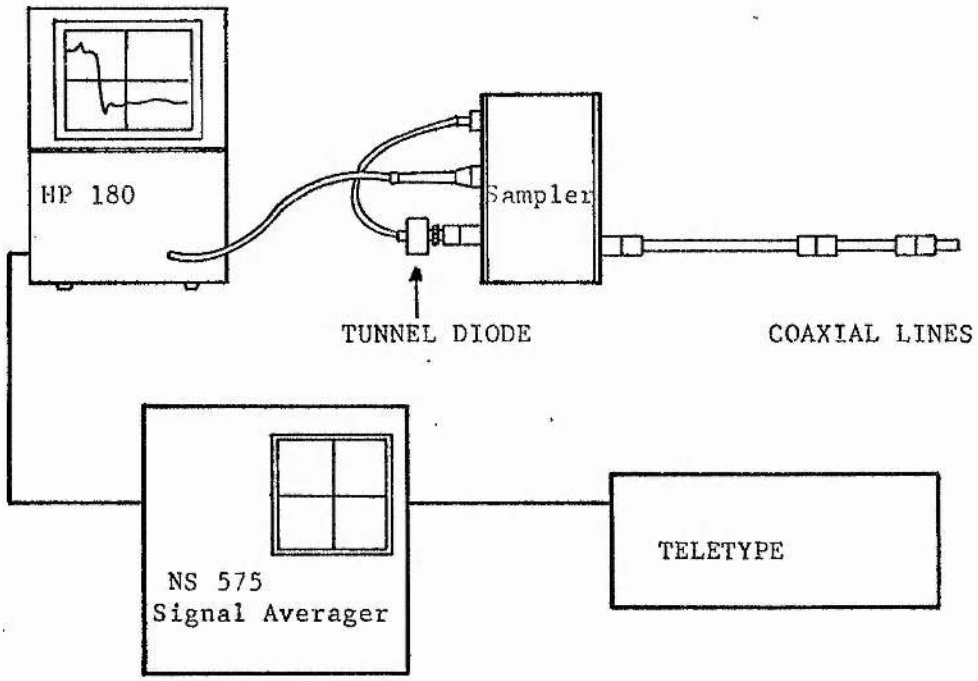
HP 180
Sampler
TUNNEL DIODE
COAXIAL LINES
NS 575
Signal Averager
TELETYPE

FIG. 5·13

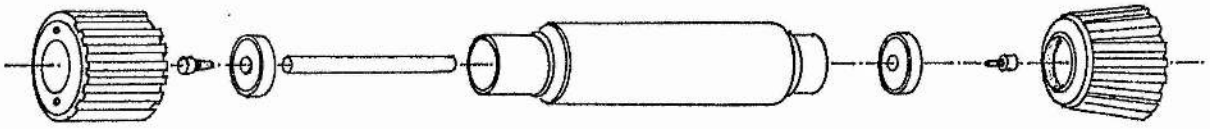

FIG. 5·14

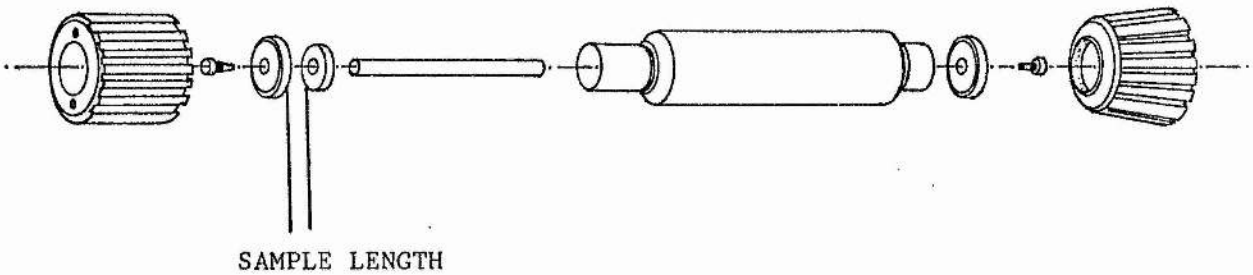

FIG. 5·15

milling machine jack the handle of which was accurately calibrated in centimetres.

FILLING THE SAMPLE CELLS

The sample cells were held vertically in a specially constructed cell holder, dismantled and filled with a dropper or a syringe. The cells were then re-assembled and inspected for air bubbles in the sample. If air bubbles were detected the procedure was repeated until an air-free sample was obtained.

5.14 TDS MEASUREMENTS

There are various methods available for measuring the dielectric response of a sample. A full account of these are given by van Gemert[129]. The method followed in this project was that of Suggett and coworkers and is known as the total reflection method[125]. On the application of a step pulse partial reflections and partial transmissions occur at the air-dielectric and dielectric-air interfaces. These multiple reflections, known as echoes, are shown in fig. (5.16)

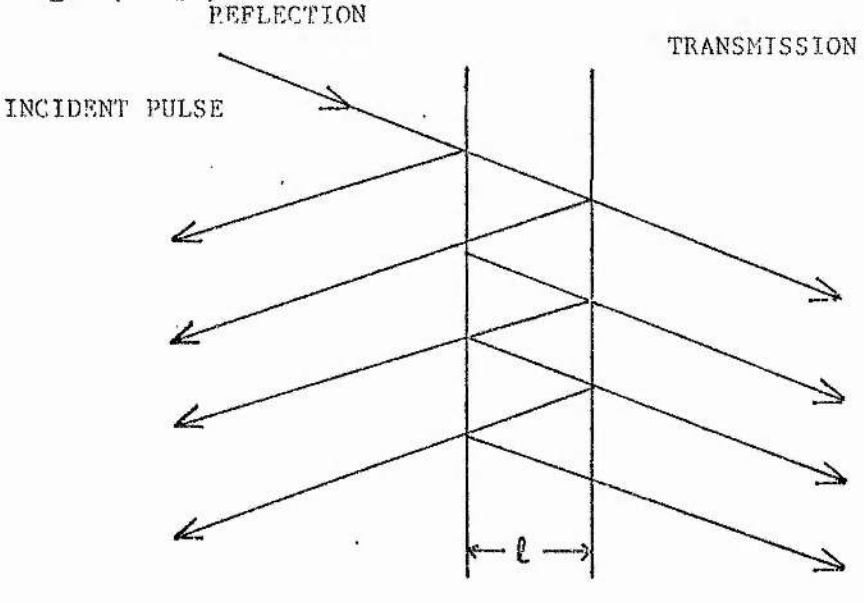

FIG 5.16

The simplest TDS method - the direct reflection method - monitors only the first reflection from the air-dielectric interface and its time window therefore only extends to the point in time at which interference from the next reflection occurs. The time separation between each reflected or transmitted pulse is proportional to the length of the sample, and for long sample cells (30cm) and samples of high permittivity e.g. formamide, can extend to almost 20 ns. One of the possibilities of extending the time range is the determination of the relationship between the totally reflected waveform and the complex permittivity of the dielectric sample. If ρ_{12} and ρ_{21} refer to the reflection coefficients at the air-dielectric and dielectric-air interfaces, τ_{12}, τ_{21} are the corresponding transmission coefficients, and υ is the propagation factor

$$\upsilon = i\omega\left[\varepsilon(i\omega)\right]^{1/2}/c \qquad (5.28)$$

The total reflection coefficient R, sometimes known as the scattering coefficient S_{11} from a length, ℓ, of sample is given to n terms by

$$R_n(i\omega) = \rho_{12} + \tau_{12}\rho_{21}\tau_{21}\exp\left(-2\upsilon\ell\right) + \tau_{12}\rho_{21}^{3}\tau_{21}\exp\left(-4\upsilon\ell\right) + \tau_{12}\rho_{21}^{(2n-3)}\tau_{21}\exp\left[-2(n-1)\upsilon\ell\right] \quad - - - - \qquad (5.29)$$

In this equation, ρ, τ and υ are complex quantities and are frequency dependent.

As $\rho_{12} = -\rho_{21}$ and $\tau_{12}\,\tau_{21} = 1-\rho^2$, the total reflection coefficient as $n \longrightarrow \infty$ is given exactly by

$$R(i\omega) = \frac{\rho\left[1-\exp\left(-2\upsilon\ell\right)\right]}{1-\rho^2\exp\left(-2\upsilon\ell\right)} \qquad (5.30)$$

where

$$\rho = \rho_{12} = \frac{1-\varepsilon^{1/2}(i\omega)}{1+[\varepsilon(i\omega)]^{1/2}} \qquad (5.31)$$

Equation (5.30) cannot be solved analytically for $\varepsilon(i\omega)$ but at least two methods of overcoming this problem are available. Restrictions may be imposed on the length of the sample; this is the thin sample method, or the equation may be solved numerically by e.g. the Newton-Raphson iterative approach[130], this is the total reflection method developed by Suggett et al[131].

5.15 PROCEDURE

The sample was placed at the end of the precision coaxial lines and terminated with a 50Ω terminator. The signal was smoothed or averaged in the NS-575 digital analyser and then stored in one half of the memory. The sample cell and the terminator were then replaced by an Amphenol short to give a reference signal. This signal was smoothed and stored in the other half of the NS-575 memory. Finally the empty sample cell with the 50Ω terminator attached was analysed and this signal was subtracted from both signals stored in the memory. This procedure cancelled any unwanted reflections from slight mismatches present in the coaxial lines and couplings. The corrected signals were then transferred onto paper tape for a complete computer analysis.

The newly constructed sample cells could not be shorted using the standard Amphenol short. They were shorted using finely cut aluminium foil which fitted tightly into the cell and provided an electrical path between the inner and outer conductors at the same point as the air-dielectric interface in the coaxial line.

5.16 TIME - REFERENCING

The signals for the dielectric sample and the short-circuit must be time referenced to the same point to prevent errors in permittivities at frequencies above a few G Hz. This was achieved using the very fast first reflection pulse on the time domain spectra

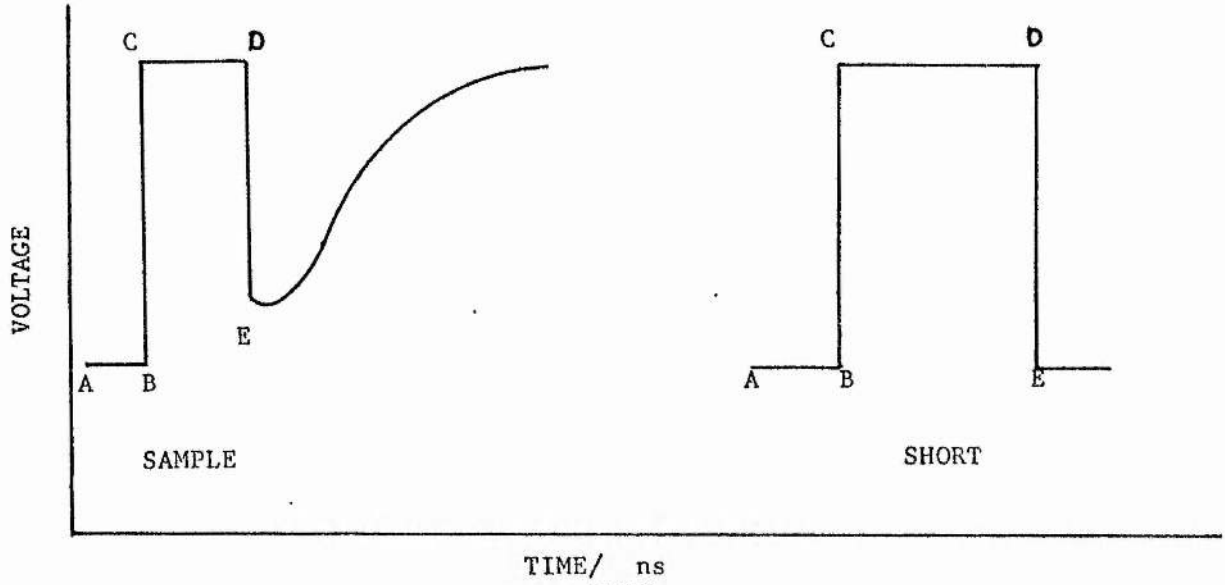

FIG. 5.17

The time referencing can best be explained with reference to fig. (5.17). In a typical sample the full time domain spectrum may extend over a 20 ns time interval. When this signal is averaged and stored in the NS-575 memory it is divided into 512 bytes. The change in the signal is therefore recorded at every 3.9×10^{-10} s The reflected pulse DE is displayed as a series of points at varying distances apart. The voltage change therefore increases or decreases at a different rate with time along DE. The point at which the largest voltage change occured was taken as the reference point for both the sample and the short. This point could be found either from the NS -575 digital address register or by the computer analysis.

5.17 CONDUCTANCE OF THE SAMPLE

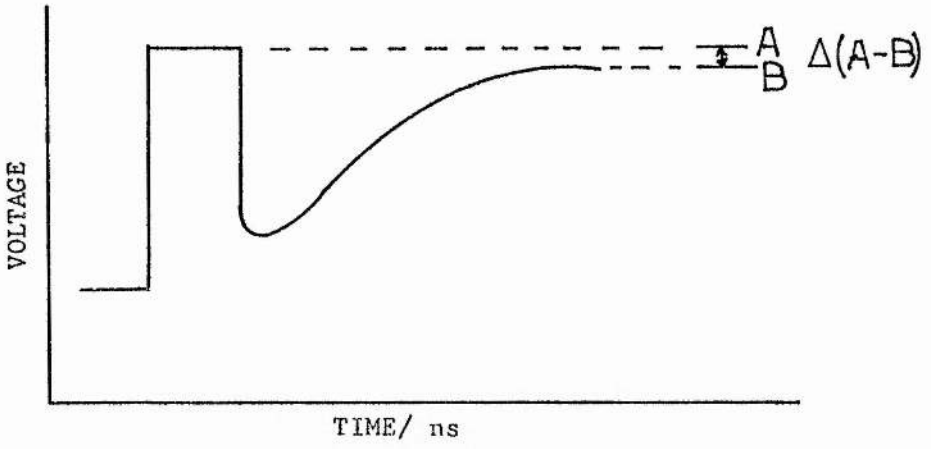

FIG. 5.18

The D.C. conductivity of a sample σ can be taken as the distance Δ (A-B) in fig. (5.18) The larger the distance AB the greater the conductivity of the sample. A large conductivity gives rise to errors in the loss factor. The effect of sample conductivity on multiple reflection methods has been considered by Fellner-Feldegg[128] and by van Gemert[132].

Fellner-Feldegg[128] has shown that if the conductivity is independent of frequency it will produce an offset of the base line of

$$S_{(11)\ cond} = (2\pi\sigma\ell)/c \qquad (5.32)$$

Van Gemert[132] however has shown that the d.c. conductivity is not independent of frequency and that the permittivity loss factor ε'' will be given by

$$\varepsilon'' + \varepsilon''_{(cond)}$$

where

$$\varepsilon''_{(cond)} = \frac{\sigma c}{\ell \pi f (1-\sigma)} \qquad (5.33)$$

and ε'' is the complex part of the dielectric permittivity $\varepsilon(i\omega)$.

In this work the conductivity of N-methylformamide

and n-methylacetamide , was too large to obtain useful dielectric information.

5.18 CALCULATIONS AND RESULTS

Propan-1-ol, formamide, N-methylacetamide and N-methylformamide were analysed by total reflection spectroscopy. The dielectric signals were analysed by computer programme to calculate the permittivities at various frequencies. The programme firstly calculated the conductance parameter σ called Δ(A - B) in fig.(5.18). If a negative value was obtained then σ was taken as zero. The time referencing procedure was then carried out with both the sample and short referenced to the same point, and the number of sampling points for the Fourier transformation was chosen. The number of points analysed depended on the desired frequency range chosen. The two signals were then Fourier transformed using the Samulon method[133]. i.e.

$$F(f) = \sum_{K=0}^{n=1} f(t) \exp\left(-2\pi f K \Delta t\right) \qquad (5.34)$$

where Δt was the sampling interval. This method was chosen to save valuable computing time. The subroutine for the Fourier transform also calculated the frequency values and presented them on a logarithmic scale. The total reflection coefficient for the samples

$$G(\omega) = \frac{F_r(\omega)}{F_i(\omega)} \qquad (5.35)$$

was evaluated and the Newton-Raphson iterative method[130] was applied to calculate the required permittivities from $G(\omega)$. The low frequency premittivity (ε_o) was known for the associated liquids analysed and this was used as

the first trial value for $\varepsilon(i\omega)$ in the iteration. The refined $\varepsilon(i\omega)$ at the lowest frequency then became the trial value at the next frequency until all the frequencies had been analysed. The calculated data for all stages of the programme for propan-1-ol are shown in appendix 5 along with the computer programme.

Two graphical methods are normally used to display dielectric data. A plot of ε^1 against ε^{11} the Cole-Cole plot[123] fig.(5.19) has the disadvantage that the parameter most accurately known, the frequency, is not directly observed. This plot for propan-1-ol is a semi-circle and the dispersion for this molecule can therefore be described by the simple Debye function[122]:

$$\varepsilon = \varepsilon_\infty + \frac{\varepsilon_0 - \varepsilon_\infty}{1 + i\omega\tau} \qquad (5.36)$$

where τ is the relaxation time of the molecule. The Debye equation may be written in various forms depending on the experimental characteristics required. Separation of equation (5.36) into its real and imaginary parts gives

$$\varepsilon' - \varepsilon_\infty = \frac{\varepsilon_0 - \varepsilon_\infty}{1 + \omega^2\tau^2} \qquad (5.37)$$

and

$$\varepsilon'' = \frac{(\varepsilon_0 - \varepsilon_\infty)\omega\tau}{1 + \omega^2\tau^2} \qquad (5.38)$$

The variation of ε^1 and ε^{11} with frequency, the Debye plots, are shown in fig. (5.20) for propan-1-ol. The frequency is displayed on a log. scale and the dielectric dispersion covers a wide range of frequency. The ε_0, ε_∞ and τ - values can be determined by using the linear relationships

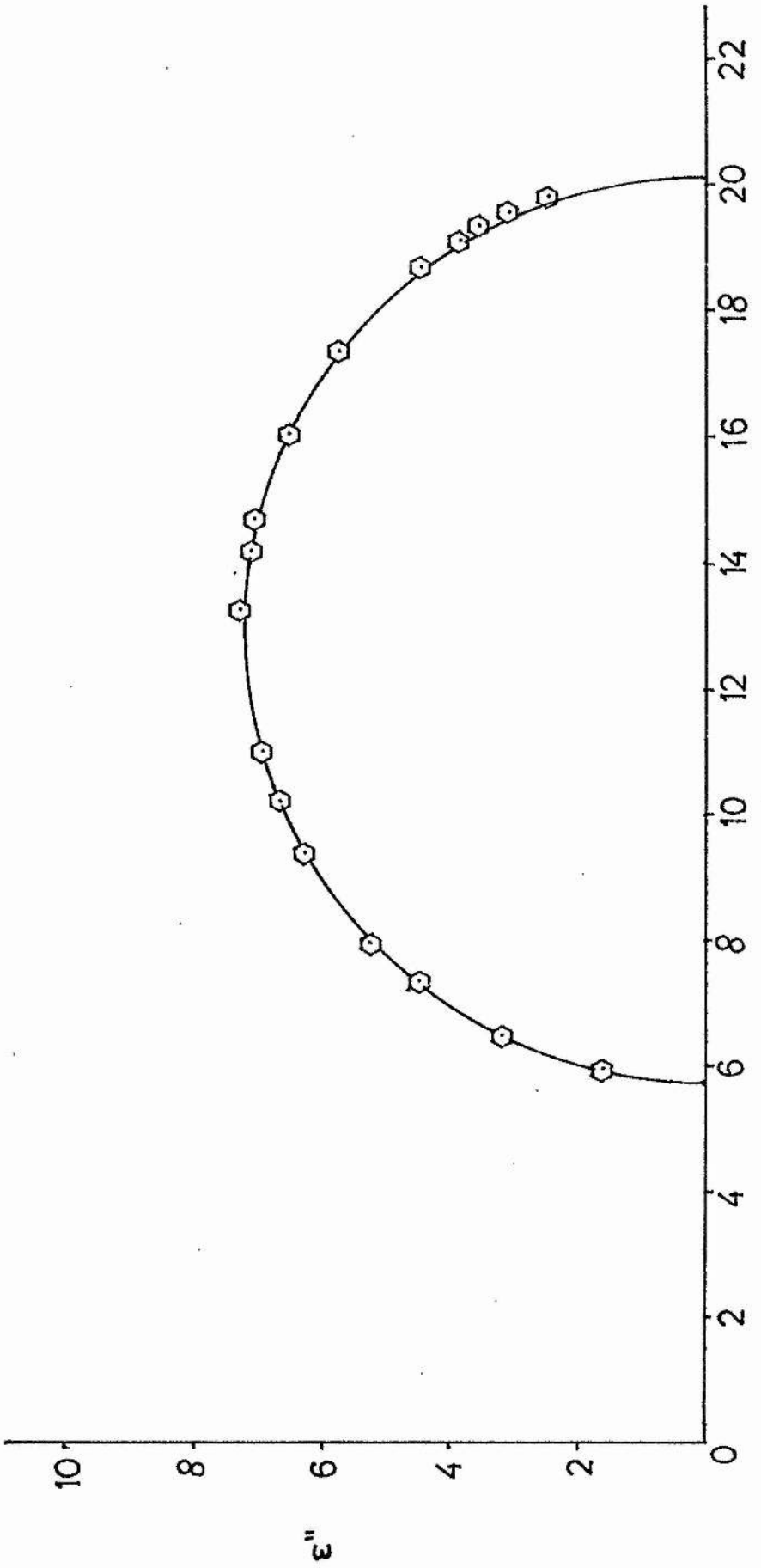

FIG. 5·19

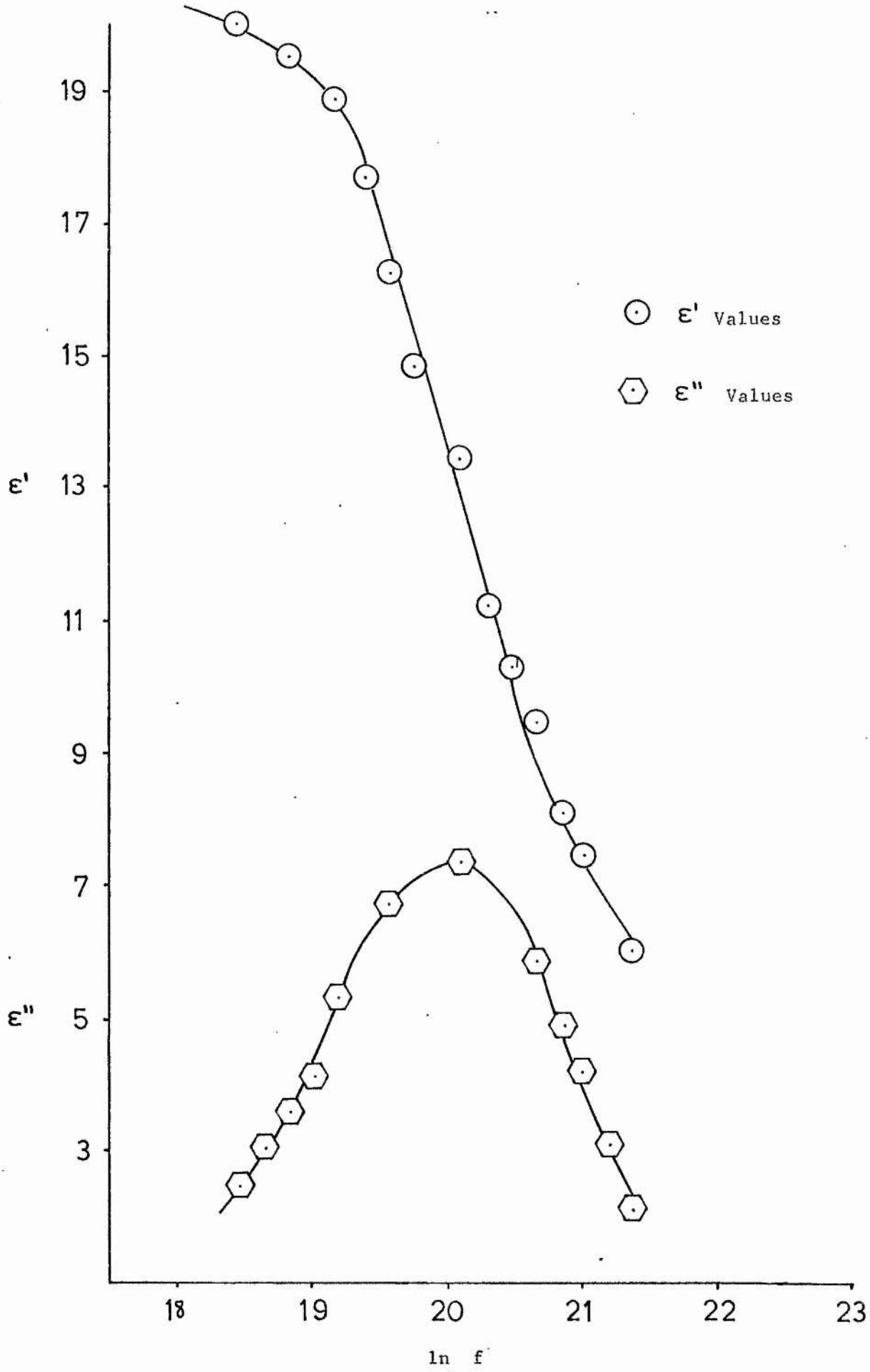

FIG. 5·20

$$\varepsilon' = \varepsilon_o - \omega\tau\varepsilon'' \qquad (5.39)$$

and

$$\varepsilon' = \frac{\varepsilon''}{\omega\tau} + \varepsilon_\infty \qquad (5.40)$$

A plot of ε' versus $\omega\varepsilon''$ will therefore give $-\tau$ as the gradient and ε_o as the intercept. The ε_o and ε_∞ values may also be found from the Cole-Cole plot. Elimination of $\omega\tau$ between equations (5.37) and (5.38) gives the Cole-Cole relation

$$\left(\varepsilon' - \frac{\varepsilon_o+\varepsilon_\infty}{2}\right)^2 + (\varepsilon'')^2 = \left(\frac{\varepsilon_o - \varepsilon_\infty}{2}\right)^2 \qquad (5.41)$$

which is the equation of a semicircle radius $\frac{\varepsilon_o - \varepsilon_\infty}{2}$ meeting at the ε' axis at ε_o and ε_∞, the centre being at $\frac{\varepsilon_o+\varepsilon_\infty}{2}$.

The relaxation time for propan-1-ol was determined from equation (5.39) and the ε_o and ε_∞ values were calculated from equation (5.41) using a regression analysis technique. These calculated values are compared with determinations using other TDR methods and with frequency domain methods in table (5. 7)

	Present Work	TDR Method	Freq. Method
ε_o	20.6	20.6,[125] 20.6[135]	20.5[136]
ε_∞	5.87	3.0," 4.2 "	
τ x10^{-12}/s	354	330," 325 "	395 "

The values obtained for propan-1-ol are therefore comparable with existing TDR methods and frequency domain methods.

Since N-methylformamide and N-methylacetamide have relaxation times not too different from propan-1-ol it was thought that this method could be used to determine ε_o, ε_∞ and τ values for these compounds. However inconclusive results were obtained for both compounds due

it is thought, to the high conductance of the samples analysed. N-methylacetamide was studied at 40°C and the results are shown in the form of a Cole-Cole plot in fig.(5.21). This figure suggests that two relaxations are occuring as the frequency increases. From frequency domain measurements however, Cole et al[134] have shown that a single relaxation process occurs in N- methylacetamide which can be described by equation (5.36).

N- methylformamide was investigated at 0°C and the results are shown as a Debye plot Fig. (5.22) Application of this data to the Cole - Cole relationship failed to produce a semicircular plot. Again Cole et al[134] have shown that N-methylformamide can be described by equation (5.36) from frequency domain measurements.

An attempt to study the dielectric behaviour of formamide by multiple reflection time domain spectroscopy proved unsuccessful due to the very fast relaxation of this molecule.

Although little success has been achieved in the study of the amides, the results of the propan-1-ol investigation indicates that time domain spectroscopic techniques are a useful tool in studying associated liquids. The relaxation times have been studied as a function of temperature for the first four alcohols[137] and the enthalpy of activation for relaxation calculated. In all four instances the energy required for relaxation was greater than that required for viscous flow. In the alcohols therefore the molecules form holes or sites for viscous flow more readily than they can reorient themselves after structural disturbance.

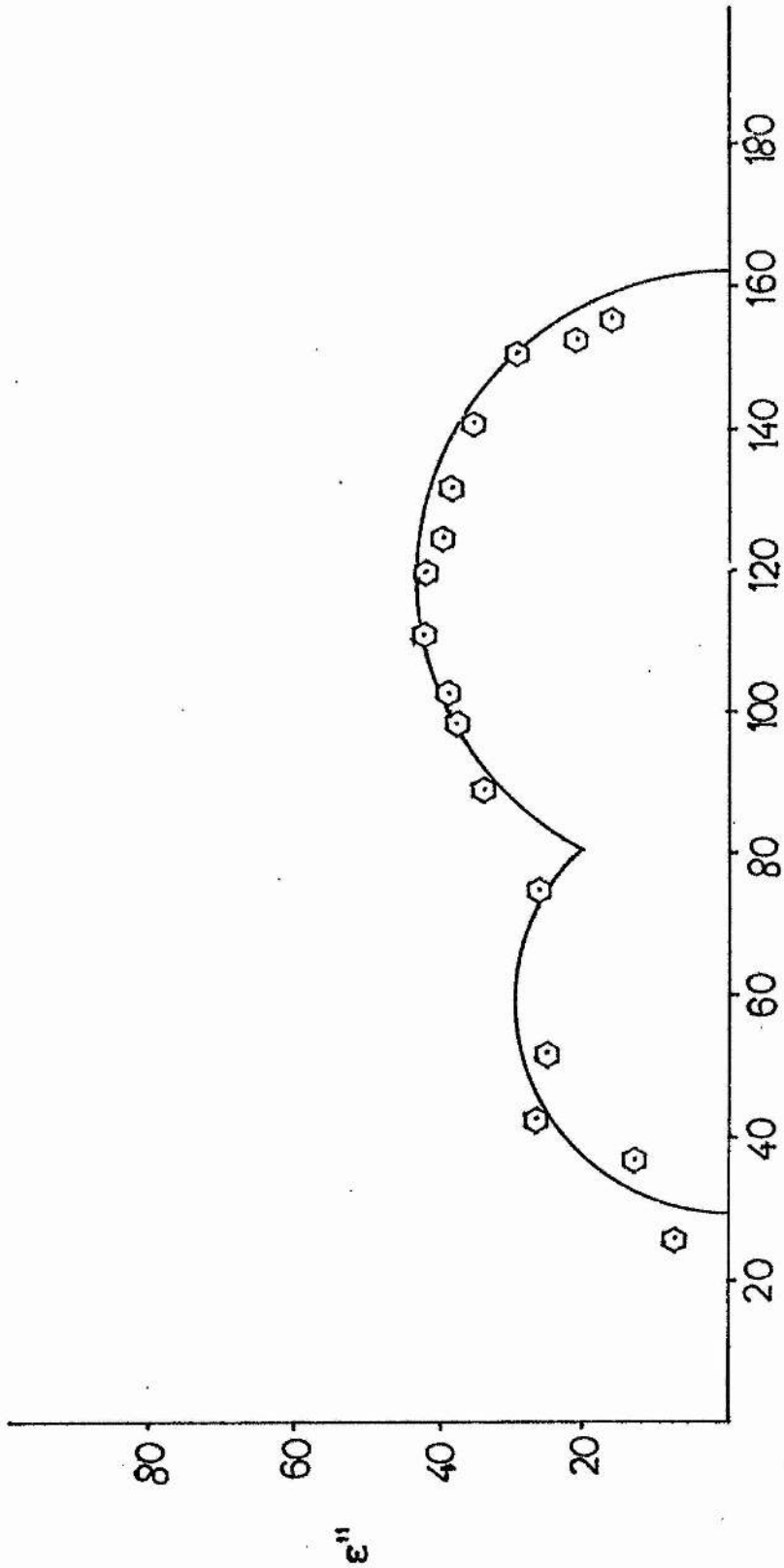

FIG. 5·21

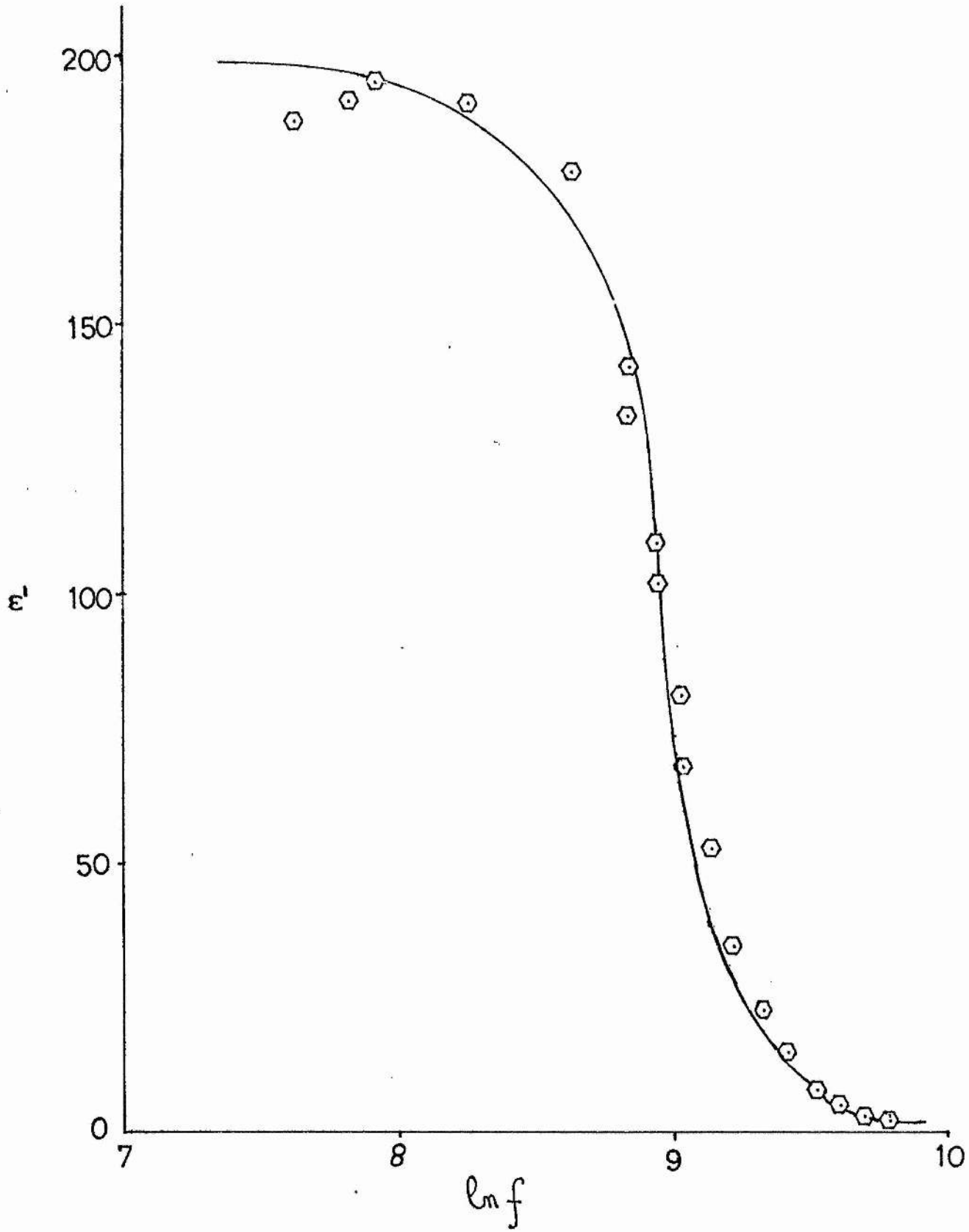

FIG. 5·22

APPENDIX 1

Density and Viscosity of water used for viscometer calibration.

Temperature/^{o}C	Density/g cm^{-3}	Viscosity/J m^{-3} s
10	0.99973	0.001306
15	0.99913	0.001138
18	0.99862	0.001053
20	0.99823	0.001002
25	0.99707	0.000890
30	0.99568	0.000797
35	0.99406	0.000719
40	0.99224	0.000653
45	0.99024	0.000596
50	0.98807	0.000547

APPENDIX 2

THALLOUS NITRATE 25°C

c / mol dm^{-3}	ρ / g cm^{-3}	η_R	$\eta_{R\,calc.}$	$\eta_R - \eta_{R\,calc.}$
0.02011	1.00196	0.99945	0.99949	-0.00004
0.03381	1.00426	0.99880	0.99887	-0.00007
0.04037	1.00584	0.99866	0.99856	0.00010
0.06364	1.01166	0.99721	0.99745	-0.00024
0.07895	1.01503	0.99705	0.99671	0.00034
0.10121	1.01955	0.99550	0.99562	-0.00012

THALLOUS SULPHATE 25°C

0.02038	1.00692	1.00595	1.00566	0.00029
0.02984	1.01104	1.00821	1.00775	0.00046
0.04002	1.01565	1.00987	1.00992	-0.00005
0.04914	1.01907	1.01133	1.01182	-0.0049
0.05975	1.02385	1.01343	1.01400	-0.00057
0.06649	1.02721	1.01524	1.01538	-0.00014
0.07702	1.03303	1.01822	1.01751	0.00071
0.08581	1.03600	1.01922	1.01927	-0.00005

THALLOUS HYDROXIDE 25°C

0.02129	1.00093	1.00293	1.00289	0.00004
0.03385	1.00424	1.00453	1.00445	0.00008
0.03926	1.00528	1.00528	1.00513	0.00015
0.05466	1.00817	1.00695	1.00702	-0.00007
0.06816	1.01002	1.00851	1.00867	-0.00016
0.13528	1.02580	1.01688	1.00168	0.00005

APPENDIX 3

LITHIUM BROMIDE 25°C

c / mol dm^{-3}	ρ / g cm^{-3}	η_R	$\eta_{R\,calc}$	$\eta_R - \eta_{R\,calc}$
0.00769	1.13060	1.00351	1.00395	-0.00044
0.03004	1.13115	1.01407	1.01430	-0.00023
0.06520	1.13367	1.02992	1.03022	-0.00030
0.09304	1.13510	1.04247	1.04271	-0.00024
0.10201	1.13528	1.04743	1.04673	0.00070
0.11530	1.13644	1.05251	1.05267	-0.00016

LITHIUM BROMIDE 35°C

0.01841	1.12254	1.00795	1.00843	-0.00048
0.06471	1.12518	1.02794	1.02810	-0.00016
0.09235	1.12667	1.03798	1.03970	-0.00172
0.10123	1.12662	1.04562	1.04342	0.00220
0.11442	1.12773	1.04855	1.04893	-0.00038

LITHIUM BROMIDE 45°C

0.01827	1.11396	1.00816	1.00799	0.00017
0.02958	1.11353	1.01255	1.01262	-0.00007
0.04473	1.11433	1.01846	1.01875	-0.00029
0.06421	1.11653	1.02731	1.02657	0.00074
0.09163	1.11797	1.03655	1.03752	-0.00097
0.11352	1.11891	1.04669	1.04622	0.00047

POTASSIUM CHLORIDE 25°C

0.00652	1.13015	1.00350	1.00285	0.00065
0.01147	1.13016	1.00440	1.00480	-0.00040
0.02740	1.13073	1.01110	1.01094	0.00016
0.05778	1.13215	1.02320	1.02245	0.00075
0.08455	1.13279	1.03270	1.03249	0.00021
0.11184	1.13415	1.04210	1.04268	-0.00058

POTASSIUM CHLORIDE 35°C

0.00647	1.12153	1.00260	1.00270	-0.00010
0.01139	1.12166	1.00420	1.00455	-0.00035
0.02720	1.12233	1.01080	1.01035	0.00045
0.05735	1.12375	1.02130	1.02120	0.00010
0.08392	1.12435	1.03070	1.03066	0.00004
0.11095	1.12566	1.04010	1.04025	-0.00015

RUBIDIUM IODIDE 25°C

0.01628	1.13105	1.00449	1.00514	-0.00065
0.02252	1.13578	1.00769	1.00696	0.00073
0.04553	1.13629	1.01360	1.01353	0.00007
0.05686	1.13799	1.01758	1.01673	0.00085
0.06757	1.13872	1.01891	1.01975	-0.00084
0.06892	1.13896	1.02007	1.02013	-0.00006
0.10238	1.14414	1.02952	1.02949	0.00003

CAESIUM CHLORIDE 25° C

0.00654	1.13106	1.00225	1.00252	-0.00027
0.01646	1.13193	1.00573	1.00592	-0.00019
0.02830	1.13300	1.00938	1.00987	-0.00049
0.05767	1.13707	1.01926	1.01954	-0.00028
0.08181	1.13998	1.02800	1.02741	0.00059
0.11064	1.14329	1.03665	1.03677	-0.00012

CAESIUM CHLORIDE 35° C

0.00381	1.12220	1.00192	1.00219	-0.00027
0.02808	1.12419	1.00901	1.00946	-0.00045
0.05724	1.12858	1.01872	1.01870	0.00002
0.08119	1.13133	1.02669	1.02622	0.00047
0.10979	1.13445	1.03493	1.03516	-0.00023

CAESIUM CHLORIDE 45° C

0.00577	1.11342	1.00278	1.00210	0.00068
0.00643	1.11389	1.00155	1.00232	-0.00077
0.01621	1.11466	1.00407	1.00542	-0.00135
0.02785	1.11531	1.01026	1.00902	0.00124
0.02858	1.11657	1.00885	1.00924	-0.00039
0.05679	1.11979	1.01774	1.01781	-0.00007
0.08056	1.12261	1.02538	1.02496	0.00042
0.10894	1.12565	1.03318	1.03345	-0.00027

CAESIUM CHLORIDE 50°C

0.00574	1.10905	1.00240	1.00206	0.00034
0.02774	1.11094	1.00836	1.00882	-0.00046
0.05658	1.11559	1.01717	1.01742	-0.00025
0.08025	1.11825	1.02525	1.02440	0.00085
0.10850	1.12113	1.03228	1.03269	-0.00041

CAESIUM BROMIDE 25°C

0.00908	1.13191	1.00299	1.00302	-0.00003
0.01692	1.13243	1.00530	1.00535	-0.00005
0.02877	1.13453	1.00880	1.00881	-0.00001
0.05525	1.13872	1.01664	1.01670	-0.00006
0.06733	1.14009	1.01928	1.01984	-0.00056
0.08441	1.14323	1.02472	1.02468	0.00004
0.11219	1.14692	1.03286	1.03251	0.00035

CAESIUM BROMIDE 3[illegible]°C

0.00901	1.12331	1.00318	1.00290	0.00028
0.01673	1.12363	1.00489	1.00514	-0.00026
0.05082	1.13010	1.01807	1.01708	0.00099
0.06683	1.13149	1.01860	1.01900	-0.00040
0.08378	1.13466	1.02464	1.02362	0.00102
0.11133	1.13810	1.03005	1.03110	-0.00105

[illegible] 45°C

0.00804	1.11482	1.00285	1.00276	0.00009
0.01665	1.11568	1.00458	1.00488	-0.00030
0.02832	1.11674	1.00807	1.00801	0.00006
0.03567	1.11665	1.00967	1.00996	-0.00029
0.05935	1.12122	1.01504	1.01617	-0.00113
0.06631	1.12276	1.01725	1.01798	-0.00073
0.08314	1.12605	1.02381	1.02235	0.00145
0.11044	1.12900	1.02946	1.02940	0.00006

[illegible] 30°C

0.01958	1.11045	1.00553	1.00555	-0.00002
0.03559	1.11414	1.00965	1.00972	-0.00007
0.05523	1.11729	1.01494	1.01476	0.00019
0.05912	1.11672	1.01543	1.01575	-0.00032
0.06605	1.11837	1.01721	1.01751	-0.00030
0.11000	1.12451	1.02892	1.02863	0.00029

[illegible] 25°C

0.01569	1.13293	1.00459	1.00453	0.00006
0.02955	1.13503	1.00789	1.00820	-0.00031
0.04518	1.13855	1.01211	1,01222	-0.00011
0.06403	1.14183	1.01661	1.01704	-0.00043
0.07188	1.14357	1.01908	1.01904	0.00004
0.08901	1.14698	1.02381	1.02339	0.00042

CAESIUM IODIDE 35°C

0.01562	1.12438	1.00433	1.00428	0.00005
0.02941	1.12622	1.00757	1.00770	-0.00013
0.06353	1.13310	1.01596	1.01595	0.00001
0.07134	1.13501	1.01773	1.01782	-0.00009
0.08832	1.13808	1.02211	1.02186	0.00025
0.10947	1.14250	1.02676	1.02688	-0.00012

CAESIUM IODIDE 45°C

0.01550	1.11581	1.00417	1.00426	-0.00009
0.02918	1.11740	1.00766	1.00765	0.00001
0.05378	1.12250	1.01347	1.01363	-0.00016
0.08086	1.12787	1.02056	1.02013	0.00043
0.09335	1.12953	1.02284	1.02311	-0.00027

CAESIUM IODIDE 50°C

0.00947	1.11027	1.00298	1.00267	0.00021
0.01544	1.11153	1.00456	1.00416	0.00040
0.02906	1.11291	1.00746	1.00747	-0.00001
0.04433	1.11705	1.01075	1.01110	-0.00035
0.05357	1.11795	1.01343	1.01329	0.00014

APPENDIX 4

METHANOL/FORMAMIDE

x_1	$\eta \times 10^2$ / J m^{-3}s				$\eta_E \times 10^2$ / J m^{-3}s
	20°C	30°C	40°C	50°c	20°C
0.0000	0.0588	0.0511	0.0447	0.0392	-
0.1194	0.0736	0.0633	0.0548	0.0478	-0.023
0.2001	0.0868	0.0738	0.0635	0.0549	-0.035
0.3194	0.1104	0.0925	0.0787	0.0673	-0.050
0.5025	0.1532	0.1250	0.1047	0.0892	-0.065
0.6681	0.2100	0.1678	0.1388	0.1167	-0.060
0.7587	0.2449	0.1954	0.1600	0.1339	-0.054
0.7999	0.2638	0.2092	0.1706	0.1428	-0.048
0.8838	0.3056	0.2399	0.1942	0.1612	-0.033
1.0000	0.3758	0.2909	0.2332	0.1918	-

x_1 is the mole fraction of formamide

ETHANOL/FORMAMIDE

x_1	$\eta \times 10^2$ / J m^{-3}s				$\eta_E \times 10^2$ / J m^{-3}s
	20°C	30°C	40°C	50°C	20°C
0.0000	0.1199	0.0992	0.0829	0.0698	
0.0919	0.1285	0.1059	0.0883	0.0745	-0.015
0.2075	0.1480	0.1209	0.1003	0.0843	-0.025
0.4151	0.1935	0.1551	0.1270	0.1050	-0.033
0.5007	0.2166	0.1724	0.1404	0.1165	-0.031
0.7138	0.2802	0.2197	0.1773	0.1462	-0.022
0.7997	0.3077	0.2403	0.1932	0.1590	-0.017
0.9103	0.3432	0.2667	0.2138	0.1759	-0.009

PROPAN-1-OL/FORMAMIDE

x_1	η X 10^2 / J m^{-3}s				η X 10^2/ J m^{-3}s
	20°C	30°C	40°C	50°C	20°C
0.0000	0.2189	0.1722	0.1372	0.1107	
0.0261	0.2173	0.1712	0.1368	0.1131	-0.007
0.0486	0.2185	0.1729	0.1385	0.1122	-0.009
0.0929	0.2219	0.1748	0.1394	0.1131	-0.012
0.0982	0.2206	0.1743	0.1397	0.1130	-0.014
0.1472	0.2284	0.1810	0.1440	0.1169	-0.015
0.1486	0.2274	0.1788	0.1431	0.1163	-0.016
0.2002	0.2346	0.1851	0.1478	0.1201	-0.017
0.3024	0.2610	0.2029	0.1615	0.1308	-0.006
0.4018	0.2857	0.2203	0.1748	0.1414	-0.003
0.5010	0.3108	0.2388	0.1885	0.1525	0.013
0.6007	0.3324	0.2544	0.2004	0.1618	0.018
0.6809	0.3529	0.2697	0.2123	0.1715	0.027
0.7927	0.3702	0.2828	0.2231	0.1810	0.026
0.9094	0.3754	0.2884	0.2293	0.1869	0.001

BUTAN-1-OL/FORMAMIDE

x_1	η X 10^2 / J m^{-3} s					η_E X 10^2/ J m^{-3} s
	20°C	25°C	30°C	40°C	50°C	20°C
0.0000	0.2945	0.2580	0.2268	0.1776	0.1409	-
0.0515	0.2883	0.2528	0.2229	0.1754	0.1402	-0.009
0.1007	0.2875	0.2524	0.2240	0.1767	0.1418	-0.016
0.1864	0.3012	0.2639	0.2340	0.1843	0.1479	-0.001
0.3350	0.3306	0.2881	0.2544	0.1996	0.1596	0.009
0.3969	0.3449	0.2999	0.2647	0.2069	0.1656	0.018
0.4991	0.3730	0.3234	0.2848	0.2221	0.1776	0.038
0.5987	0.3951	0.3421	0.3007	0.2343	0.1872	0.052
0.6991	0.4121	0.3561	0.3131	0.2440	0.1954	0.060
0.8044	0.4122	0.3567	0.3139	0.2456	0.1977	0.052
0.9082	0.4018	0.3492	0.3085	0.2446	0.1978	0.033

METHANOL - FORMAMIDE			
X_1	ΔG^*/ kJ mol^{-1}	ΔH^*/ kJ mol^{-1}	ΔS^*/ J $K^{-1} mol^{-1}$
0.000	9.97 9.96 *	9.72 9.54 *	-0.84 -1.34*
0.1194	10.48	10.49	0.02
0.2001	11.05	11.17	0.41
0.3194	11.42	12.17	2.49
0.5025	12.20	13.49	4.34
0.6681	12.96	14.74	5.99
0.7587	13.34	15.23	6.34
0.7999	13.51	15.57	6.89
0.8838	13.87	16.18	7.75
1.0000	14.37	17.04	8.97
		17.15**	

* Ref. Irving & Simpson

** Ref: K.Tyuzyo

ETHANOL-FORMAMIDE			
X_1	ΔG^*/ kJ mol^{-1}	ΔH^*/ kJ mol^{-1}	ΔS^*/ $J \cdot K^{-1} mol^{-1}$
0.000	12.58	13.29	2.39
0.0920	12.67	13.47	2.71
0.2075	12.90	13.97	3.60
0.4151	13.35	15.09	5.85
0.5007	13.54	15.56	6.78
0.7138	13.95	16.43	8.31
0.7997	14.09	16.67	8.65
0.9103	14.24	16.93	9.01

PROPAN-1-OL - FORMAMIDE			
X_1	ΔG^*/ kJ mol^{-1}	ΔH^*/ kJ mol^{-1}	ΔS^*/ J $K^{-1} mol^{-1}$
0.0000	14.62	17.08	8.25
0.0261	14.57	16.89	7.78
0.0486	14.56	16.68	7.10
0.0929	14.54	16.92	8.00
0.0982	14.53	16.74	7.42
0.1472	14.55	16.83	7.66
0.1486	14.53	16.82	7.68
0.199	14.57	16.79	7.44
0.2002	14.55	16.82	7.63
0.3024	14.65	17.35	9.04
0.4018	14.73	17.69	9.94
0.5010	14.78	17.94	10.60
0.6007	14.82	18.18	11.27
0.6809	14.78	18.27	11.71
0.7927	14.72	18.12	11.41
0.9094	14.54	17.96	10.47

BUTANOL-1-OL - FORMAMIDE			
X_1	ΔG^*/ kJ mol^{-1}	ΔH^*/ kJ mol^{-1}	ΔS^*/ J $K^{-1} mol^{-1}$
0.000	15.83	18.58	9.23
0.0515	15.71	18.13	8.13
0.1	15.64	17.79	7.24
0.186	15.62	17.89	7.62
0.33	15.60	18.33	9.18
0.39	15.57	18.52	9.91
0.499	15.57	18.73	10.61
0.59	15.50	18.89	11.35
0.69	15.38	18.87	11.71
0.80	15.13	18.60	11.65
0.90	14.79	17.92	10.51

```
                C       CVTDS
0001                    LOGICAL*1 RCARD(80),ITITLE(80)
0002                    COMPLEX FT1(50),FT2(50),GT(50),E,ENEW,FUNC,DERV
0003                    COMMON F
0004                    REAL T(1200),V(1200),TT(1200),T1(1200),T2(1200),T3(1200),T4(1200),
                       1V1(1200),V2(1200),V3(1200),V4(1200),F(50)
0005                    INTEGER MM(600),X(1200),IX(8,54),IT(1200),OPTITL,SIZE,SUBT,CARD
0006                    EQUIVALENCE (X(1),IX(1,1))
0007                    READ(5,13)NLL,DIV,CALIB,NF,R,S,DIST
0008                 13 FORMAT(I3,2F10.0,I3,3F10.0)
                C       IF CARD=1 NO CARDS ARE PRODUCED
                C       IF CARD =2 THE PROG. PUNCHES CARDS
                C       DIST=SAMPLE CELL LENGHT IN CMS.
                C       R=REAL PART OF E IN THE NEWTON-RAPHSON ITERATIONS
                C       S=IMAGINARY PART OF E IN THE NEWTON-RAPHSON ITERATION AND IS ENTER
                C       -ED WITH A NEGATIVE SIGN
                C       NLL IS THE NUMBER OF POINTS COUNTED BACKWARDS FROM THE TIME REFERE
                C       -NCING POINT
                C       DIV IS THE NUMBER OF DIVISIONS ON THE T.D.R. SCOPE USED FOR CALIBR
                C       ATION
                C       CALIB IS THE NUMBER OF CHANNELS EQUIVALENT TO THAT NUMBER OF DIVIS
                C       -IONS
0009                    KOUNT=0
0010                 10 KOUNT=KOUNT+1
0011                    IF(KOUNT.GT.2) GOTO 2400
0012                    READ(5,100)KODE,CARD
0013                100 FORMAT(A4,I1)
0014                    WRITE(6,121)
0015                121 FORMAT(1H1,'
                       1TIME DOMAIN SPECTROSCOPY'/)
0016                    WRITE(6,120)KODE
0017                120 FORMAT(1H0,'   TAPE VALIDATION CODE    ',A4/)
                C       READ TAPE TITLE
0018                    READ(5,127) TIMSCL,IDENT
0019                127 FORMAT(F10.0,I1)
                C          IDENT=1    SAMPLE + 50-OHM TERMINATOR
                C          IDENT=2    SHORT CIRCUIT
                C       READING FROM TDS-SCOPE IS IN NANOSECONDS/DIVISION
0020                161 WRITE(6,162)TIMSCL
```

```
0021          162 FORMAT(1HO,'    TIME SCALE ,F9.4,' NANOSECONDS/DIVISION ')
0022              DO 205 J=1,64
0023              READ(5,110)(IX(L,J),L=1,8)
0024          110 FORMAT(8(I9,1X))
0025          205 CONTINUE
                  C     PRINT OUT VOLTAGES IN SEQUENCE
0026          605 T(1)=TIMSCL*10.0/512.0
0027              DO 606 J=2,510
0028          606 T(J)=T(J-1)+TIMSCL*10.0/512.0
0029              DO 607 J=1,510
0030          607 V(J)=X(J)
0031              NPRINT=170
0032          778 CONTINUE
0033              WRITE(6,261)
0034          261 FORMAT(1HO,4X,'TIME (NS)',5X,'SIGNAL LEVEL',6X,'TIME (NS)',5X,
                 1'SIGNAL LEVEL',6X,'TIME (NS)',5X,'SIGNAL LEVEL')
0035              DO 300 J=1,NPRINT
0036              MN=3*(J-1)+1
0037              M1=MN
0038              M2=M1+1
0039              M3=M2+1
0040              WRITE(6,251)T(M1),V(M1),T(M2),V(M2),T(M3),V(M3)
0041          251 FORMAT(1H ,3(F13.6,2X,F12.0,5X))
0042          300 CONTINUE
0043              IF(IDENT-1)2339,2100,2200
0044         2100 CONTINUE
0045              DO 2110 J=1,510
0046              T1(J)=T(J)
0047         2110 V1(J)=V(J)
0048              GOTO 10
0049         2200 CONTINUE
0050              DO 2210 J=1,510
0051              T2(J)=T(J)
0052         2210 V2(J)=V(J)
0053              GOTO 10
0054         2339 CONTINUE
0055              GOTO 10
0056         2400 CONTINUE
0057              GOTO 26
```

```
0058          5 WRITE(7,2402)(T1(J),V1(J),T2(J),V2(J),J=1,510)
0059       2402 FORMAT(E12.4,2X,E12.4,2X,E12.4,2X,E12.4)
0060         25 CONTINUE
C
C     CALCULATION OF CONDUCTANCE PARAMETER
C
0061          PHT1=0.0
0062          PHT2=0.0
0063          DO 1100 J=1,20
0064       1100 PHT1=PHT1+V1(J)
0065          PHT1=PHT1/20.0
0066          DO 1110 J=491,510
0067       1110 PHT2=PHT2+V1(J)
0068          PHT2=PHT2/20.0
0069       1113 CONTINUE
0070       1115 CONTINUE
0071          COND=PHT1-PHT2
0072          IF(COND.LT.0.0) GOTO 1120
0073          GO TO 1130
0074       1120 COND=0.0
0075       1130 CONTINUE
0076          WRITE(6,2782)
0077       2782 FORMAT(1H1)
0078          WRITE(6,1140)PHT1,PHT2,COND
0079       1140 FORMAT(1HO,'PHT1= ',E10.4,' PHT2= ',E10.4,' COND= ',E10.4)
0080          CONTINUE
C
C     RE-REFERENCING TIME SCALES OF V1 AND V2
C
0081         53 CONTINUE
0082         54 CONTINUE
0083          NMN=510
0084          DMAX=V1(2)-V1(3)
0085          DO 2700 J=4,NMN
0086          D=V1(J-1)-V1(J)
0087          IF(D.GT.DMAX) GOTO 2660
0088          GOTO 2663
0089       2660 N1MAX=J
0090          DMAX=D
```

```
0091          2005 FORMAT(1H ,E10.4,5X,I5)
0092          2663 CONTINUE
0093          2700 CONTINUE
0094               WRITE(6,2005)DMAX,N1MAX
0095               DMAX=V2(2)-V2(3)
0096               DO 2710 J=4,NMN
0097               D=V2(J-1)-V2(J)
0098               IF(D.GT.DMAX)GOTO 2705
0099               GOTO 2706
0100          2705 N2MAX=J
0101               DMAX=D
0102          2706 CONTINUE
0103          2710 CONTINUE
0104               WRITE(6,2005)DMAX,N2MAX
0105               IF(N2MAX-N1MAX) 2720,2720,2730
0106          2720 NSTART=N1MAX-NLL
0107               NSTOP=NMN
0108               DO 2721 J=NSTART,NSTOP
0109               K=J+1-NSTART
0110               V1(K)=V1(J)
0111               T1(K)=T1(J)-T1(NSTART)
0112          2721 CONTINUE
0113               NSTART=N2MAX-NLL
0114               NSTOP=NMN-(N1MAX-N2MAX)
0115               DO 2722 J=NSTART,NSTOP
0116               K=J+1-NSTART
0117               V2(K)=V2(J)
0118               T2(K)=T2(J)-T2(NSTART)
0119          2722 CONTINUE
0120               GOTO 2750
0121          2730 NSTART=N2MAX-NLL
0122               NSTOP=NMN
0123               DO 2731 J=NSTART,NSTOP
0124               K=J+1-NSTART
0125               V2(K)=V2(J)
0126               T2(K)=T2(J)-T2(NSTART)
0127          2731 CONTINUE
0128               NSTART=N1MAX-NLL
0129               NSTOP=NMN-(N2MAX-N1MAX)
```

```
0130              DO 2732 J=NSTART,NSTOP
0131              K=J+1-NSTART
0132              V1(K)=V1(J)
0133              T1(K)=T1(J)-T1(NSTART)
0134         2732 CONTINUE
0135         2750 CONTINUE
0136              NMN=NSTOP-NSTART
0137         2401 FORMAT(1H ,4(E11.4,5X))
0138         2760 CONTINUE
0139              GMN=NMN
0140              NS=5
0141              GS=NS
0142              DO 2780 J=1,510
0143         2780 CONTINUE
0144              DELTAT=(TIMSCL*DIV)/CALIB*1.0E-09
                  C
                  C      CARRY OUT FOURIER TRANSFORMS ON EACH SIGNAL AND FIND RATIO
                  C
0145              CALL CVFTR(V1,FT1,DELTAT,NMN,NS,NF)
0146              CALL CVFTR(V2,FT2,DELTAT,NMN,NS,NF)
0147              DO 3000 J=1,NF
0148         3000 GT(J)=FT1(J)/FT2(J)
0149              WRITE(6,3001)(FT1(J),FT2(J),GT(J),J=1,NF)
0150         3001 FORMAT(1H ,6X,6E12.4//)
                  C      NEWTON-RAPHSON SOLUTION FOR COMPLEX PERMITTIVITY FROM TOTAL
                  C      SCATTERING COEFFICIENT.
                  C
0151              E=CMPLX(R,S)
0152              DO 4000 J=1,NF
0153              ECOND = COND*2.9979E+10/(DIST*3.14159*F(J)*(1.0-COND))
0154              DO 4100 I=1,20
0155              CALL CVNEWT(E,DIST,FUNC,GT(J),F(J))
0156              CALL CVDERV(E,DIST,DERV,F(J))
0157              ENEW=E-FUNC/DERV
0158              EPS=(REAL(E)-REAL(ENEW))**2+(AIMAG(E)-AIMAG(ENEW))**2
0159              E=ENEW
0160              IF(EPS-0.01)4200,4200,4100
0161         4100 CONTINUE
0162              WRITE(6,4101)F(J),EPS
```

```
0163          4101 FORMAT(1HO,'NO CONVERGANCE AT A FREQUENCY OF ',E10.4,' ,EPS HAS A
                  1VALUE OF'E10.4,' AT THE LAST ITERATION')
0164          4200 CONTINUE
0165               E=ENEW
0166               E1=REAL(E)
0167               E2=AIMAG(E)
0168               E3=E2+ECOND
0169               SLOGF=0.43429*ALOG(F(J))
0170               WRITE(6,4300)F(J),SLOGF,E1,E2,E3,ECOND,I
0171          4300 FORMAT(E10.4,5X,E10.4,4(5X,E10.4),I3)
0172               IF(CARD.LT.2)GOTO 4000
0173          4013 WRITE(7,4016)F(J),E1,E2,E3,SLOGF
0174          4016 FORMAT(E10.4,5X,E10.4,5X,E10.4,5X,E10.4,5X,E10.4)
0175          4000 CONTINUE
0176          9999 CONTINUE
0177               CALL EXIT
0178               END
```

```
      C     FOURIER TRANSFORM SUBROUTINE
0001        SUBROUTINE CVFTR(Y,FTRANS,DELTAT,NMN,NS,NF)
0002        DIMENSION Y(1200),F(50)
0003        COMPLEX FTRANS(50),A,CMPLX
0004        COMMON F
0005        WRITE(6,15)DELTAT,NMN
0006     15 FORMAT(1H ,'DELTAT='E10.4,5X,'NMN='I4)
0007        DO 10 K=2,NMN
0008        Y(K-1)=Y(K)-Y(K-1)
0009     10 CONTINUE
0010        GMN=NMN
0011        F1=1/((GMN-1)*DELTAT)
0012        FH=GMN/2*F1
0013        RF1=ALOG(F1)
0014        RFH=ALOG(FH)
0015        DELF=(RFH-RF1)/NF
0016        NR=NF-1
0017        F(1)=F1
0018        N=1
0019        DO 12 J=2,NR
0020        F(J)=EXP(RF1+(N*DELF))
0021        N=N+1
0022     12 CONTINUE
0023        F(NF)=FH
0024        NJ=NMN-1
0025        DO 50 J=1,NF
0026        FTRANS(J)=(0.0,0.0)
0027        DO 60 K=1,NJ
0028        IF(Y(K)) 70,60,70
0029     70 CONTINUE
0030        THETA=6.2831854*DELTAT*F(J)*(K-1)
0031        A=CMPLX(COS(THETA),-SIN(THETA))
0032        FTRANS(J)=(Y(K)*A) + FTRANS(J)
0033     60 CONTINUE
0034     50 CONTINUE
0035        RETURN
0036        END
```

```
      C     SUBROUTINE TO CALCULATE DERIVATIVE FOR NEWTON-RAPHSON SEQUENCE
0001          SUBROUTINE CVDERV(E,DIST,DERV,FR)
0002          COMPLEX E,Z,P,EPZ,A,B,C,DERV
0003          Z=CSQRT(E)
0004          P=CMPLX(0.0,-4.19158*DIST*FR*1.0E-10)
0005          EPZ=CEXP(P*Z)
0006          A=-1.0*(1.0-EPZ)/((1.0+Z)**2-(1.0-Z)**2*EPZ)
0007          B=(-1.0*(1.0-Z**2)*P*EPZ)/(2.0*Z*((1.0+Z)**2-((1.0-Z)**2)*EPZ))
0008          C=-1.0*(1.0-Z**2)*(1.0-EPZ)*(2.0*(1.0+Z)+(1.0-Z)*EPZ*(2.0-P*(1.0-Z
             1)))/(2.0*Z*((1.0+Z)**2-(1.0-Z)**2*EPZ)**2)
0009          DERV=A+B+C
0010          RETURN
0011          END
```

```
      C     SUBROUTINE TO CALCULATE FUNCTION VALUE FOR NEWTON-RAPHSON SEQUENCE
0001        SUBROUTINE CVNEWT(E,DIST,FUNC,GT,FR)
0002        COMPLEX E,GT,P,Z,PZ,EPZ,FUNC,CMPLX,CSQRT,CEXP
0003        Z=CSQRT(E)
0004        P=CMPLX(0.0,-4.19158*DIST*FR*1.0E-10)
0005        EPZ=CEXP(P*Z)
0006        FUNC=((1.0-Z)/(1.0+Z)*(1.0-EPZ))/(1.0-((1.0-Z)/(1.0+Z))**2*EPZ)+GT
0007        RETURN
0008        END
```

```
DELTAT=0.1974E-10      NMN= 491
DELTAT=0.1974E-10      NMN= 491
      -0.4927E 05 -0.3354E 05 -0.2438E 06  0.1761E 06  0.6752E-01  0.1863E 00

      -0.6436E 05 -0.2728E 05 -0.2204E 06  0.2074E 06  0.9312E-01  0.2114E 00

      -0.7944E 05 -0.1337E 05 -0.1821E 06  0.2392E 06  0.1247E 00  0.2372E 00

      -0.9011E 05  0.9251E 04 -0.1307E 06  0.2609E 06  0.1667E 00  0.2619E 00

      -0.9172E 05  0.3851E 05 -0.7734E 05  0.2717E 06  0.2200E 00  0.2750E 00

      -0.8171E 05  0.7151E 05 -0.1718E 05  0.2837E 06  0.2685E 00  0.2717E 00

      -0.5520E 05  0.1060E 06  0.6725E 05  0.2844E 06  0.3096E 00  0.2673E 00

      -0.2700E 04  0.1316E 06  0.1784E 06  0.2449E 06  0.3459E 00  0.2630E 00

       0.7001E 05  0.1194E 06  0.2617E 06  0.1266E 06  0.3958E 00  0.2651E 00

       0.1315E 06  0.5851E 05  0.2818E 06 -0.1893E 05  0.4506E 00  0.2379E 00

       0.1410E 06 -0.4047E 05  0.2224E 06 -0.1843E 06  0.4652E 00  0.2036E 00

       0.5456E 05 -0.1452E 06 -0.7839E 04 -0.2920E 06  0.4919E 00  0.2000E 00

      -0.8494E 05 -0.1223E 06 -0.2143E 06 -0.1624E 06  0.5264E 00  0.1716E 00

      -0.1529E 06  0.3431E 05 -0.2482E 06  0.1372E 06  0.5303E 00  0.1548E 00
```

```
 0.1344E 06 -0.3784E 05  0.2147E 06 -0.1153E 06  0.5594E 00  0.1243E 00
-0.8422E 05 -0.9108E 05 -0.1720E 06 -0.1237E 06  0.5736E 00  0.1168E 00
 0.2687E 04  0.1058E 06  0.3561E 05  0.1810E 06  0.5659E 00  0.9650E-01
 0.2708E 05 -0.9643E 05  0.2401E 05 -0.1769E 06  0.5555E 00  0.7766E-01
-0.7448E 04  0.8662E 05 -0.1891E 04  0.1448E 06  0.5987E 00  0.4361E-01
-0.5281E 05 -0.4898E 05 -0.1005E 06 -0.9619E 05  0.5178E 00 -0.8166E-02
 0.1577E 05 -0.4434E 05  0.4643E 05 -0.9094E 05  0.4570E 00 -0.5993E-01
 0.2834E 05 -0.1465E 05  0.4924E 05 -0.5304E 05  0.4147E 00  0.1493E 00
 0.1169E 05 -0.1239E 05  0.2395E 05 -0.6672E 05  0.2202E 00  0.9618E-01
-0.7800E 04 -0.7438E 04 -0.2276E 05  0.1143E 05  0.1426E 00  0.3984E 00
 0.8634E 04  0.7218E 04  0.4378E 04 -0.1445E 05 -0.2917E 00  0.6858E 00
 0.2025E 03  0.8336E 04 -0.2327E 04  0.4993E 04  0.1356E 01 -0.6727E 00
 0.5281E 04  0.1739E 04 -0.6705E 04  0.2443E 05  0.1100E-01 -0.2192E 00
-0.9249E 04  0.3885E 04 -0.1841E 05 -0.7939E 04  0.3469E 00 -0.3607E 00
-0.4565E 04  0.3959E 03 -0.1596E 05  0.5934E 04  0.2594E 00  0.7161E-01
```

.1034E 09	3	0.0	0.2003E 02	-.2456E 01	-.2456E 01
.1242E 09	2	0.0	0.1975E 02	-.3008E 01	-.3008E 01
.1492E 09	2	0.0	0.1947E 02	-.3493E 01	-.3493E 01
.1793E 09	2	0.0	0.1931E 02	-.4139E 01	-.4139E 01
.2154E 09	2	0.0	0.1890E 02	-.5275E 01	-.5275E 01
.2587E 09	2	0.0	0.1763E 02	-.6306E 01	-.6306E 01
.3108E 09	2	0.0	0.1623E 02	-.6675E 01	-.6675E 01
.3734E 09	2	0.0	0.1486E 02	-.6594E 01	-.6594E 01
.4486E 09	2	0.0	0.1434E 02	-.6438E 01	-.6438E 01
.5389E 09	2	0.0	0.1344E 02	-.7199E 01	-.7199E 01
.6474E 09	3	0.0	0.1121E 02	-.7042E 01	-.7042E 01
.7778E 09	2	0.0	0.1036E 02	-.6043E 01	-.6043E 01
.9344E 09	2	0.0	0.9492E 01	-.5868E 01	-.5868E 01
.1123E 10	3	0.0	0.8147E 01	-.4853E 01	-.4853E 01
.1349E 10	2	0.0	0.7469E 01	-.4203E 01	-.4203E 01
.1620E 10	3	0.0	0.6640E 01	-.3122E 01	-.3122E 01
.1946E 10	3	0.0	0.6045E 01	-.2137E 01	-.2137E 01
.2338E 10	3	0.0	0.5166E 01	-.1444E 01	-.1444E 01
.2809E 10	3	0.0	0.4410E 01	-.8253E 00	-.8253E 00
.3375E 10	3	0.0	0.4213E 01	-.1617E 00	-.1617E 00
.4054E 10	3	0.0	0.3306E 01	-.1828E 00	-.1828E 00
.4870E 10	3	0.0	0.2780E 01	-.5836E-01	-.5836E-01
.5851E 10	7	0.0	0.1750E 01	0.5684E 00	0.5684E 00
.7029E 10	3	0.0	0.1349E 01	0.3106E 00	0.3106E 00

REFERENCES

1. D.I. Mendelejew, Works, Vol. IV (Leningrad,1937)
2. H. Eyring, S. Glasstone and K. Laidler, The theory of Rate Processes (McGraw-Hill, New York, 1941)
3. R.J. Podolsky, J. Amer. Chem. Soc., 1958, 80, 4442
4. O.Y. Samoilov, Structure of Aqueous Electrolyte Solutions and the Hydration of Ions (Consultants Bureau, New York, 1965)
5. P. Debye and E. Hückel, Phys.Z., 1923, 24,185
6. N. Bjerrum, K.danske vidensk. Selsk., 1926, No.9,7
7. L. Onsager, Phys.Z., 1927,28, 277
8. H. Falkenhagen, M. Leist and G. Kelbg,Ann. Phys.Lpz., 1952, 11, 51
9. S. Arrhenius, Meddel. Vetenskapsakad. Nobelinst., 1913, 2,25
10. M. Born, Z.Phys.,1920, 1, 45
11. R.A. Robinson and R.H. Stokes, Electrolyte Solutions (Butterworths, London, 1959)
12. D.A. Owensby, A.J. Parker and J.W. Diggle, J. Amer. Chem.Soc., 1974, 96, 2682
13. I. Newton, Philosophiae Naturalis Principia Mathemetica (1687)
14. P.Navier, Mem.de l'Acad. des Sciences, 1823,6, 389
15. G.G. Stokes, Math. and Phys. Papers, Vol.1 (Cambridge 1880)
16. R.H. Stokes and R. Mills, The Viscosity of Electrolytes (Pergamon Press, Oxford, 1965)
17. G. Jones and M. Dole, J. Amer. Chem. Soc., 1929 51, 2950

18. H. Falkenhagen and M. Dole, Z. Phys. Chem. (Frankfurt) 1929, 6, and Phys. Z., 1929, 30,611

19. H.S. Frank and W.Y. Wen, Discuss. Faraday Soc., 1957, 24, 133

20. A. Dinsdale and F. Moore, Viscosity and its Measurement (Chapman and Hall, London, 1962)

21. J.F. Swindells, R. Ullman and H. Mark, Techniques of Organic Chemistry, Vol.I, ed. Weissberger (Interscience London, 3rd edn., 1959)

22. R. G. Hagen, Ann.d.Phys., 1839, 46, 423

23. J.L. Poiseuille, Mém.Savants Étrangers, 1846, 9, 433

24. O. Reynolds, Phil.Trans.A., 1883, 174, 935; 1886,177,171

25. E. Hagènbach, Ann. Phys., Liepzig (Pogg.Ann.), 1860, 109, 385

26. L.R. Wilberforce, Phil.Mag., 1891,31, 407

27. M. Couette, Ann.d.Chim. et Phys., 1890, 21,433

28. F. Finkener and R. Gartenmeister, Z.Phys.Chem.(Frankfurt), 1890, 6, 524

29. P. Boussinesq, Compt. Rend., 1890, 110, 1160; 1891,113, 9

30. L. Ubbelohde, Ind. Eng. Chem., Anal.Ed., 1937,9, 85

31. L.D. Eicher and B. Zwolonski, J.Phys.Chem.,1971,75, 2016

32. J. Einfeldt and E. Gerdes,Z.Phys.Chem.(Liepzig,1971, 246 221

33. W. Adolph and W. Siedel,Z.Phys.Chem.(Frankfurt),1974, 93, 173

34. G. Jones and S.K. Talley,J.Amer.Chem.Soc.,1933,55,624

35. J.F. Swindells,R.Coe and D.Godfrey,J.Res.Nat.Bur.Stand., 1952,48,1

36. R.C. Hardy and R.L.Cottingham,J.Res.Nat.Bur.Stand., 1949, 42,573

37. Hanbook of Chemistry and Physics,52nd Ed., 1971-72 p.F36

38. J.McDowall,Ph.D.thesis,St. Andrews,December, 1973

39. M.R. Lipkin,J.A.Davison,W.T.Harvey and S.S.Kurtz,Jr., Ind.Eng.Chem.Anal.Ed., 1944, 16, 55

40. L.R. Dawson,E.D. Wilhoit and P.G. Sears,J.Amer.Chem. Soc., 1957,79, 5906

41. J.M.Notley and M. Spiro, J.Chem.Soc.,(B), 1966,362

42. Moisture Determinations by the Karl Fischer Reagent (BDH Ltd.,London,1967)

43. H.Lund and J.Bjerrum,Ber.Deut.Chem.Gesell. 1931,64,210

44. S.Young,J.Chem.Soc.,1902,707

45. J.F. Mathews and J.J.McKetta,J.Phys.Chem.1961,65,758

46. J.L.Poiseuille,Ann.Chem.Phys.(3),1847,21,76

47. S.Arrhenius,Z.Physik.Chem.,1887,1,285

48. E.Grüneisen,Wiss.Abhandl.Physik.Tech.Reichsanstalt, 1905,4,151,237

49. A.Einstein,Ann.Physik,1906,19,289;1911,34,591

50. H.Falkenhagen and E.L.Vernon,Phil.Mag., 1932,14,537

51. H.S. Harned and B.B.Owen,The Physical Chemistry of Electrolyte Solutions (Reinhold,NewYork, 3rd ed.,1958), p.240

52. M.Kaminsky,Disc.Faraday Soc.,1957,24,171

53. F.Pitts, Proc. Roy. Soc. A, 1953,217,43

54. C.W.Davies and V.E.Malpass, Trans. Faraday Soc.,1964, 60,2075

55. R.W.Gurney,Ionic Processes in Solution(MacGraw-Hill, New York,1953)

56. G.Jones and S.K.Talley,J.Amer.Chem.Soc.,1933,55,4124

57. G.Jones and H.J.Fornwalt, J.Amer.Chem.Soc.,1936,58,619

58. M.Kaminsky,Z.Phys.Chem. (Frankfurt),1957,12,206

59. D.Feakins and K.G.Lawrence,J.Chem.Soc. A,1966,212

60. R.T.M. Bicknell,K.G.Lawrence,M.A. Seeley,D.Feakins and L.Werblan,J.C.S. Faraday I. 1976.72,307

61. J.E.Desnoyers and G.Perron,J.Solution Chem.,1972,1,199

62. A.Martell and L.G.Sillen,Stability Constants (Chemical Society,London,1964)

63. V.S.K. Nair and H.N.Nancollas,J.Chem.Soc., 1957,318

64. L.Onsager and R.M.Fuoss,J.Phys.Chem.,1932,36,2689

65. C.W.Davies and E.C.Righellato, Trans.Faraday Soc., 1930,26,592

66. R.P.Bell and J.H.B.George,Trans.Faraday Soc.,1953,49,619

67. R.P.Bell and M.H.Panckhurst,J.Chem.Soc., 1956,2836

68. W.T.Lindsay,J.Phys.Chem.,1962,66,1341

69. E.Hückel and H.Schaaf,Z.Phys.Chem(Frankfurt),1959,21,326

70. C.W.Davies and V.E.Malpass,Trans.Faraday Soc.,1964,60 2078

71. J.H.B.George,J.A.Rolfe and L.A.Woodward,Trans.Faraday Soc., 1953,49,375

72. P.B.Davis,W.S.Putnam and H.C.Jones,J.Franklin Inst., 1915,180,567

73. P.B.Davis and H.I.Johnson,Carnegie Institution of Washington Publication No.260, 1918,71

74. J.M.McDowall and C.A.Vincent,J.C.S. Faraday I, 1974,70,1862

75. P.Bruno,C.Gatti and M.Della Monica, Electrochim.Acta, 1975,20,533

76. J.M.McDowall,N.Martinus amd C.A.Vincent,J.C.S. Faraday I,1976,72,654

77. M.Kaminsky,Disc.Faraday,Soc., 1957,24,127

78. W.M.Cox and J.H.Wolfenden,Proc.Roy.Soc.A,1934,145,486

79. E.R.Nightingale,Jnr.,J.Phys.Chem.1959,63,1381

80. B.S.Krumgal'z,Zhur,Fiz.Khim,1973,47,1691

81. R.J.Gillespie,Rev.Pure Appl.Chem.,1959,9,1

82. C.M.Criss and M.J.Mastroianni ,J.Phys.Chem.,1971,75,2532

83. D.F.-T.Tuan and R.M.Fuoss,J.Phys.Chem., 1963,67,1343

84. R.W.Kunze and R.M. Fuoss,J.Phys.Chem., 1963,67,385

85. N-P.Yao and D.N.Bennion,J.Phys.Chem.,1971,75,1727

86. J.M.Notely and M.Spiro,J.Phys.Chem.1966,70,1502

87. B.S.Krumgal'z,Zhur.Fiz.Khim.,1971,45,2559

88. A.Sacco,G.Petrella and M.Castagnolo,J.Phys.Chem. 1976,80,749

89. C.M.Criss,R.P.Held and E. Luksha,J.Phys.Chem, 1968 72,2970

90. C.M.Criss and M.Salomon,Physical Chemistry of Organic Solvent Systems,A.K.Covington and T,Dickinson Ed.,(Plenum Press,New York,N.Y.1973),Chapter 2

91. C.M.Criss and E.M.Luksha,J.Phys.Chem.,1968,72,2966

92. H.S.Frank and M.W.Evans,J.Chem.Phys. 1945,13,507

93. J.Padova,Water and Aqueous Solutions,Ed.Horne,1971, Chapter IV.

94. J.O'M.Bockris,Quart.Rev., 1949,3,173

95. O.Ya.Samoilov,Disc.Faraday Soc., 1957,24,141

96. E.Darmois,J.Phys.radium, 1941,2,2

97. E.R.Nightingale,Jnr. and R.F.Benck,J.Phys.Chem,1959,63,1777

98. D.Feakins,D.J.Freemantle and K.G.Lawrence,J.C.S. Faraday I,1974,70,795

99. F.J. Millero, Chemical Reviews, 1971, 71 147

100. P.Bruno and M.Della Monica,Electrochem.Acta,1976,21,799

101. S.Arrhenius,Meddel.Vetenskapsakad.Nobelinst,1916,3,20

102. E.N.daC.Anrade,Phil.Mag., 1934,17,497,698

103. G.Somsen and C,de Vissier, Rec. Trav. Chim., 1972, 91, 942

104. A.J.Parker,Quart.Rev.London,1962,16,163

105. R.J.Bearman and P.F.Jones,J.Chem.Phys.,1960,33,1432

106. G.A.Ratcliff and M.A.Khan, Can.J.Chem.Eng.,1971,49,125

107. R.J.Fort and W.R.Moore,Trans,Faraday Soc., 1966,62,1112

108. H.M.N.H. Irving and R.B.Simpson,J.inorg. nucl.chem., 1970,32,901

109. E.W.Merry and W.S.Turner,J.Chem.Soc., 1914,105,748

110. Z.Kozlowski,Lodzkie Towarzystoo Naukowe Soc. Scient. Lodz.Acta Chim., 1971,16,17

111. M.Liler and D.Kosanovic,Hydrogen Bonding,ed.Hadzi (Pergamon Press,London,1959)

112. K.Tyuzyo,Bull.Chem.Soc.Japan,1957,30,782

113. N.I.Joukovsky,Bull.Soc.Chim.Belg.,1934,43,397

114. T.Erdey-Grúz,E.Kugler and L.Majthényi, Electrochim. Acta,1968,13,947

115. F.Dolezalek,Z.Phys.Chem.1913,83,73

116. R.H.Hind,E.McLaughlin and A.R.Ubbelohde ,Trans.Faraday Soc.,1960,56,328

117. J.Frenkel,Kinetic Theory of Liquids (Oxford University Press,London,1946)

118. M.Tamura and M.Kurata,Bull.Chem.Soc.Japan. 1952,25,32

119. F.Mato and J.L.Hernandez,Anal,de Fiz.y.Quim.,1967, 63(B),13

120. S.A.Rice,J.P.Boon and H.T.Davis,Simple Dense Fluids, ed.Frisch and Salsburg,(Academic Press,London, 1968) p.257-8

121. C.D.Sinclair and C.A.Vincent, J.C.S. Faraday 1,1974, 70,1926

122. P.Debye,Polar Molecules (Catalog Co., New York, 1929)

123. K.S.Cole and R.H.Cole, J.Chem.Phys., 1941,9,341

124. H.Fellner-Feldegg,J.Phys.Chem,1969, 73,616

125. A.Suggett,P.A.Mackness,M.J.Tait,H.W.Loeb and G.M.Young, Nature,1970,228, 456

126. H.Fellner-Felldeg,J.Phys.Chem.,1972,76,2116

127. G.P.deLoor,M.J.C. van Germert and H.Gravesteyn, Chem.Phys.Lett. 1973,18, 295

128. See reference 126

129. M.J.C. van Gemert, Philips Res. Repts.1973,28,530

130. R.K.Mackie,T.M.Shephard and C.A.Vincent,Mathematical Methods for Chemists (Butterworths,London,1973)

131. A.H.Clark,P.A. Quickenden and A.Suggett,J.C.S. Faraday II,1974,70,1847

132. M.J.C. van Gemert.J.Chem.Phys.,1974 60.3963

133 H.A.Samulon,Proc.IRE,1951,39,175

134. S.J.Bass,W.I.Nathan,T.M.Meighan and R.H.Cole,J.Phys. Chem.,1964,68,509

135. M.J.C. van Gemert,Thesis,University of Lieden, 1972

136. S.K.Garg and C.P.Smyth,J.Phys.Chem.,1965,69,1294

137. H.W.Loeb, G.M.Young,P.A.Quickenden and A.Suggett, Ber. Bunsenges,Phys.Chem.,1971,75,1155